A GLOBAL APPROACH TO THE HYDROGEN PRODUCTION,
CARBON ASSIMILATION AND NITROGEN METABOLISM OF
<u>RHODOBACTER CAPSULATUS</u>
BY PHYSIOLOGICAL AND MICROARRAY ANALYSES

A THESIS SUBMITTED TO
THE GRADUATE SCHOOL OF NATURAL AND APPLIED SCIENCES
OF
MIDDLE EAST TECHNICAL UNIVERSITY

BY

NİLÜFER AFŞAR

IN PARTIAL FULFILLMENT OF THE REQUIREMENTS
FOR
THE DEGREE OF DOCTOR OF PHILOSOPHY
IN
BIOLOGY

SEPTEMBER 2012

Approval of the Thesis;

A GLOBAL APPROACH TO THE HYDROGEN PRODUCTION, CARBON ASSIMILATION AND NITROGEN METABOLISM OF <u>RHODOBACTER CAPSULATUS</u> BY PHYSIOLOGICAL AND MICROARRAY ANALYSES

submitted by **NİLÜFER AFŞAR** in partial fulfillment of the requirements for the degree of **Doctor of Philosophy in Biological Sciences Department, Middle East Technical University** by,

Prof. Dr. Canan Özgen   _____
Dean, Graduate School of **Natural and Applied Sciences**

Prof. Dr. Musa Doğan   _____
Head of Department, **Biological Sciences**

Prof. Dr. Meral Yücel   _____
Supervisor, **Biological Sciences Dept., METU**

Examining Committee Members:

Prof.Dr. Emel Arınç   _____
Biological Sciences Dept., METU

Prof. Dr. Meral Yücel   _____
Supervisor, Biological Sciences Dept., METU

Prof. Dr. Ufuk Gündüz   _____
Biological Sciences Dept., METU

Assoc. Prof. Dr. Ayşegül Gözen   _____
Biological Sciences Dept., METU

Assoc. Prof. Dr. Füsun Eyidoğan   _____
Elementary Education Department, Başkent University

Date: 14.09.2012

I hereby declare that all information in this document has been obtained and presented in accordance with academic rules and ethical conduct. I also declare that, as required by these rules and conduct, I have fully cited and referenced all material and results that are not original to this work.

Name, Last name : Nilüfer, Afşar

Signature :

ABSTRACT

A GLOBAL APPROACH TO THE HYDROGEN PRODUCTION, CARBON ASSIMILATION AND NITROGEN METABOLISM OF <u>RHODOBACTER CAPSULATUS </u>BY PHYSIOLOGICAL AND MICROARRAY ANALYSES

Afşar, Nilüfer

Ph.D., Biological Sciences Department

Supervisor: Prof. Dr. Meral Yücel

September 2012, 225 pages

One of the most important parameters affecting hydrogen production in photofermentation process is the type of carbon and nitrogen sources. For this reason in this research, the effect of different nitrogen sources (5mM ammonium chloride and 2mM glutamate) and acetate concentrations (40-80mM) on metabolism of *Rhodobacter capsulatus* were investigated.

First of all, physiological experiments were carried out to compare growth, hydrogen production and substrate utilization behaviors of *R. capsulatus* on different nitrogen sources and acetate concentrations. For further understanding of hydrogen production, carbon assimilation and nitrogen metabolism; microarray analysis were conducted. For this purpose, an Affymetrix GeneChip for *R. capsulatus* was custom designed and manufactured. An efficient RNA isolation protocol from *R.*

capsulatus was optimized for use of microarray analysis. Validation of the microarray experiments and custom designed *R. capsulatus* were carried out by RT-qPCR analysis.

On 5mM ammonium chloride containing medium, transcription of genes related to transport, assimilation and utilization of acetate were significantly up-regulated compared to 2mM glutamate medium. On the other hand, nitrogenase enzyme encoding genes were significantly down-regulated on ammonium chloride containing medium.

Although transcription of genes that take role in acetate assimilation did not show a significant difference on 80mM acetate compared to 40mM acetate; TCA cycle, photosynthetic apparatus, electron transport and Calvin cycle related genes were significantly down-regulated on 80mM acetate.

From microarray data analysis results, it was suggested for the first time that *Rhodobacter capsulatus* might assimilate acetate by using two different routes using glyoxylate cycle and/or ethylmalonyl-CoA pathway.

Keywords: Photofermentation, biohydrogen, Rhodobacter capsulatus, microarray, nitrogen source, carbon source

ÖZ

RHODOBACTER CAPSULATUS'UN HİDROJEN ÜRETİMİ, KARBON ASİMİLASYONU, VE AZOT METABOLİZMASINA FİZYOLOJİK VE MİKRODİZİN ANALİZLERİ İLE GLOBAL BİR YAKLAŞIM

Afşar, Nilüfer

Doktora., Biyolojik Bilimler Departmanı

Tez Yöneticisi: Prof. Dr. Meral Yücel

Eylül 2012, 225 sayfa

Fotofermentasyon sürecinde hidrojen üretimini etkileyen en önemli parametrelerden biri karbon ve azot kaynaklarının türüdür. Bu nedenle bu araştırmada, farklı azot kaynaklarının (5mM amonyum klorür ve 2mM glutamat) ve asetat konsantrasyonlarının (40-80mM) *R. capsulatus*'un metabolizması üzerine etkisi incelenmiştir.

İlk olarak, farklı azot kaynakları ve asetat konsantrasyonlarında *R. capsulatus*'un büyüme, hidrojen üretimi ve substrat kullanım davranışlarını karşılaştırmak için fizyolojik deneyler yapılmıştır. Hidrojen üretimi, karbon asimilasyonu, azot metabolizması ve bunların denetim mekanizmalarının daha iyi anlaşılması için mikrodizin analizi yapılmıştır. Bu amaca yönelik olarak *R. capsulatus* için bir Affymetrix çipi tasarlanmış ve üretilmiştir. *R. capsulatus* bakterisinden miktar ve kalite olarak mikrodizin deneylerinde kullanılabilecek yeterlilikte RNA eldesi

sağlayan bir izolasyon prosedürü optimize edilmiştir. Mikrodizin deneylerinin ve *R. capsulatus* çipinin doğrulanması eş zamanlı kantitatif PZR analizi ile gerçekleştirilmiştir.

5mM amonyum klorür içeren besiyerinde 2mM glutamat içeren besiyerine göre; asetatın taşınması, asimilasyonu ve kullanımıyla ilişkili genlerin ifadesi anlamlı bir şekilde artmıştır. Diğer taraftan, nitrojenaz enzimini kodlayan genlerin ifadesi amonyum klorür içeren besiyerinde belirgin bir şekilde azalmıştır.

Asetat asimilasyonunda rol alan genlerin ifadesinde 80mm asetatta 40mm asetat ile karşılaştırıldığında anlamlı bir fark görülmemiştir. Ancak sitrik asit döngüsü, fotosentetik aparat, elektron taşıma ve Calvin döngüsü ile ilişkili genlerin ifadesi 80mM asetat içeren ortamda anlamlı ölçüde azalmıştır.

Mikrodizin veri analizi sonuçlarına bakıldığında, *Rhodobacter capsulatus*'un asetat asimilasyonunu iki farklı yolla glioksilat çevrimi ve / veya etilmalonil-KoA yolağı kullanılarak gerçekleştirebileceği ilk kez önerilmiştir.

Anahtar kelimeler: Fotofermentasyon, biyohidrojen, *Rhodobacter capsulatus*, mikrodizin, azot kaynağı, karbon kaynağı

To my mom and dad

ACKNOWLEDGEMENTS

I am thankful to all of the present and past Hydrogen Research Laboratory members Assoc. Prof. Dr. Yavuz Öztürk, Assist. Prof. Dr. Başar Uyar, Assist. Prof. Dr. Gökhan Kars, Assist. Prof. Dr. Kamal Elkahlout, Elif Boyacıoğlu Genç, Endam Özkan, Dominic Deo Androga, Efe Boran, Begüm Peksel, Gökçe Avcıoğlu, Burcu Özsoy and Gülşah Pekgöz for their help, friendship and the great atmosphere they create.

I am thankful to my precious best friends Buket Başmanav, Çiğdem Koşe and Melis Akman for their love and moral support. I am very lucky to have you in my life. I would also like to thank to a very special person, Ozan Erkal for his existence and never ending support.

Finally, I am expressing my deepest love and appreciation to my mom Nesrin Afşar, to my dad İbrahim Afşar and to the rest of my family for their never ending patience, care and love. They have always believed in me and supported me.

TABLE OF CONTENTS

LIST OF TABLES

xviii

LIST OF FIGURES

LIST OF ABBREVIATIONS

A	Irradiated area (m2)
Acetyl-CoA	Acetyl coenzyme A
ADP	Adenosine di-phosphate
ADP	Adenosine di-Phosphate
ATP	Adenosine tri-phosphate
B. subtilis	Bacillus subtilis
bch	Bacteriochlorophyll
BP	Biebl Pfenning
bp	Base pair
cDNA	Complementary DNA
crt	Carotenoids
Cyt	Cytochrome
DFE	Dark fermenter effluent
DMSO	Dimethyl sulfoxide
Dnase	Deoxyribonuclease
E.coli	Escherichia coli
Fd	Ferredoxin
Fe	Iron
GC	Gas chromatography
GCOS	GeneChip® Operating Software
gdw	Gram dry weight
HPLC	High performance liquid chromatography
hup$^-$	Uptake hydrogenase deficient
LHI and LHII	Light harvesting I and II complexes, respectively
Light intensity	W/m2
Mg	Magnesium

mM	millimolar
mmol	Millimole
Mo	Molybdenum
mRNA	Messenger RNA
NAD	Nicotinamide adenine dinucleotide
Nif	Nitrogen fixation
OD	Optical density
ORF	Open reading frame
PCR	Polymerase chain reaction
PHB	Poly-β-hydroxy butyric acid
PNS	Purple non-sulfur
PS	Photosystem
R. capsulatus	*Rhodobacter capsulatus*
R. palustris	*Rhodopseudomonas palustris*
R. sphaeroides	*Rhodobacter sphaeroides*
R.rubrum	*Rhodospirillum rubrum*
RC	Reaction center
RNA	Ribonucleic acid
rRNA	Ribosomal RNA
RT-PCR	Real time quantitative PCR
t	Time (hour)
TCA	Tricarboxylic acid
TE	Tris ethylene diamine tetra-acetic acid
TMAO	Nitrous oxide trimethyl-amine-N-oxide
tRNA	Transfer RNA
UV	Ultraviolet
V	Volume (ml or L)

CHAPTER 1

INTRODUCTION

Growing human population is increasing the world's energy demand every day. The energy consumption rate is expected to rise by 44% by 2030 (McKinlay and Harwood, 2010). Today, 80% of global energy demand is met by fossil fuels (oil, coal and gas). Due to the fact that, the rate of fossil fuel consumption is higher than the rate of the fossil fuel production by the nature (Jain, 2009), fossil fuel reserves will be depleted. Ediger et al. (2006) estimated in their model that the fossil fuel production peak has already been reached in Turkey and the total fossil fuel production will come to an end by 2038. Another problem with fossil fuels is that their combustion contributes to emission of pollutants such as CO_2 and cause global climate change (Das and Veziroğlu, 2001). International Energy Agency (IEA) reported that energy-related CO_2 emissions will increase by 20% between 2010 and 2035 which will give rise to a long-term rise in the average global temperature in excess of 3.5°C. In order to reduce energy-related CO_2 emissions it is needed to increase usage of renewable alternative recourses (World Energy Outlook 2011 Fact Sheet). Hydrogen is seen as a good alternative to fossil fuels since its combustion with oxygen gives only water as by product and does not result in air pollution (Das and Veziroğlu, 2008).

1.1 Hydrogen Production from Biomass

Heat of combustion of hydrogen is compared to various fuels in Table 1.1. It is seen that combustion of hydrogen gives the highest amount of energy per unit mass.

Table 1. 1 Heat of combustion of various fuels (Jain, 2009)

Fuel	Energy (Kcal/g)
Hydrogen	34.0
Petroleum	10.3—8.4
Paraffin	10.3—9.8
Graphite (Coal)	7.8
Castor oil	9.4
Wood	4.2

Hydrogen can be generated from natural gas by steam reforming, coal gasification and water electrolysis. However, these conventional routes still utilize non-renewable energy sources and for that reason they are not sustainable. On the other hand, hydrogen production from biomass can provide sustainable and renewable energy. There are two main strategies for the production of hydrogen from biomass which include (Manish and Banerjee, 2008):

(1) Thermochemical processes such as pyrolysis and gasification

(2) Nonthermal biological processes using microorganism

Biological hydrogen production processes by using microorganisms has several advantages over other hydrogen production methods (Basak and Das, 2007; Redwood et al., 2009):

(1) They are environmentally friendly

(2) They utilize renewable energy resources such as agricultural wastes

(3) They can be operated under mild operating conditions at ambient temperature and atmospheric pressure. For this reason, they are less energy intensive.

1.2 Biological Hydrogen Production Processes

Microorganisms belonging to significantly different taxonomic and physiological groups can produce biohydrogen. All biological hydrogen production processes are dependent on the presence of a hydrogen producing enzyme such as hydrogenase or nitrogenase (Kotay and Das, 2008). Biological hydrogen production by use of microorganisms can be grouped into four major categories (Das et. al., 2008):

1. Biophotolysis of water by algae (direct biophotolysis) and cyanobacteria (indirect photolysis)

2. Dark fermentation by fermentative bacteria

3. Photofermentation by photosynthetic bacteria

4. Integrated systems using dark fermentative and photosynthetic bacteria
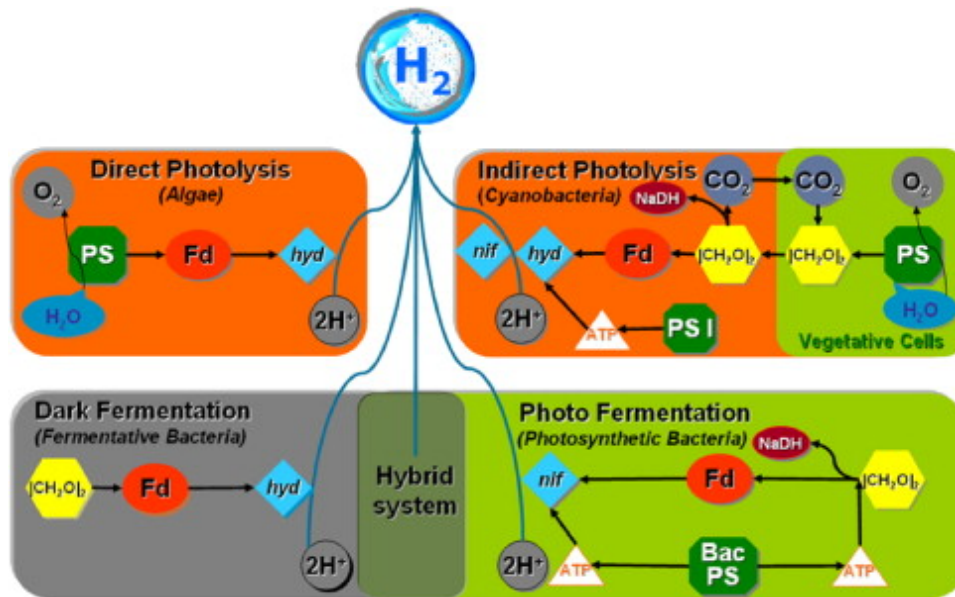
Figure 1. 1 Biological hydrogen production processes using microorganisms (Kotay and Das, 2008)

1.2.1. Biophotolysis

Biophotolysis is the biological splitting of water into hydrogen and oxygen. This type of biological hydrogen production can be performed by some green algae via direct biophotolysis and some cyanobacteria via indirect biophotolysis.

Green algae can produce biological hydrogen via direct biophotolysis. In this process, light energy captured by photosystem II (PSII) apparatus produces electrons. Electrons are then carried to ferredoxin using the light energy captured by photosystem I (PSI). Finally, a reversible hydrogenase captures electrons from the reduced ferredoxin and produces H_2 (Figure 1.2) according to the following general reaction (Das and Veziroğlu, 2008).

$2H_2O + light\ energy \rightarrow 2H_2 + O_2$ (1.1)
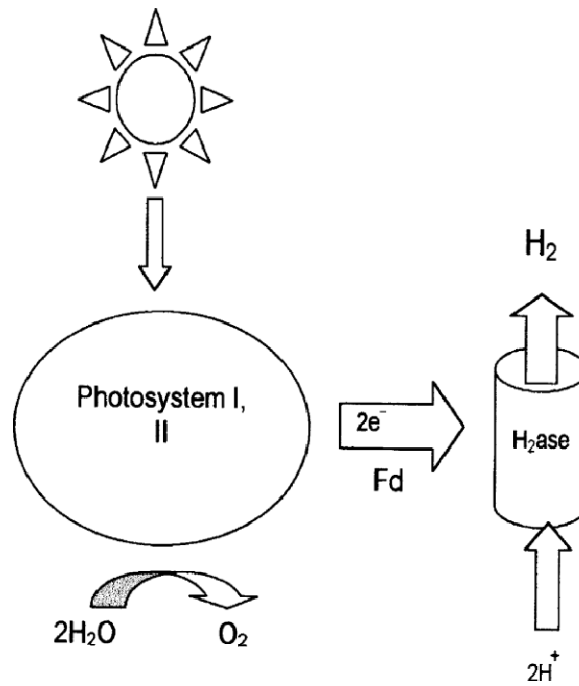
Figure 1. 2 Direct photolysis by green algae (Hallenbeck and Benemann, 2002)

Biohydrogen production via direct biophotolysis is attractive since it generates hydrogen directly from water which is an abundant and easily obtainable substrate (Hallenbeck et al., 2009). On the other hand, O_2 generated as a byproduct of the function of PS2, is a powerful inhibitor of all H_2-related reactions including gene expression, mRNA stability and enzymatic catalysis. For that reason, direct biophotolysis can operate only for short periods of time (a few min), before the accumulated O_2 inhibits the H_2 production process (Eroğlu and Melis, 2011).

Cyanobacteria can evolve biological hydrogen via indirect photolysis. In indirect biophotolysis, the problem of inhibition of H_2 production processes by O_2 is solved since oxygen generation and hydrogen production reactions occur in separate stages (Figure 1.3). In the first stage, CO_2 is fixed from air and energy-rich organic compounds are synthesized. In the second stage, the organic compounds are then used by hydrogenases for biological hydrogen production (Hallenbeck and Benemann, 2002).

The biochemical equations of indirect biophotolysis are shown in the equation below (Das et al., 2008):

$$12H_2O + 6CO_2 \rightarrow C_6H_{12}O6 + 6O_2 \qquad (1.2)$$

$$C_6H_{12}O_6 + 12H_2O \rightarrow 12H_2 + 6CO_2 \qquad (1.3)$$
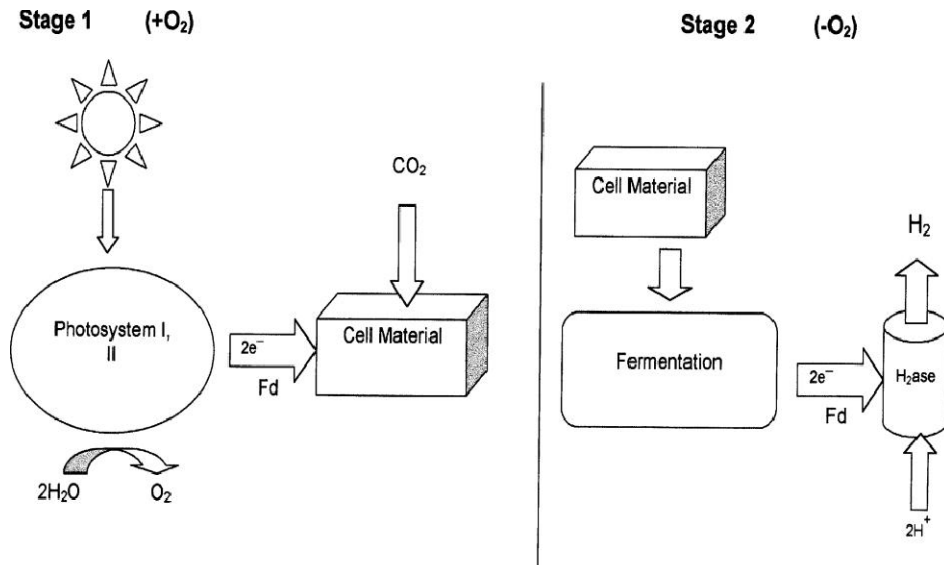
Figure 1. 3 Indirect photolysis (Hallenbeck and Benemann, 2002)

In addition to the capacity to fix CO_2 via photosynthesis, some cyanobacteria also have the ability to fix atmospheric nitrogen via nitrogenase enzyme. In these microorganisms, the heterocysts are differentiated to promote an O_2 free environment for nitrogenase enzyme for generation of H_2 (Das et al., 2008; Eroğlu and Melis, 2011). Disadvantages of biological hydrogen production via indirect biophotolysis are: lower photochemical efficiency and presence of uptake hydrogenase enzymes that consume H_2 (Nath and Das, 2004).

1.2.2 Dark Fermentation

Dark fermentation is an anaerobic process and takes place only in the absence of oxygen (Das and Veziroglu, 2008). A variety of fermentative bacteria can be used to decompose carbohydrate rich substrates to hydrogen, organic acids (acetic, lactic, butyric etc.) and alcohols (ethanol, buthanol, etc.) (Hallenbeck and Ghosh, 2009). These bacteria do not use the energy of the sun for H_2 production. Instead, they depend on the catabolism of organic substrates, which must be present in the growth medium (Melis and Melnicki, 2006). Dark fermentation reactions can take place at mesophilic (25-40°C), thermophilic (40-65°C), extreme thermophilic (65-80°C) or hyperthermophilic temperatures (>80°C) (Levin et al., 2004).

Hydrogenase enzyme is responsible for hydrogen production in anaerobic dark fermentation. Pyruvate is the key intermediate in all fermentation pathways leading to hydrogen production from the glycolytic breakdown of carbohydrate-derived sugars (Figure 1.4). Product distribution and type of the hydrogenase enzyme used can differ according to the type of microorganism, oxidation state of the substrate and environmental conditions such as pH and hydrogen partial pressure (Hallenbeck and Ghosh, 2008; Hallenbeck, 2009).

There are some advantages of biological hydrogen production via dark fermentation such as:
(1) No direct solar input is required and H_2 can be produced during whole day
(2) A variety of wastes and energy crops can be used as substrate
(3) It requires a simple reactor technology.

7

On the other hand, biological hydrogen production via dark fermentation route also has some disadvantages such as:

(1) Low hydrogen yields (Nath and Das, 2004; Hallenbeck and Ghosh, 2009).

(2) Low substrate conversion efficiencies (Das et al., 2008).
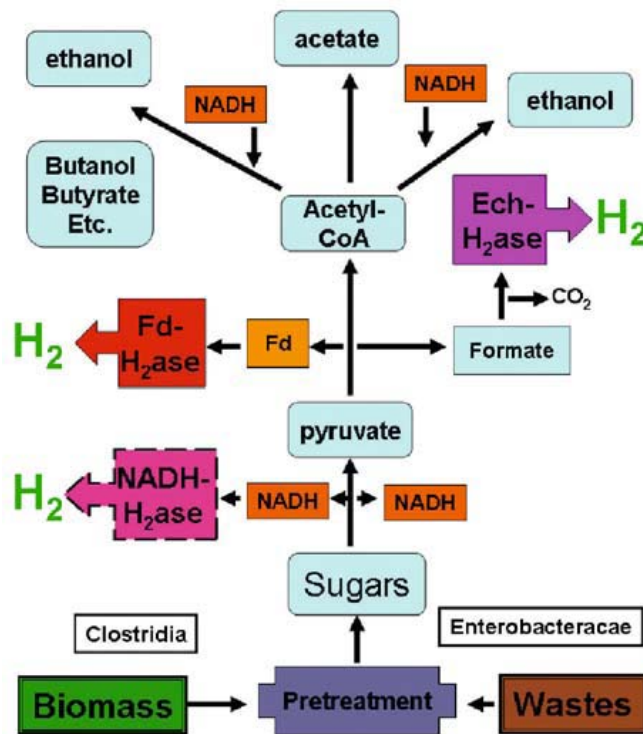
Figure 1. 4 Dark fermentation by fermentative bacteria (Hallenbeck et al., 2009)

1.2.3. Photofermentation

Purple non sulfur bacteria (PNS) can produce biological hydrogen via photofermentation. It takes place under illumination, ammonium limited and oxygen free conditions. Nitrogenase is the key enzyme responsible for hydrogen production. In this process, photosynthetic apparatus of anoxygenic phototrophs absorbs sunlight and performs electron transport to generate a proton motive force

which is required for ATP synthesis. ATP and electrons are then utilized by nitrogenase enzyme for hydrogen production (Figure 1.5). PNS bacteria obtain electrons from utilization of organic compounds (usually small organic acids) as substrate (Hallenbech and Ghosh, 2009; Eroğlu and Melis, 2011).

The biochemical reaction for photofermentation is as follows (Das et al., 2008):

$$CH_3COOH + 2H_2O + \text{light energy} \rightarrow 4H_2 + 2CO_2 \qquad (1.4)$$
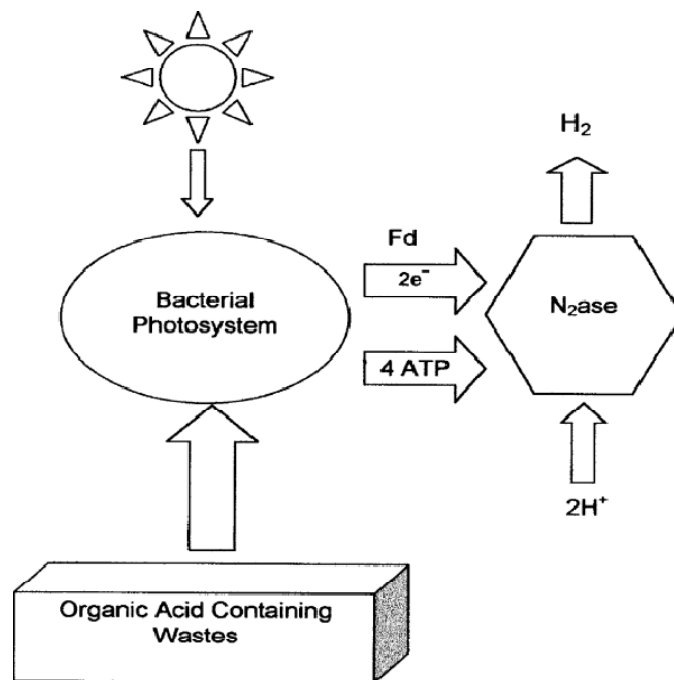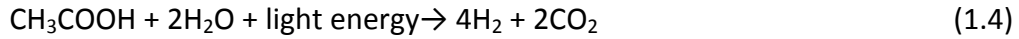
Figure 1. 5 Photofermentation by PNS bacteria (Hallenbeck and Benemann, 2002).

Among the biological hydrogen production mechanisms, photofermentation by using PNS bacteria offer some advantages over other biological hydrogen production routes (Kars and Gündüz, 2010; Basak and Das, 2007; Eroglu and Melis, 2011):

(1) Substrate to product conversion efficiency is high.

(2) O_2 which is a repressor for biological hydrogen systems is not generated.

(3) PNS bacteria can utilize a wide wavelength of light. They can absorb and use both the visible (400–700 nm) and near infrared (700–950 nm) regions of the solar spectrum

(4) PNS bacteria can utilize a wide variety of organic substrates such as organic acids, sugars, fatty acids or waste products of factories. Therefore, they have a potential application in waste treatment processes.

The drawbacks of photofermentative biological hydrogen production by PNS bacteria are: low light conversion efficiencies, high energy demand by nitrogenase; requirement of expensive hydrogen impermeable photobioreactors

1.2.4. Integrated Systems

Integration of photo-fermentation and dark-fermentation is a promising way for the enhancement of overall H_2 production yields when compared to single stage dark-fermentation or photo-fermentation processes. In the first stage of the system, anaerobic dark fermentative bacteria convert carbohydrate containing substrate to hydrogen, CO_2 and low molecular weight organic acids. In the second stage, the effluents of dark fermentation containing organic acids (such as acetate and lactate) are fed to the photobioreactors. Finally, PNS bacteria perform photofermentation and utilize the end products of dark fermentation for further hydrogen production (Redwood et al., 2009; Das et al., 2008).

When glucose is the sole substrate in dark fermentation and acetate is the main product, a theoretical maximum yield of 12 mol H_2/mol glucose could be expected to be produced in an integrated dark and photo fermentation system. The biochemical reactions of the system are as follows (Kotay and Das, 2007):

Stage 1: Dark fermentation of 1 mole of glucose yields 4 moles of and 2 moles of acetate:

$$C_6H_{12}O_6 + 2H_2O \rightarrow 4 H_2 + 2CH_3COOH + 2 CO_2 \qquad\qquad (1.5)$$
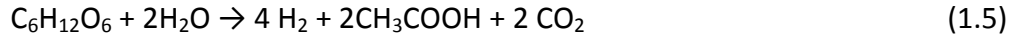
Stage 2: Photofermentation of 2 moles of acetate coming from dark fermentation yields additional 8 moles of H_2

$$2CH_3COOH + 4H_2O + \text{"light energy"} \rightarrow 8H_2 + 4CO_2 \qquad\qquad (1.6)$$
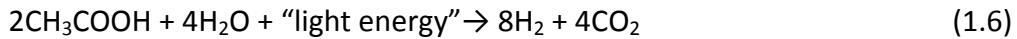
In an EU 6th framework project HYVOLUTION, integration of dark fermentation and photofermentation approach has been adapted to achieve a cost effective biological hydrogen production from biomass, ranging from energy crops to bio-residues from agro-industries (Claassen and Vrije, 2006). During this project, various feedstocks like sugar beet molasses miscanthus (Uyar et al., 2009), (Özgür et al., 2010), potato steam peel (Afsar et al., 2011), sugar beet thick juice (Özkan et. al., 2011) were used as substrates in integrated dark and photofermentation processes.

1.3 Parameters Affecting Photofermentation

There are some parameters that affect photofermentation procesess such as: pH, temperature, light intensity, molecular oxygen and type and concentration of carbon and nitrogen sources.

It is known that optimum temperature for biohydrogen production by PNS bacteria is in between 30–35°C (Sasikala et al., 1993) and 30 °C is found to be the preferred temperature for hydrogen production of *R. capsulatus* (Sevinç et al., 2012).

The optimum pH interval for hydrogen production is in between 6.5 and 7.5. It is known that the hydrogen yield and efficiency decreases below or above these values (Sasikala et al., 1993).

PNS bacteria require light for hydrogen production and it is known that the light intensity applied to the photobioreactors directly affects biological hydrogen yield. A previous study with *R. sphaeroides* has shown that hydrogen production increases as the light intensity increases. However, a further increase in light intensity after 270 W/m^2 does not have an influence on hydrogen production of PNS bacteria (Uyar et al., 2007).

Molecular oxygen can inhibit biological nitrogen fixation both at the transcriptional level by repressing the nitrogenase synthesis and at the post tranlational level by switching off the nitrogenase activity (Goldberg et al., 1987).

Type and concentration of the carbon source significantly influence photofermentation processes. Previous studies showed that initial concentration of acetate has a significant influence on which metabolic pathway is taken by PNS bacteria for acetate consumption (Barbosa 2001; Nath et al.,2005; Özgür et al.,2009; Özsoy, 2012). A decrease in acetate concentration from 22 to 6 mM caused a decrease in hydrogen generation with *Rhodopseudomonas* species and higher acetate concentrations were suggested to increase hydrogen production (Barbosa et al., 2001). Highest hydrogen production was observed with *R. capsulatus* on 40mM acetate containing medium. On the other hand, a further increase in acetate concentration from 40mM to 50mM decreased hydrogen yields (Özgür et al., 2009).

Type and concentration of nitrogen source is another important parameter which affects photofermentation process. Biological hydrogen production is repressed or inhibited when ammonium is present in the medium (Koku et al., 2002). It was reported with *R. sphaeroides* that ammonium can totally inhibit hydrogen production when ammonium concentration is 3 mM or above (Akköse et al., 2009). Although glutamate is known to be the most efficient nitrogen source for hydrogen

production and high concentrations of glutamate also inhibit hydrogen production of PNS bacteria (Koku et al., 2002).

1.3. Purple Non Sulfur Bacteria

Purple bacteria are gram negative prokaryotes and widely found in nature in aquatic and terrestrial environments. Purple sulfur bacteria were initially told as "non sulfur" since it was believed that PNS bacteria lacked the ability to use hydrogen sulfide as electron donor when grown photoautotrophically. However, later studies showed that PNS bacteria can also oxidize hydrogen sulfide but at lower concentrations (less than 0.5 mM) compared to sulfur. Another difference in the sulfide metabolism of PNS bacteria and purple bacteria is that the S° produced by purple bacteria is stored intracellularly in sulfur globules (Figure 1.6a). On the other hand, If PNS bacteria oxidize sulfide, the S° produced remains outside the cell (Figure 1.6b). Utilization of sulfide by PNS bacteria has an environmental effect since; H_2S which is poisonous to many organisms can be converted into nontoxic forms of sulfur such as elemental sulfur (S°) and sulfate (SO_4^{2-}) (Madigan et al. 2009).

a   b
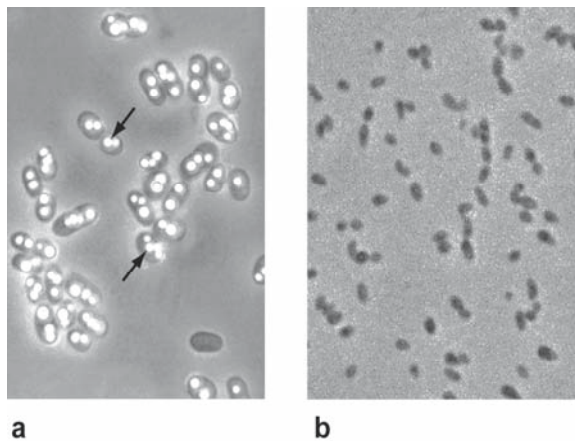
Figure 1.6 Phase photomicrographs of phototrophic purple bacteria. (a) Cells of a strain of the purple sulfur bacterium *Thermochromatium tepidum* (1.5 µm wide). *B*right refractile intracellular sulfur globules are shown with arrows. (b) Cells of

13

Rhodobaca bogoriensis, a purple nonsulfur bacterium (0.8 μm wide) (Madigan et al. 2009)

Classification of purple bacteria on the basis of 16SrNA sequencing have demonstrated that purple sulfur bacteria are species of gamma proteobacteria while PNS bacteria are either alpha- or beta proteobacteria (Imhoff , 2006). Twenty genera of PNS bacteria have been identified and all of them are gram negative proteobacteria. The most widely used species in laboratory studies belong to the genera of *Rhodobacter* and *Rhodopseudomonas* (Madigan et al. 2009)*.* Cell suspensions appear in different colors from beige, olive-green, peach brown, brown, brown-red, red or pink due to the presence of photosynthetic pigments (Imhoff, 2006).

1.3.1 *Rhodobacter capsulatus*

Rhodobacter capsulatus is known to be the most metabolically diverse and flexible species in bacteria world. It is capable of photosynthesis, aerobic respiration, anaerobic respiration and fermentation. The different growth modes of *R. capsulatus* are given in Table 1.2. Like other PNS bacteria *R. capsulatus* takes role in the anoxic cycling of carbon both as primary producers via CO_2 fixation (photoautotrophy) and as light-stimulated consumers via reduction of organic compounds (photoheterotrophy). Photosynthetic pigments (bacteriochlorophyll and carotenoids) are located in the cytoplasmic membrane and internal membrane systems which are vesicles, lamellae or membrane stacks. They grow phototrophically under oxygen free conditions in the presence of light. Photosynthetic pigment synthesis and internal membrane formation are inhibited by oxygen. The preferred mode of growth is photoheterotrophy since growth is best in media that contain readily useable organic compounds (Imhoff, 2006; Madigan et al., 2009; Koku, 2002).

14

Table 1. 2 The different growth modes of R. capsulatus

Mode of Growth	Carbon Source	Electron Source	Notes:
Photoheterotrophy	Organic carbon	Organic carbon	Good growth, H_2 production (under anaerobic conditions, in the absence of ammonia)
Photoautotrophy	CO_2	H_2	In the absence of organic carbon. H_2 is consumed.
Aerobic respiration (chemoheterotrophy)	Organic carbon	Organic carbon	In the presence of O_2. Stops H_2 production.
Anaerobic respiration (chemoheterotrophy)	Organic carbon	Organic carbon	Under anaerobic, low light conditions. Requires a terminal electron acceptor other than O_2 such as nitrate, DMSO or TMAO. No H_2 production. Marginal growth.
Fermentation	Organic carbon	Organic carbon	Under anaerobic-dark conditions. No H_2 production. Poor growth.

1.3.1.1. Photoheterotrophic Metabolism

R. capsulatus is seen as one of the most promising biological hydrogen producers in large scale photofermentation applications. It has the ability to generate biohydrogen during photoheterotrophic growth on organic acids or sugars under nitrogen limited conditions (Basak and Das, 2007). *R. capsulatus* can use atmospheric N_2 as the sole nitrogen source via nitrogen fixation. Nitrogenase enzyme catalyzes reduction and assimilation of atmospheric N_2 to ammonia. H_2 is produced as a byproduct in small amount during this reaction. However, in the absence of N_2, nitrogenase acts as an ATP-powered hydrogenase and exclusively generates hydrogen (McKinlay and Harwood, 2010).

The photoheterotrophic metabolism of PNS bacterium is summarized in Figure 1.7. Under photoheterotrophic growth conditions, TCA cycle and photosynthetic apparatus work in parallel. The carbon substrate is fed into the TCA cycle where it is oxidized to produce CO_2 and electrons. Photosynthetic apparatus capture solar energy to produce a cyclic electron flow. As a result, a proton gradient is generated and utilized by ATP synthase to make ATP, by NADH dehydrogenase reverse activity, and by the Rnf complex to reduce ferredoxin. Succinate dehydrogenase feeds electrons to the ubiquinol pool. Photoheterotrophic conditions can cause over-reduction of the photosynthetic electron transport. The excess electrons (derived from the TCA cycle or reverse NADH dehydrogenase activity) need to be removed. They can be dissipated via evolution of hydrogen, fixation of carbon dioxide in the Calvin cycle or PHB synthesis. During exponential growth, the Calvin cycle utilizes most of the excess electrons via reduction of carbon dioxide into biosynthetic intermediates. Only small portion of electrons generated from organic substrate oxidation is utilized for hydrogen production. However, in the stationary phase, biosynthesis almost stops and majority of organic carbon is oxidized into carbon dioxide and most of the electrons are directed toward hydrogen production (Golomysova et al., 2010; Koku et al.,2002)

1.3.1.2. Photosynthetic Membrane Apparatus

The photosynthetic membrane apparatus of purple non sulfur bacteria is composed of the photosynthetic reaction center and light harvesting complexes. Pigments are non-covalently bound to proteins of these complexes. Bacteriochlorophyll (bch) is
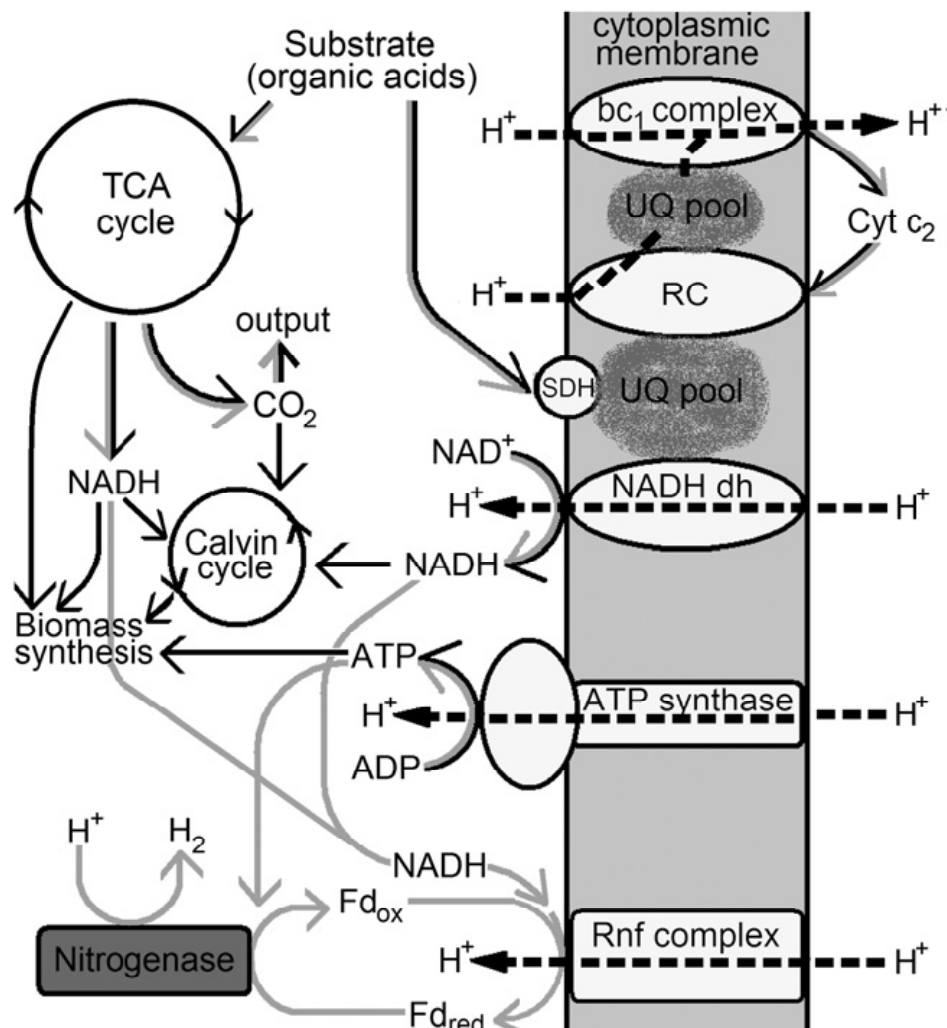
Figure 1.7 Photoheterotrophic metabolism of PNS bacteria. Black arrows represent key flows for growth and grey arrows represent key flows for hydrogen production. UQ: ubiquinone, H^+: protons, RC: photosynthetic reaction center, SDH: succinate dehydrogenase, NADH dh: NADHde hydrogenase, Fd: ferredoxin, Rnf (Rhodobacter nitrogen fixation) complex: ferredoxin:NAD(D) oxidoreductase (Golomysova et al., 2010).

the main light harvesting pigment which absorbs light in the far-red region in between 800-875nm. Carotenoids (crt) are accessory pigments. In addition to light harvesting they are also involved in photoprotection and structure stabilization. They absorb green light at 450 nm and 550nm. Using these pigments, PNS bacteria can grow photosynthetically by using the far-red and green light that has not been filtered out by the organisms that contain Chlorophyll a that strongly absorbs red

light in between 680-700nm. The harvesting of light is performed by two integral membrane pigment protein complexes termed as LH2 (encoded by puc operon) and LH1 (encoded by pufB and pufA). They function to absorb solar energy and to transfer that energy to the photosynthetic reaction centers (RC). Photosynthetic reaction centers are membrane spanning complexes of polypeptide chains and cofactors that catalyze the first steps in the conversion of light energy to chemical energy during photosynthesis. Purple non sulfur bacterial reaction center consists of three protein subunits: L (light subunit encoded by pufL), M (medium subunit encoded by pufM) and H (heavy subunit encoded by puhA). The prosthetic groups are bound to the L and M subunits. These are two BChls (special pair), two accessory BChls in close proximity to the special pair, two bacteriopheophytins (BChl lacking the central Mg^{+2}), and a pair of quinones (QA, QB), a non heme iron and a carotenoid. Light energy is absorbed by the LH2, transferred to the LH1, and then trapped by the RC. In the RC, the special pair Bchl a molecules is oxidized and electron flow occurs across the photosynthetic membrane to a primary electron acceptor, ubiquinone, which is reduced. Subsequently, the electron is transferred to the secondary electron acceptor. A second RC turnover results in the full reduction of UQB - to $UQBH_2$. The reduced ubiquinone leaves the RC and transfers its electron to the cytochrome bc1 complex and replaced by an oxidized ubiquinone (Q). Electrons are transferred from cytochrome bc1 back to the RC by cytochrome c. Protons are pumped across the membrane by cytochrome bc1 and an electrochemical gradient that drives ATP synthesis via the ATP synthase is generated (Law et al., 2004; Hu et al.,2002). The photosynthetic membrane apparatus is illustrated in Figure 1.8 and the structure of ATP synthase is given in Figure 1.9.
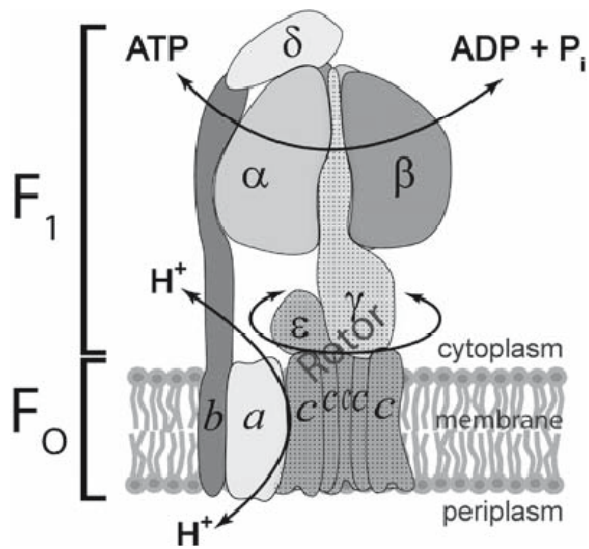
Figure 1. 8 ATP synthase componants (Feniouk, 2009).
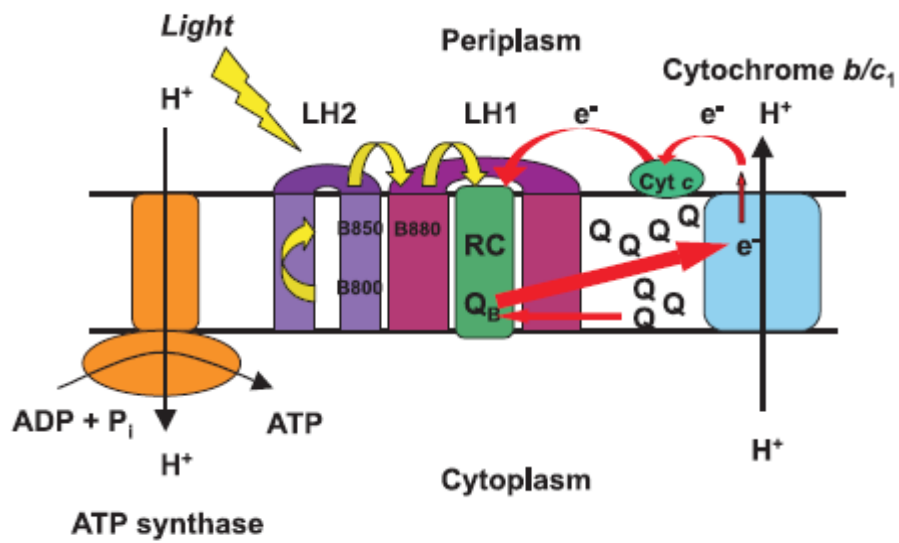
Figure 1. 9 Photosynthetic apparatus (Law et al., 2004)

1.3.1.3. Electron Transport

In *Rhodobacter capsulatus* there are three main types of electron transport chains. These are cyclic photosynthetic chain, aerobic respiratory chain and anaerobic respiratory chains. During transport of electrons through carriers, protons are pumped from the cytoplasm to the periplasm which results in the formation of a proton gradient used for ATP generation (Zannoni, 1995).

Under photoheterotrophic conditions, *R. capsulatus* performs anoxygenic photosynthesis by the cyclic electron transfer between the reaction center and the cytochrome bc1 complex via the lipid soluble ubiquinone pool and the electron carriers. R. capsulatus electron carriers are soluble cytochrome c_2 (cyt c_2) or membrane-bound cytochrome c_y (cyt c_y). Under aerobic conditions photosynthetic activity is avoided and *R. capsulatus* carries out aerobic respiration. Aerobic respiratory electron transfer possesses two different terminal oxidases, the cytochrome cbb_3 oxidase and the quinol oxidase. Electrons can be transferred from cyt bc_1 complex to cyt cbb_3 oxidase via quinol pool and cytochrome c carriers (cyt c_2 and cyt c_y) or directly from cyt bc_1 complex to terminal electron acceptor O_2 (Figure 1.10). Cyt bc_1 complex (ubihydroquinone: cytochrome c oxidoreductase) is a multisubunit integral membrane protein and consists of three metal containing subunits, Cyt b, Cyt c_1 and the 'Rieske' iron sulfur protein. The structural genes encoding these three structural subunits are pet A, B and C (Gray, K. A. and Daldal, F., 1995). Under anaerobic conditions *R. capsulatus* can perform anaerobic respiration and electrons are transported from ubiquinol to terminal acceptors other than oxygen via nitrate, nitrite, nitric oxide and nitrous oxide trimethyl-amine-N-oxide (TMAO), dimethyl sulfoxide (DMSO) reductases (Zannoni, 1995).
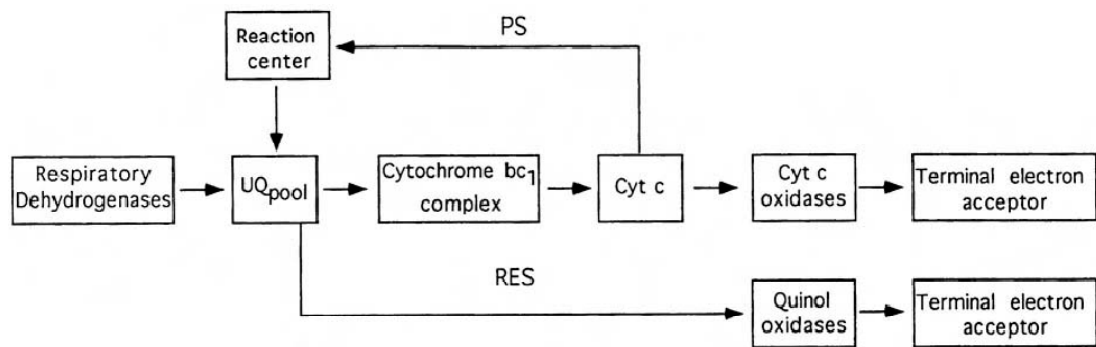
Figure 1. 10 Photosynthetic and aerobic respiratory electron transport chains of *R. capsulatus* (Gray and Daldal, 1995)

1.3.1.4. Metabolic Routes for Organic Carbon Metabolism

PNS bacteria can utilize a variety of different sugars (glucose, fructose) and organic acids (acetate, lactate, malate) during photoheterotrophic growth mode. An overall central carbon metabolism is summarized in Figure 1.11 (Tabita, 1995). Acetate is the main by-product of dark fermentation of fermentative bacteria. For this reason, it has been a desired substrate for growth and hydrogen production of PNS bacteria for photofermentation. Being a central intermediate of the carbon metabolism, acetate can be utilized through different metabolic routes, including polyhydroxybutyrate (PHB) synthesis for storage purposes, or a tricarboxylic acid (TCA) cycle for energy purposes and biomass accumulation.

Figure 1. 11 Metabolic routes for Organic Carbon Metabolism (Tabita, 1995).

1.3.1.4.1. Acetate Assimilation Pathways

Acetate like many other compounds (fatty acids, alcohols or polyhdroxyalkanoates) enter central carbon metabolism at the level of acetyl-CoA (Meister et al., 2005) (Figure 1.12). Conversion of acetate into acetyl-CoA is catalyzed by the enzyme,

acetate co-A ligase which is also known as acetyl-CoA synthetase. This enzyme is present in both prokaryotes and eukaryotes, and generates acetyl-CoA from acetate, coenzyme A (CoA) and ATP. The chemical reaction which is catalyzed by acetate co-A ligase is given below.

ATP + acetate + CoA $\leftrightarrow$ ADP + phosphate + acetyl-CoA $\hspace{2cm}$ (1.7)
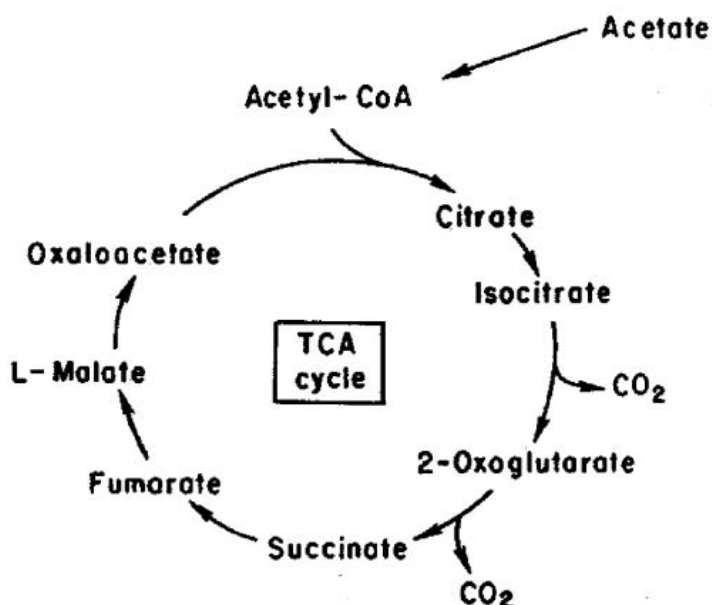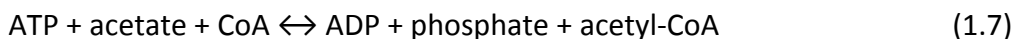
Figure 1. 12 Acetate entry to TCA cycle

Many of the C_4 acids in the TCA cycle are utilized for biosynthesis of cellular building blocks. Growth of bacteria on C_2 compound acetate is only possible only when the intermediates of the TCA cycle are replenished. In PNS bacteria, acetate assimilation can occur via three different metabolic routes which are glyoxylate cycle, ethlymalonyl-CoA pathway and citramalate cycle. In all approaches, the aim is to convert acetyl-CoA into malate so that TCA cycle intermediates can be replenished for the biosynthesis of the cellular blocks (Tang et al., 2011).

The two unique enzymes of the glyoxylate cycle are isocitrate lyase and malate synthase. The cycle starts when acetyl-CoA enters the TCA cycle via condensation of oxaloacetate to citrate by the action of citrate synthase. Isocitrate lyase then cleaves isocitrate to succinate and glyoxylate, and finally malate synthase condenses glyoxylate and acetyl-CoA to generate malate and CoA. With the action of other TCA cycle enzymes, the net fixation of two molecules of acetyl-CoA to one molecule of malate is obtained (Figure 1.13) (Erb et al., 2010). Among the PNS bacteria, *Rhodopseudomonas palustris* uses glyoxylate cycle for acetate assimilation (Laguna et al., 2011).
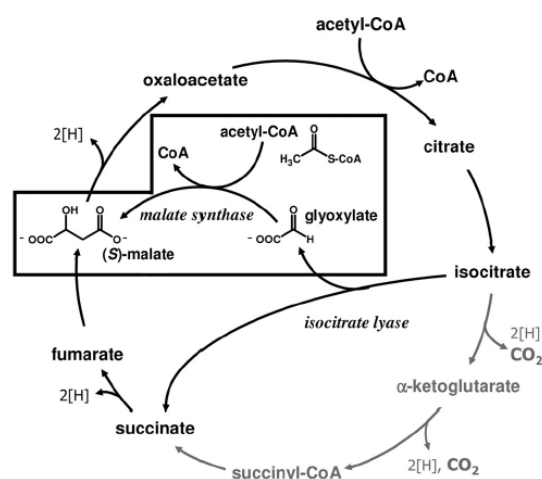
Figure 1. 13 Glyoxylate cycle (Erb et al., 2010)

There are also organisms which lacked isocitrate lyase gene and activity such as *Rhodobacter sphaeroides and Rhodospirillum rubrum* (Berg and Ivanovsky, 2009). In these bacteria, an alternative isocitrate independent acetate assimilation strategy has been evolved. Ethlymalonyl-CoA pathway forms malate from acetyl-CoA and glyoxylate, but this reaction is not direct and takes place with the action of two separate enzymes which are L-malyl-CoA/β-methylmalyl-CoA lyase and malyl-CoA thioesterase (Erb et al., 2010). The intermediates and enzymes of the ethlymalonyl-CoA pathway are given in the Figure 1.14.

24
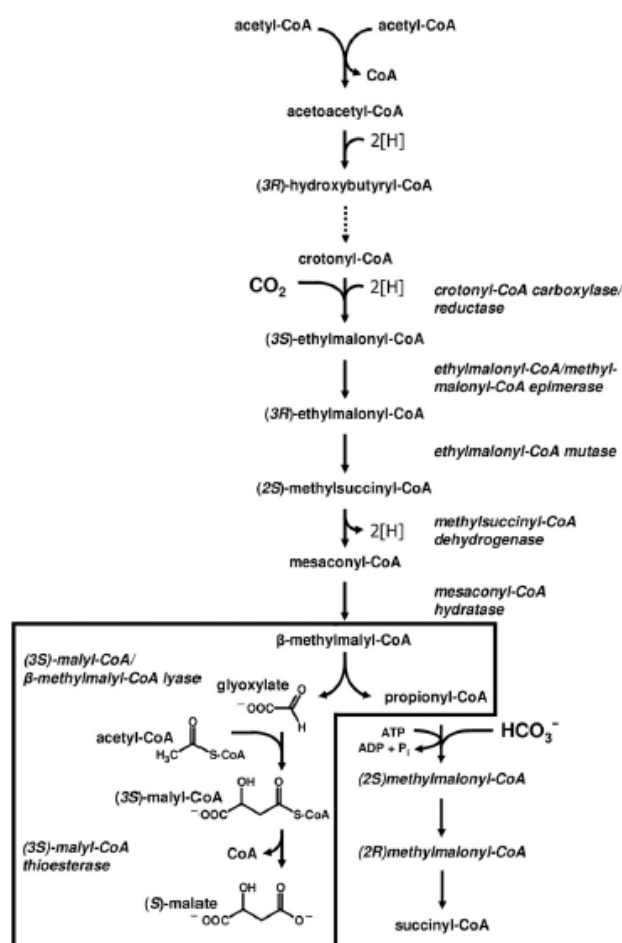
Figure 1. 14 Ethlymalonyl-CoA pathway (Erb et al., 2010)

Another alternative to glyoxylate cycle for acetate assimilation in isocitrate lyase negative PNS bacteria is proposed for *Rhodospirillum rubrum*. This route is called as citramalate cycle (Ivanovsky et al., 1997). Main reactions of the proposed citramalate cycle are shown in Figure 1.15. Another study later showed the coexistance of activity of citramalate cycle enzymes and a unique ethylmalonyl-CoA pathway enzyme (crotonyl-CoA reductase) together and suggested that this bacterium is capable of using both citramale cycle and ethylmalonyl pathway depending on the growth conditions (Berg and Ivanovsky, 2009).
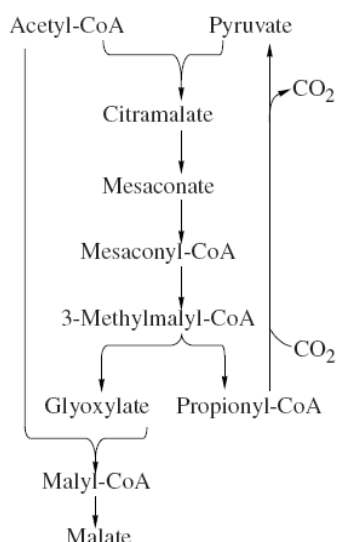
Figure 1. 15 Citramalate cycle (Berg and Ivanovsky, 2009)

R. capsulatus possesses the structural genes for glyoxylate cycle (isocitrate lyase and malate synthase), ethylmalonyl-CoA pathway and citramalate pathway. It was obseved that literature data on the activity of isocitrate enzyme of *R. capsulatus* are open to discussion. It is known that isocitrate lyase activity can differ when different strains used (Tabita, 1995) and even with the same strain of *R. capsulatus* different results can be obtained by different observers (Petushkova and Tsyganov, 2011). Meister et al. (2005) showed that *R. capsulatus* lacked isocitrate activity and synthesis of malate from glyoxylate was due to activity of L-malyl-CoA/β-methylmalyl-CoA lyase and rather than malate synthase. Based on these results, it was proposed that *R. capsulatus* operates an alternative pathway for acetate assimilation. They suggested that β-methylmalyl-CoA was an intermediate in the unknown acetate assimilation pathway and citramalate might be the source. Later studies showed that β-methylmalyl-CoA is also an intermediate of ethylmalonyl-CoA pathway pathway and can be produced from mesaconyl-CoA by the ethylmalonyl-CoA pathway enzyme mesaconyl-CoA hydratase (Zarzycki et al., 2008; Alber et al., 2006) and no other detailed study has been conducted related to acetate metabolism of this bacterium.

1.3.1.5. Nitrogen Fixation and Hydrogen Production

Rhodobacter capsulatus can fix atmospheric nitrogen by catalysis of an enzyme called nitrogenase. The genes required for nitrogen fixation are commonly called *nif* genes. *R. capsulatus* possesses a molybdenum-dependent nitrogenase (Mo-nitrogenase) consist of two dissociable two components. The smaller dinotrogenase reductase component is known as Fe protein (encoded by nifH) and functions as an ATP-dependent electron donor to the larger dinitrogenase component which is known as the MoFe protein (encoded by nifDK). The dinitrogenase component contains two types of metal clusters, the M-cluster (FeMo cofactor), which represents the site of substrate reduction, and the P-cluster that transfer electrons and protons to the FeMo cofactor. The enzyme mechanism involves reduction of the Fe protein by electron donors such as ferredoxin, transfer of single electrons from the Fe protein to the MoFe protein (which requires MgATP hydrolysis) and, finally, an internal electron transfer by the P cluster to the FeMo cofactor substrate-binding site. In addition to Mo-nitrogenase, *R. capsulatus* also contains an iron-only nitrogenase (Fe-nitrogenase), which does not contain any heterometal in its active center (FeFe-cofactor). Genes specific for Fe nitrogenase are encoded by *anf* for (alternative nitrogen fixation) genes (Dixon and Kahn, 2004; Rubio and Ludden, 2008).

All nitrogenases reduce N_2 to NH_3 with the obligate production of molecular hydrogen as side product as seen in the reaction below:

$$N_2 + 8H+ + 8e- + 16\ ATP \leftrightarrow 2\ NH_3 + H_2 + 16\ ADP + 16\ Pi \qquad (1.8)$$
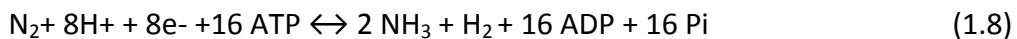
In the absence of N_2, nitrogenase behaves as an ATP-powered hydrogenase and generates H_2 as the main product.

$$2H+ + 2e- + 4\ ATP \leftrightarrow H_2 + 4\ ADP + 4\ Pi \qquad (1.9)$$
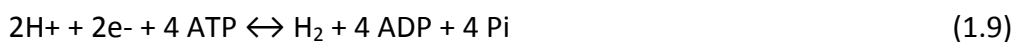
Rhodobacter capsulatus genome contains more than 50 nitrogen fixation (nif) related genes, most of them are grouped in four unlinked regions of the chromosome A, B, C, and D.

Region A: contains genes take role in electron supply to nitrogenase (*rnfABCDGEH*, *rnfF*, and *fdxN*), FeMoco biosynthesis (*nifEN*, *nifQ*, *nifSV*, and *nifB1*), and nitrogen regulation (*nifA1*).

Region B: contains the structural genes of Mo-nitrogenase, *nifHDK*, the nitrogen regulatory genes *rpoN* and *nifA2*, the FeMoco biosynthesis gene *nifB2*, genes involved in molybdenum uptake (*modABC*), and two molybdenum regulatory genes (*mopA*, *mopB*).

Region C: contains the *ntrBC* genes coding for a two-component regulatory system, which acts on top of the nitrogen regulatory cascade.

Region D: contains the nitrogen regulatory *anfA* gene and the structural genes of Fe-nitrogenase, *anfHDGK*.

1.3.1.5.1. Regulation of Nitrogen Fixation

Nitrogen fixation is a highly energy-demanding process, for that reason its synthesis and activity is highly regulated according to a number of environmental factors like (1) availability of ammonium, (2) oxygen partial pressure, (3) availability of molybdenum, (4) the C/N ratio at which carbon and nitrogen sources are consumed, (5) availability of iron, (6) temperature and (7) in photosynthetic bacteria light intensity (Masepohl and Kranz, 2009).

R. capsulatus has been a model organism in nitrogen fixation regulatory studies. *R. capsulatus* sense fixed nitrogen level by the Ntr system. (Masepohl and Kranz, 2009; Masepohl and Hallenbeck, 2010) Ntr system is composed of the bifunctional enzyme GlnD (uridylyltransferase/UMP-removing enzyme), two PII-like signal transduction proteins, GlnB and GlnK, and the two-component regulatory system NtrB–NtrC. Actually, the Ntr system does not sense nitrogen status directly from ammonium but it senses the ratio of ammonium assimilation product glutamine (Gln) to the carbon skeleton 2-oxoglutarate (2-ketoglutarate) and the energy source ATP. These metabolites bind synergistically to GlnD, GlnB, and GlnK and regulate the activity of different target proteins: NtrB, NifA1, NifA2, and DraT. The cascade that controls nitrogen fixation in *R. capsulatus* is shown in Figure 1.16. Upon nitrogen depletion, NtrC is phosphorylated. The phosphorylated form of NtrC activates transcription starting at the RpoD (RNA polymerase, sigma 70) dependent nifA1, nifA2, and anfA promoters and under molybdenum repression activates anfA transcription. NifA1, NifA2, and AnfA activate transcription starting at RpoN (RNA polymerase subunit, sigma 54 specific for nitrogen control) dependent nif and anf promoters. When ammonium added to a nitrogen-fixing culture, regulation occurs at three steps. First, GlnB interacts with NtrB, and NtrB–GlnB triggers dephosphorylation of NtrC. Second, GlnB and GlnK interact with NifA1 and NifA2, which in turn are no longer able to activate transcription of nif genes. Ammonium addition also inactivates AnfA. Third, DraT is transiently activated by interaction with GlnB or GlnK, and in turn, DraT modifies nitrogenase so that it is turned into an inactive state. When ammonium is utilized, DraG turns nitrogenase back to its active form. (Masepohl and Hallenbeck, 2010). The ammonium transporter (AmtB) also takes role in control of nitrogen fixation. In the presence of ammonium in the medium, AmtB forms a complex with GlnK. The AmtB-GlnK complex keeps DraG seperated from its substrate NifH and allows the accumulation of inactive state of nitrogenase (Masepohl and Hallenbeck, 2010).

29
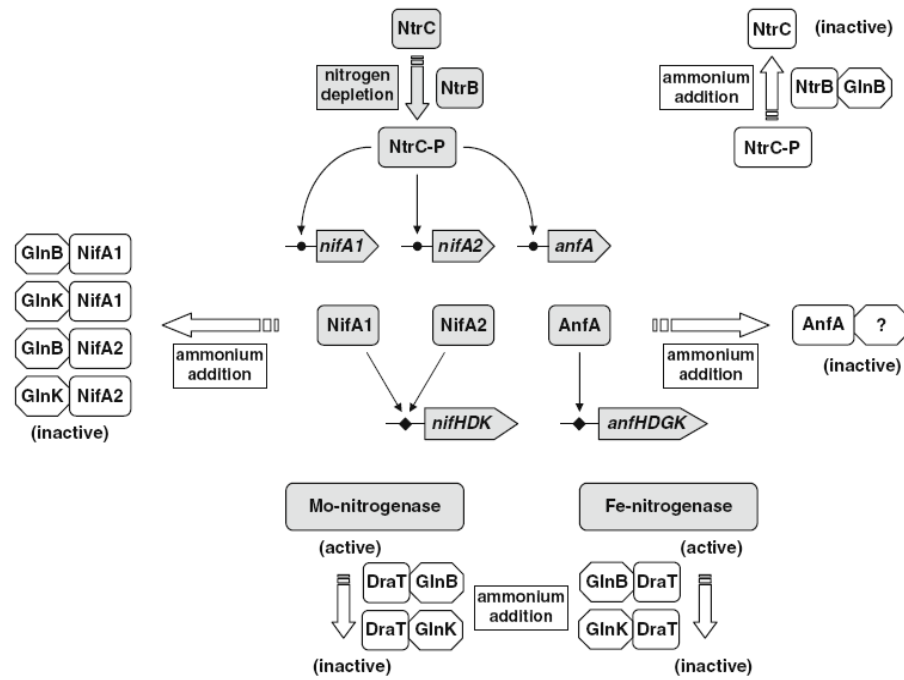
Figure 1. 16 Nitrogen control of nitrogen fixation by GlnB and GlnK in *R. capsulatus*. The regulatory cascade leading to synthesis of Mo and Fe nitrogenase is highlighted in grey. RpoD-dependent nifA1, nifA2, and anfA promoters are shown with filled circles. NifA1, NifA2, and AnfA activate transcription starting at RpoN-dependent nif and anf promoters are shown with filled diamonds (Masepohl and Hallenbeck, 2010).

In addition to mentioned specific regulatory genes, a two component global regulatory system RegA-RegB is involved in nitrogen fixation regulation. This regulatory system activates expression of genes involved in photosynthesis, carbon dioxide assimilation, nitrogen fixation and represses expression of uptake hydrogenase genes.

1.3.1.6. Hydrogenases

The hydrogenase enzymes are also involved in hydrogen metabolism and can catalyze both the oxidation (uptake hydrogenases) and production of hydrogen.

$$H_2 \leftrightarrow 2H^+ + 2e^- \tag{1.9}$$
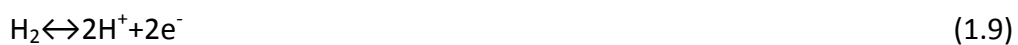
Hydrogenases are classified in two main groups according to their phylogenetic origin, the [NiFe]hydrogenases and the [FeFe]hydrogenases, which contain a Ni and an Fe atom or two Fe atoms, respectively, liganded by cysteine residues, at their active site (Vignais et al., 2006). *R. capsulatus* contains uptake hydrogenases that consume the H_2 produced by nitrogenase. The *R. capsulatus* uptake hydrogenase belongs to membrane-associated respiratory uptake [NiFe]-hydrogenases. The structural genes that encode the small and large subunits are called as S (encoded by hupS) and L (encoded by hupL), respectively. In addition to the structural genes, the hydrogenase gene cluster (*hup* genes) contains some additional genes which encodes proteins required for maturation of the heterodimeric enzyme (hyp genes), and the regulation of hydrogenase gene transcription. Uptake hydrogenases are linked to the quinone pool of the respiratory chain in the membrane by a third subunit which is a cyt *b* encoded by the third gene of the structural operon hupC. The uptake hydrogenase can also supply electrons to the Complex I (NADH: ubiquinone oxidoreductase) for CO_2 reduction, and to the Rnf complex which is involved in electron transfer to nitrogenase (Vignais , 2009).

1.3.1.6.1. Regulation of Uptake Hydrogenase

R. capsulatus controls the transcription of uptake hydrogenases by using a specific system that senses H_2. The HupUV protein is the H_2-sensor for the the two-component HupT/HupR regulatory system, which regulates the transcription of hydrogenase genes according to H_2. In the presence of H_2, HupR activates hupSL transcription in a non phosphorylated state. However, in the absence of H_2, HupR is phosphorylated by HupT~P and it does not trigger transcription of hydrogen uptake structural genes. In addition to this specific sensing mechanism, transcription of uptake hydrogenase structural genes are also controlled by RegA/RegB global regulatory system which represses transcription of HupSLC.

1.3.1.7 Calvin-Benson-Bassham Cycle and Redox Balance

R. capsulatus can fix inorganic CO_2 via Calvin-Benson-Bassham Cycle like other Purple non sulphur bacteria. The unique enzymes of the Calvin cycle are ribulose 1,5-bisphosphate carboxylase-oxygenase (RubisCO) and phosphoribulokinase (PRK). Phosphoribulokinase phosphorylates ribulose 5-phosphate and produces ribulose 1,5-bisphosphate which is the CO_2 acceptor. RubisCo catalyzes the actual CO_2 fixation reaction by combining CO_2 with ribulose 1,5-bisphosphate to form two molecules of 3-phosphoglycerate (Tabita, 1995; Tichi and Tabita, 2001). It is known that Calvin Cycle is active not only during photoautotrophic growth mode but also during photoheterotrophic mode. Under photoheterothrophic growth conditions, rather than generating organic carbon Calvin cycle operates to balance the redox potential of the cell. The excess reducing equivalents which are not used for biosynthesis can be used for CO_2 fixation via Calvin cycle or dissipated as H_2 via nitrogenase enzyme activity (Figure 1.17) (McKinlay and Harhood, 2011; Öztürk et al., 2012).
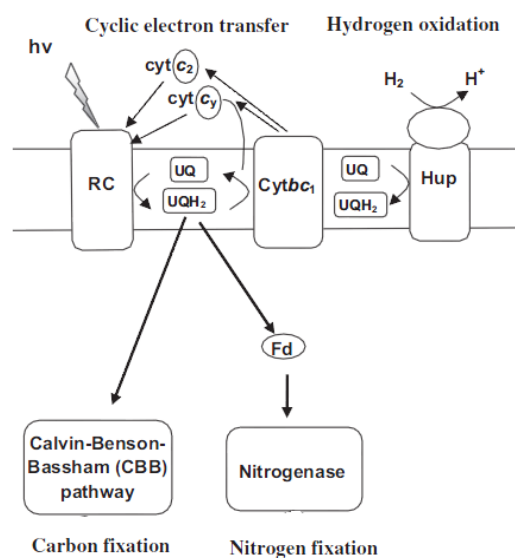
Figure 1. 17 Redox balancing pathways during photoheterotrophic growth of *R. capsulatus* (modified from Öztürk et al., 2012).

1.4. Microarray Technology

Microarrays are miniaturized, ordered arrangements of biological materials located at certain positions on a solid support and used to study interactions between biological molecules. The biological material used in microarrays can be DNA, proteins or carbohydrates. However the working principle in all types is the same. A mixture of labeled biological molecules "target" are hybridized with the "probes" (DNA, proteins or carbohydrates) which are immobilized onto a solid surface. By this way, biological interaction between molecules can be studied. Basic principle of DNA, proteins or carbohydrate microarrays is given in Figure 1.18. DNA microarrays will be discussed in detail in the next section.
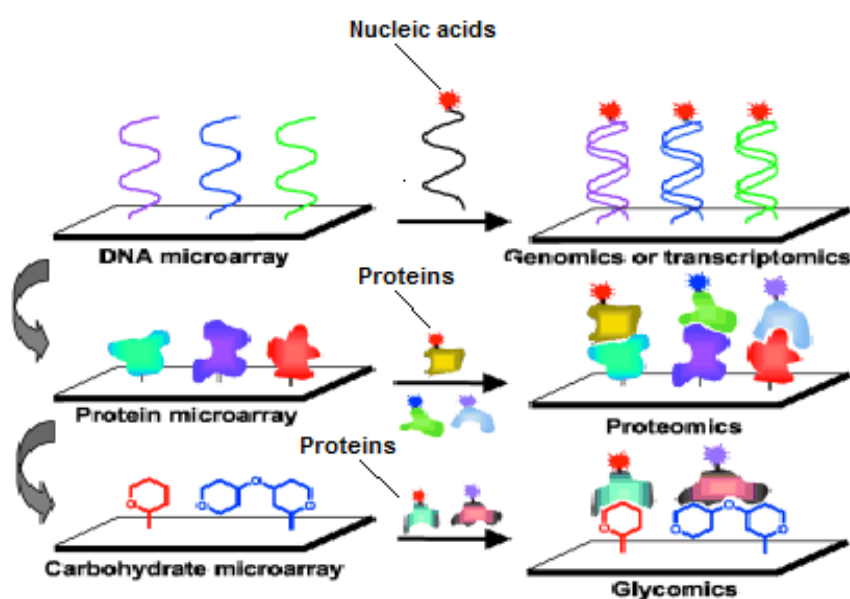
Figure 1. 18 Different types of microarrays: DNA, Protein and carbohydrate microarrays (Modified from Shin et al., 2005)

1.4.1. DNA Microarrays

DNA microarrays are extensions of a conventional membrane-based hybridization technique, Southern blot that has been used for detection and characterization of nucleic acids in biological samples. The main principle behind microarrays is that, an unknown sample (target) is applied to an ordered array of immobilized DNA molecules of known sequence (probe) to produce complementary base specific hybridization pattern (Zhou and Thompson, 2004).

Studying gene expression by microarray has several advantages over conventional nucleic acid-based approaches:

1. Microarray is a high throughput technology. Expression of thousands of genes can be compared rapidly at the same time on the same chip (Letowski, 2003).

2. High sensitivity can be obtained in probe-target hybridization since microarray requires a very small volume of probe and the target nucleic acid is restricted to a small area (Zhou and Thompson, 2004).

3. Nonspecific binding possibility is very low. Organic and fluorescent compounds that might attach to microarrays during fabrication and application can be removed. These properties results in significantly less background signal noise than that can occur in conventional techniques (Zhou and Thompson, 2004).

4. Hybridization and detection of the target can be performed in a simple and rapid way which allows real-time data analysis in field scale heterogeneous environments (Zhou and Thompson, 2004).

5. Microarray technology can be automated and for that reason it is much more cost-effective compared to conventional detection methods (Zhou and Thompson, 2004).

Major applications of DNA microarrays can be summarized as follows: gene expression profiling, pathogen detection and characterization, comparative genome hybridization, genotyping , whole genome resequencing, determining

protein-DNA interactions, mutation and single nucleotide polymorphism (SNP) detection, regulatory RNA studies, alternative splicing detection, RNA binding protein analysis, microRNA studies, and DNA methylation profiling (Hobman, 2007).

According to the differences in the array manufacture method microarray systems can be divided into two major groups: spotted microarray and in situ synthesised oligonucleotide microarrays.

Spotted microarrays: The probes are the chemically synthesized oligomers or products of the polymerase chain reaction (PCR) generated from genes, open reading frames (ORFs), cDNA libraries or clone collections. The probes are then printed onto glass surface by robotic spotting (Figure 1.19).
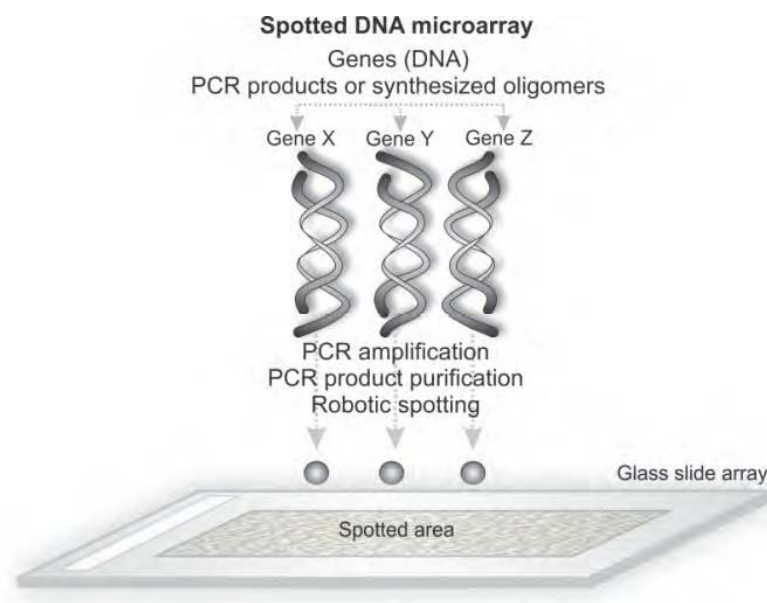
Figure 1. 19 Probe preparation and array printing for spotted microarray (modified from Saei and Omidi, 2011).

For spotted DNA microarray sample preparation, RNA is isolated from control and treated samples. RNAs are converted into cDNA. Then cDNAs are labelled with with two different fluorescent dyes (for example, Cy3 and Cy5) and hybridized on to the array (Hobman, 2007). After washing step, arrays are scanned twice for two different wavelengths corresponding to the fluorescent dyes used. The relative signal intensity obtained is used to determine ratios of mRNA abundance for the genes (Schulze and Downward, 2001). Main steps in spotted microarray procedure are summerized in Figure 1.20.
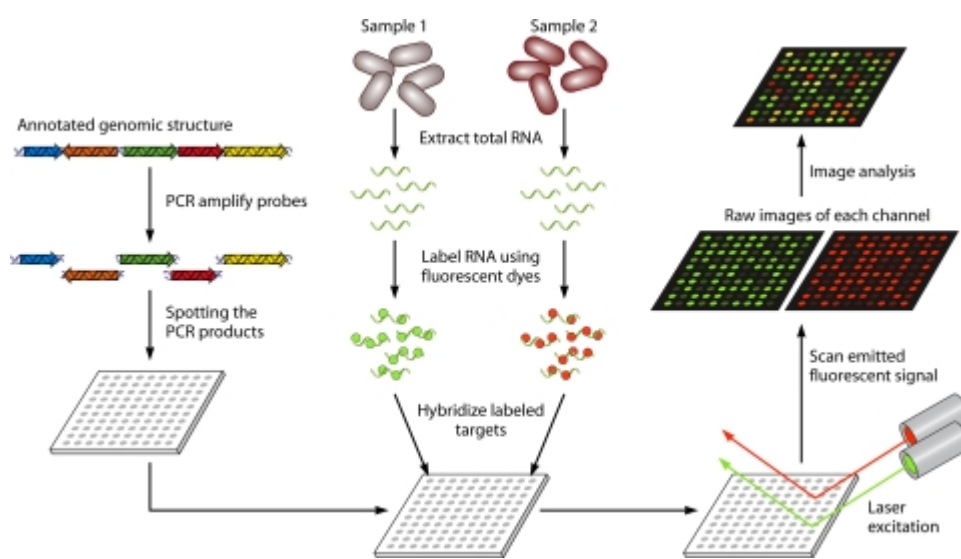
Figure 1. 20 Spotted microarray protocol (Miller and Tang, 2009).

By using spotted microarray method, researchers can construct in their own labs. In-house spotted arrays are widely preferred in research since their production is relatively cheap. A single printing machine can be used to print arrays for a large number of individual projects or research groups in the same facility. In addition to their cost effectiveness, in-house spotted arrays offers a great flexibility to researcher about what can be printed on the glass slide array (Hobman, 2007) and arrays may be customized differently for each experiment. The disadvantage of spotted microarray method is the lack of standardization due to different labeling

methods and fluorescent dyes used in detection. Hybridization and array washing methods used by different laboratories might result in different results (Hobman, 2007).

In situ synthesized oligonucleotide microarrays:

In oligonucleotide microarrays, the probes are synthesized in situ directly onto the surface of the chip instead of printing presynthesized probes. The most widely used microarrays with in situ synthesized probes are the GeneChips manufactured by Affymetrix (Santa Clara, CA, USA) (Ehrenreich, 2006). Affymetrix chip technology will be discussed in detained in the next part.

1.4.1.1. Affymetrix Microarrays

Affymetrix GeneChips are the most widely used DNA microarrays. The major advantages of using Affymetrix microarrays are the reproducibility of the manufacturing process and the standardization of methods, kits, instrumentation, and hardware used in the protocol when compared to spotted glass microarrays. Affymetrix Probes are 25mer oligonucleotides (Hobman, 2007). Due to their short length, multiple probes per target are included to improve sensitivity, specificity, and statistical accuracy. In this technology, the specificity is further increased by the use of probe sets (11 to 15 probe pairs). Each probe set contains one perfect-match probe and one mismatch probe that contains a single different base in the middle of the probe (i.e., position 13 of a 25-bp probe). Each member of the probe set is placed in a different feature, which allows the mismatch probe to behave as a negative control to identify possible nonspecific cross-hybridization events (Miller and Tang, 2009).

Probes are synthesized in situ by using a photolithographic method rather than spotting the probes as in spotted microarrays. Photolithography method used in the manufacture of Affymetrix GeneChips is summarized in Figure 1.21. A quartz wafer (microarray surface) is coated with a layer of a light-sensitive compound. By this way, the microarray surface is chemically protected from a nucleotide addition until illumination with UV light. Photolithographic masks are used to target specific nucleotides to exact probe locations on the wafer. When UV light reaches to on a particular feature area, it removes the protecting groups from the array surface and allows the addition of a single protected nucleotide. Application of repeated cycles of masking, light exposure, and addition of the specific base enables the synthesis of 25mer oligonucleotide (Miller and Tang, 2009).

In situ probe synthesis approach by using photolithography is advantageous. First, microarrays can be manufactured directly from sequence databases and by this way the uncertain and burdensome aspects of sample handling and tracking are removed. Second, a high degree of precision in each cycle is ensured and microarray-to-microarray variations are minimized. The drawbacks of the photolithographic approach are the high costs of the photomasks and time-consuming design and manufacture of the arrays (Zhou and Thompson, 2004).

The overall procedure used for prokaryotic target preparation for Affymetrix GeneChip® array is summarized in Figure 1.22.

Affymetrix offers a variety of catalog prefabricated GeneChip® arrays for many eukaryotic and prokaryotic organisms. In addition, it also manufactures user defined custom arrays for high-content designs such as whole genomes of organisms not represented on their catalog or combination designs, such as multiple bacterial organisms as described in GeneChip® CustomExpress™ Array Design Guide.

Figure 1. 21 Photolithography used for Affymetrix GeneChip® manufacturing (Miller and Tang, 2009).
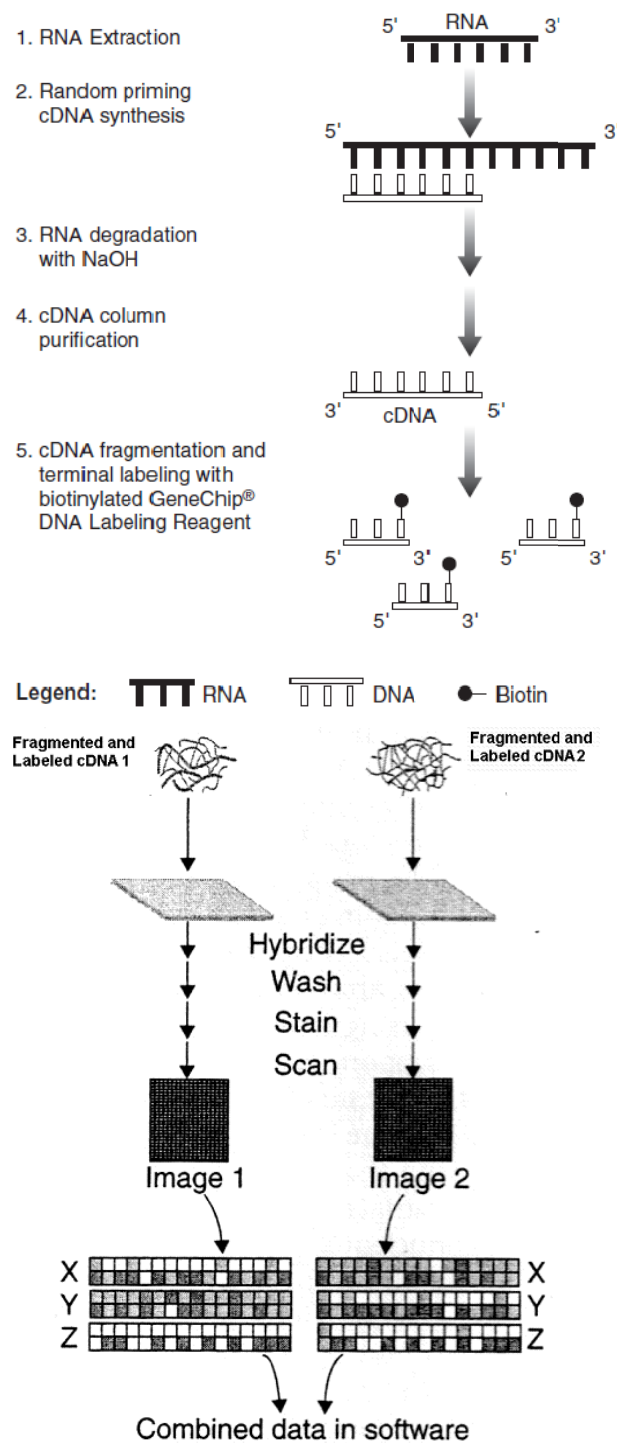
Figure 1. 22 Affymetrix protocol (Hobman, 2007).

1.4.2. Microarray Validation by RT-qPCR

For validation of microarray based gene expression, real time quantitative PCR (RT-qPCR) remains the gold standard which allows for a rapid, sensitive and easy confirmation (VanGuilder et al*.,* 2008; Arikawa et al., 2008). This method enables detection of the quantity of mRNA by measuring the fluorescence generated during amplification process in PCR reaction.

RT-qPCR involves three main steps 1) Reverse transcription where mRNA is converted to cDNA 2) Amplification of cDNA 3) Detection and quantification of the amplicon. Detection of the product can be performed by using fluorescent dyes which can bind to DNA specifically or nonspecifically.

SYBR Green is a dye used for non-specific detection. SYBR Green based detection is the most widely used method in qPCR experiments due to its low cost, simplicity, and flexibility compared to other specific detection methods (such as TaqMan chemistry) which require expensive oligonucleotide probes labeled with fluorescent reporter dyes (Boehm et al.2004). SYBR Green is a fluorescent dye which binds to any double-stranded DNA molecule by intercalating between base pairs in a non specific way. For this reason, it is important to use primer pairs that are highly specific to their target sequence to avoid production of nonspecific products.

Otherwise non specific amplification or primer dimer formation would occur and contribute to the fluorescent signal which might cause overestimation of the target (Smith and Osborn, 2009).

Fluorescence signal increases after each cycle as the SYBER Green binds to double stranded product. The threshold cycle (Ct) parameter is the cycle number when a significant increase in fluorescence signal is detected above the background fluorescence. The initial amount of starting material is inversely proportional to Ct

value. In other words, the greater the quantity of target in the starting material, the smaller is the Ct value due to faster rise in fluorescent signal (Wong and Medrano, 2005).

1.4.2.1. Relative Quantification

Relative quantification is the most widely used method for RT-qPCR quantification. Relative quantification involves the calculation of gene expression levels as the target/reference ration gene of each treated sample divided by the target/reference ratio of the control sample. Reference gene is a housekeeping gene whose expression level does not show a difference in all experimental conditions and in all samples (such as 16srRNA). Normalization to a reference gene results in the correction of sample to sample variations caused by differences in the initial quality and quantity of the nucleic acid (Roche Applied Science Technical Note No. LC 13/2001).

1.4.2.2. Evaluation of RT-qPCR Assay Parameters

There are several parameters that can help researcher to validate RT-qPCR assay:

No Template Control (NTC): Contains water instead of template. Normally, amplification signal in NTC is not expected. Presence of amplification signals in the NTC sample might indicate contamination or primer dimer formation problems (D'haene et al., 2010)

Positive Control: Contains a different template where the target gene is known to be expressed. It is used to check the quality of primers and reagents in the reaction mix (Eurogentec qPCR-guide).

PCR Efficiency: It is the indicator of the amplification performance and can be determined by constructing a standard curve. Standard curve is obtained by serial dilutions for both the target and reference gene. If the slope of the standard curve is -3.32, PCR efficiency is 100%. PCR efficiency between 90%-110% which refers to a slope between -3.1 and -3.58 is acceptable (D'haene et al., 2010).

R square (R^2): R^2 is a statistical parameter and indicates how well the data points lie on one straight line. If the R^2 < is 0.95, it indicates that pipetting errors, diluting of inhibitory factors. An R^2 >0.985 is acceptable.

Melt curve analysis: Non-specific products can be detected by performing a melt curve analysis after PCR reaction. At the beginning of the analysis, reaction mix is at a low temperature and the fluorescence signal is high due to SYBR Green bound double stranded PCR products. As the reaction temperature is increased, the fluorescence will drop suddenly when the temperature reaches the melting temperature (Tm) of a nucleic acid. The instrument is set to measure the fluorescence of all samples continuously as the temperature increases. Every PCR product has a different Tm depending on the length and base composition (GC content). For this reason any contaminating product or primer dimers would seen as an additional peak different from the desired amplicon peak. An example of melt curve is given in Figure 1.23 and the additional peak other than the specific PCR product shows the presence of primer dimer formation (Roche Applied Science Technical Note No LC 1/99).
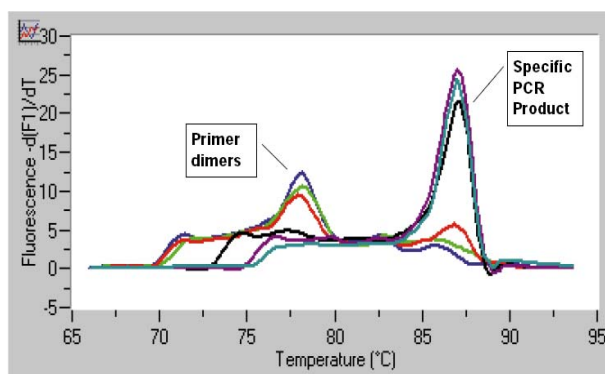
Figure 1. 23 Primer dimer (Roche Tech Note LC 1/99)

1.5 Aim of the Study

In photofermentative hydrogen production, types of the nitrogen and carbon sources are two important parameters which affect growth and hydrogen production capacities of PNS bacteria. *Rhodobacter capsulatus* is known to be the most widely used photofermentative PNS bacteria for biological hydrogen production. The effect of different nitrogen sources and acetate concentrations on transcriptome of *R. capsulatus* has not been investigated at whole genome level yet. The main objective of this study was to investigate the hydrogen production, carbon assimilation, and nitrogen metabolism of *R. capsulatus* on different nitrogen sources (5mM ammonium chloride vs 2mM glutamate) and acetate concentrations (40-80mM).

For this purpose, the first approach was to achieve physiological experiments in batch type photobioreactors under photofermentative growth mode of *R. capsulatus.*

As a second approach microarray analysis were carried out by using custom-designed Affymetrix GeneChips.

Validation of the microarray experiments was achieved by RT-qPCR analysis. Finally, microarray data analysis was carried out by using Genespring GX11 software.

CHAPTER 2

MATERIALS AND METHODS

2.1. Materials

Wild type *Rhodobacter capsulatus* strain SB1003 (gifted by Prof. Patrick Hallenbeck (Microbiologie et immunologie, Université de Montréal, Montreal, Canada) and DSM 1710 (DSMZ, German Collection of Microorganisms and Cell Cultures, Braunsweig, Germany) were used in physiological experiments. For to study gene expression, *Rhodobacter capsulatus* strain SB1003 was used in microarray and qPCR experiments. The chemicals used in this study were supplied by Merck, Sigma, Applichem, Fermentas, Invitrogen and Affymetrix.

2.2. Methods

Bacteria were spread on MPYE agar plates to obtain single colonies. The components were dissolved in distilled water and 1.5 % agar (m/v) was added for solidification of the medium (Daldal et al., 1986). Medium was autoclaved for sterilization (1.06 Bar, 121°C for 30 min) and poured into sterile petri plates. The composition and preparation of the MPYE medium is given in Appendix A.

20mM Acetate was added as the carbon source and 10mM glutamate was added as the nitrogen source to minimal Biebl and Pfennig (BP) medium (Biebl and Pfennig, 1981) for growth of bacteria. The components of BP medium were dissolved in

distilled water and pH was set to 6.3-6.4 by using pH meter. After autoclave sterilization, iron-citrate, vitamin and trace element solution were added. The composition of the BP media, iron-citrate, vitamin (biotin, thiamin and niacin) and trace element solutions are given in Appendix A.

The effect of different nitrogen sources on *R. capsulatus* metabolism was studied by comparing 5mM ammonium chloride (NH_4Cl) and 2mM glutamate, carbon source was 40mM in both conditions. In order to investigate the effects of different initial carbon sources, nitrogen source was kept constant as 2mM glutamate and 40mM, 60mM and 80mM acetate concentrations were used as carbon source. Except the carbon and nitrogen sources, other components of the BP medium (Biebl and Pfennig, 1981) were same. The nitrogen and carbon sources and their concentrations are given in Table. 2.1

Table 2. 1 Nitrogen and carbon sources used in the experiments

Condition	Carbon Source	Nitrogen Source
1	40mM Acetate	5mM NH_4Cl
2	40mM Acetate	2mM Glutamate
3	60mM Aceate	2mM Glutamate
4	80mM Acetate	2mM Glutamate

2.3. Experimental Set-up

The photobioreactors with 150 ml volume were inoculated with freshly grown bacteria by 10%. In order to obtain an anaerobic atmosphere, photobioreactors were flushed with argon. The reactor bottles were illuminated with 100W tungsten lamps. Light intensity was set to 200 W/m^2 at the surface by a lux meter (Lutron LX-

105 Light Meter). The experiments were carried out at 30°C in a cooled incubator (Nüve, ES 250 cooled incubator) and repeated 4 times.

The evolved gas during experiments was measured by the water displacement method (Uyar et al., 2007). Graduated glass collection tubes filled with distilled water were connected to the reactor bottles by capillary tubes. Gas generated in the reactors were collected in the collection tubes and replaced with water. The schematic diagram and the photograph regarding the experimental set-up are given in Figure 2.1 and Figure 2.2 respectively.
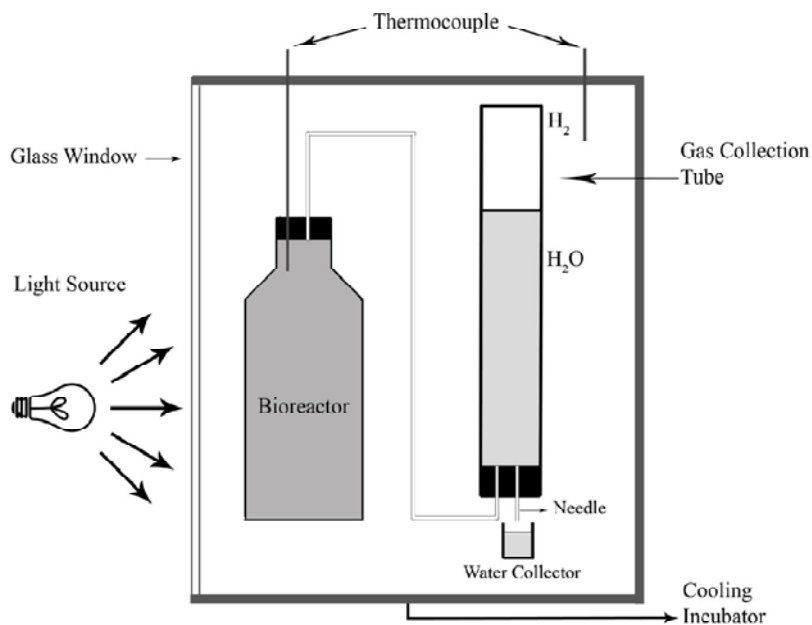
Figure 2. 1 Figure Schematic diagram of the experimental set-up (Sevinç, 2010).

Figure 2. 2 The photograph of the experimental set-up

2.4. Analyses

Daily samples (2.5 ml) were taken from the photobioreactors in order to obtain physiological parameters such as gas composition, optical density, pH and organic acid consumption (Figure 2.3). 2ml sterile distilled water was injected into the photobioreactors in order to balance the pressure.
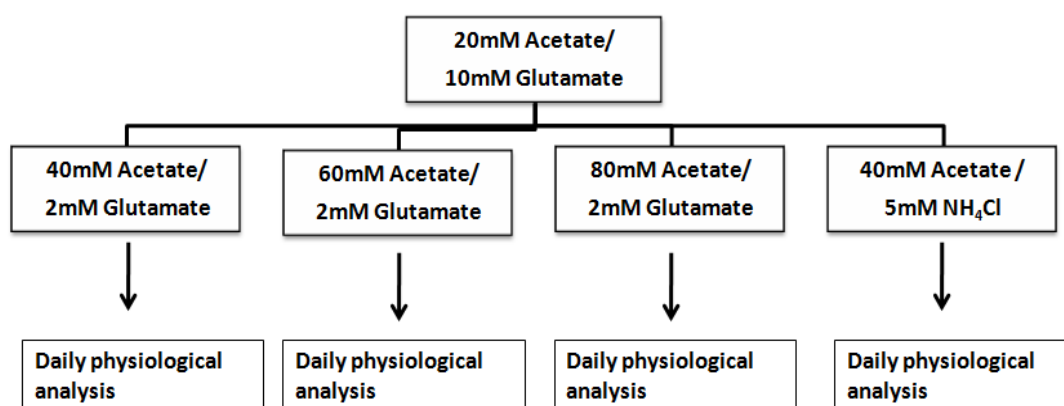
Figure 2. 3 Conditions for physiological sample collection

2.4.1. Gas Composition Analysis

The composition of the gas generated during the experiments was analyzed by a Gas Chromatograph (GC) (Agilent Technologies 6890N). GC instrument was equipped with a thermal conductivity detector and a Supelco Carboxen 1010 column. Gas samples (100 μL) were collected from the headspace of the photobioreactors by using a gas-tight syringe (Hamilton, 22 GA 500μL gas tight No. 1750). The oven, injector and detector temperatures were 140°C, 160°C and 170°C, respectively. Argon was used as carrier gas at a flow rate of 26ml/min. The temperatures of oven, injector and detector were 140 °C, 160 °C and 170 °C, respectively. The GC instrument was controlled by using Agilent Chemstation ver.B.01.01 software (Agilent Technologies).

2.4.2. Optical density measurement

The optical densities of cultures were determined spectrophotometrically (Shimadzu UV-1201) at 660 nm. A time based growth curve was obtained by using the daily optical density values.

2.4.3. Organic Acid Analysis

For organic acid analysis, samples were centrifuged at 13,600 rpm for 10 minutes in a bench-top centrifuge (Eppendorf MiniSpin) to precipitate the cells. The pellet was discarded and supernatant part was taken into a new clean eppendorph. The supernatant was filtered with 45 μm nylon filters (Millipore, 13 mm) to get rid of impurities. Then the samples were analyzed by High Performance Liquid Chromatography (HPLC) which was equipped with Alltech IOA-1000 (300mm ×7.8 mm) column. 10 μL of sample was injected into the system by the autosampler (Shimadzu SIL-20AC). Organic acids were detected the at 210 nm wavelength by using a UV detector (Shimadzu SPD-20A). During analysis, the oven temperature

was kept at 66 °C. The mobile phase was 0.085 M H_2SO_4 with a flow rate of 0.4 ml/min with a low gradient pump (Schimadzu LC-20AT).

2.4.4. pH Analysis

The pH analyses of the cultures were done by the use of a pH meter (Mettler Toledo 3311). The pH meter was calibrated with pH 7 and pH 4 solutions before use.

2.5. Microarray Analysis

In order to investigate global transcript profile of *Rhodobacter capsulatus* on different nitrogen sources and different acetate concentrations, microarray analysis was carried out.

2.5.1. Design of Affymetrix GeneChip®

A microarray chip for *Rhodobacter capsulatus* was not commercially available. For that reason, a GeneChip® array was custom designed and manufactured by Affymetrix, Santa Clara, California. Physical map of the entire genome of the bacterium *Rhodobacter capsulatus* was constructed by Prof. Dr. Robert Haselkorn's team (Haselkorn et al., 2001, Strnad et al., 2010). The nucleotide sequence of the bacterium is available in GenBank with the accession numbers CP001312 for the chromosome and CP001313 for the plasmid pRCB133.

The genome of *R. capsulatus* consists of a circular chromosome and a single plasmid which are 3,738,958 and 132,962 base pair lengths, respectively. Both the chromosome and the plasmid have GC rich sequences (66.6%). Coding region of the genome is 91% and there are 3531 open reading frames (ORF) on chromosome and 154 ORFs on the plasmid. In addition, there are 53 tRNA and 4 rRNA operons. In ORFs, 3100 genes possess identified function and 610 of them have similarities with

hypothetical genes in the databases. On the other hand, the remaining ORFs do not have any homologues in the databases.

Considering these characteristics of *R. capsulatus* genome, expression chip of the whole genome is designed according to the GeneChip® Custom Expression Array Desgin Guide. A sequence file in FASTA format, an instruction file (including the name, the product, role and description of the probe sets with the name of the genes) and a design request form were prepared and sent to Affymetrix Custom Array Design Team. In addition to ORFs, 200 intergenic sequences with bigger than 300bp length were also added to sequence file. The coding strand of the ORFs and both strands of the intergenic regions were present on the genechip and represented by separate probe sets.

The feature size of the antisense DNA array was 11 micron and the format was 100-3660. 13 probe sets were selected from the 600 bases proximal to 3' end of each gene and intergenic region sequences by a perfect match (PM)/mismatch (MM) probe strategy. In PM Probe sets, 25 bp are perfectly complementary to the target. On the other hand, in MM Probe sets there is a mismatch in the middle base to capture non-specific hybridization. A total of 4,052 probe sets are placed on the microarray. The name of the *R. capsulatus* array was designated as Affymetrix.GeneChip ® TR_RCH2a520699F.

Some probes were placed onto the array for the target preparation control, hybridization control, alignment control and quality control. The target preparation controls were Poly-A Controls which are dap, lys, phe, thr, trp genes derived from *B. subtilis*. Hybridization controls were bioB, bioC, bioD genes derived from *E.coli* and cre gene derived from P1 bacteriophage. Alignment and chip quality controls were located on the edges, at the corner blocks, on blocks left free at the center of the chip and in the chip name.

51

2.5.1. RNA Isolation and Characterization

RNA samples were collected from 40mM acetate/ 5mM NH_4Cl, 40mM acetate / 2mM glutamate, 80mM acetate /2mM glutamate containing photobioreactors after 16h of inoculation (Figure 2.4). For RNA isolation, $1.5x10^9$ bacterial cells (OD_{660} = 1.2, 1ml) were transferred to a microcentrifuge tube and centrifuged for 15 min at 12000 rpm at 4°C in a cooling centrifuge (Sigma 4K15). Supernatants were discarded. The pellets were frozen with liquid nitrogen and stored at -80°C until RNA isolation.
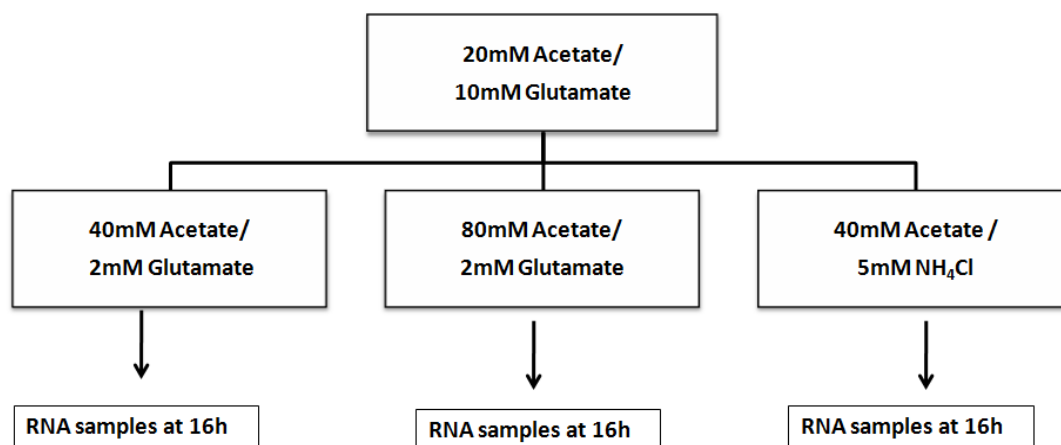
Figure 2. 4 Sample collection for RNA samples

Total RNA isolation was performed according to protocol given for Invitrogen TRIzol® Max Bacterial RNA Isolation Kit with some modifications. The cell pellets were resuspended in 200 µl of 5 mg/ml lysozyme solution (Sigma, activity ≥ 40,000 units/mg protein) by vortexing for 10 seconds. The lysozyme solution was prepared in Tris EDTA (TE) buffer. The composition of TE buffer is given in Appendix B. Then the samples were incubated at 37 °C for 10 min in a heater block (WTW-CR 3200). After incubation, 20 µl of 3 mg/ml Proteinase K (AppliChem, activity 37.5 m Anson U) was added onto samples and vortexed for 1 minute. Then the samples were kept

at room temperature for 5 minutes. 200 µl cold chloroform (Merck) was added onto the samples and mixed by vigorous shaking for 15 seconds. The samples were kept at room temperature for 6 minutes and centrifuged at 12,000g for 15 minutes at 4 °C. Following centrifugation, the mixture separated into 3 phases: a lower phase contained the TRIzol® Reagent, cell debris and proteins (red); a middle phase contained the DNA, and a colorless upper aqueous phase contained RNA. RNA remained in the upper aqueous phase. The volume of the aqueous phase was about 60% of the volume of TRIZOL Reagent used for homogenization (approximately 600-650µl for 1ml Trizol). 600 µl upper aqueous phase was transferred to a new RNase-free microcentrifuge tube. Then 500 µl of cold isopropanol was added and mixed by inverting 40 times and kept at room temperature for 10 minutes. The microcentrifuge tubes were then centrifuged at 17,000g for 10 minutes at 4 °C. At this step, RNA was precipitated and a clear pellet at the bottom of the microcentrifuge tubes was formed. The supernatant was discarded and RNA pellet was washed with 1 ml of 80% ethanol (Merck) by vortexing and centrifugated at 20,000g for 10 minutes at 4 °C. The supernatant was removed and RNA pellet was briefly air dried for few minutes for to remove the residual ethanol. RNA pellet was dissolved in 20 µl of RNase free ultra pure water (MilliQ) by incubating at 60 °C for 10 minutes and stored at -80 °C for further use.

The quantity and quality (purity and integrity) of the isolated RNA was tested. For an efficient prokaryotic microarray analysis, isolated RNA should have $OD_{260/280}$ ratio between 1.8 and 2.1 and its concentration should be higher than 555ng/µl. The concentration of total RNA was measured by a micro-volume spectrophotometer (AlphaSpec™) at 260 nm wavelength using 1 µl of total RNA. The quality of isolated RNA was determined by Agilent 2100 Bioanalyzer Expert-Prokaryote Total RNA Nano Chip according to the protocol given in Agilent RNA 6000 Nano Kit Quick Start Guide.

2.5.2. cDNA synthesis

The Poly-A RNA Control Stock containing polyadenylated transcripts for *B. subtilis* genes was serially diluted as recommended for 100 format array. 2 μL of the Poly-A RNA Control Stock was added to 38 μL of Poly-A Control Dilution Buffer for the First Dilution (1:20) and vortexed and spinned down to collect the liquid at the bottom of the tube. 2 μL of the first dilution was added to 38 μL of Poly-A Control Dilution Buffer to prepare the Second Dilution (1:20), vortexed and spinned down to collect the liquid at the bottom of the tube. 2 μl of second dilution was used in cDNA synthesis reaction mix. The First Dilution of the poly-A RNA controls was allowed to be stored up to six weeks at −20°C and frozen-thawed up to eight times. However the second dilution, was prepared freshly for each experiment.

30 μl of RNA/Primer hybridization mix was prepared by addition of 10μg of total RNA, 10 μl of 100 ng/μl random primers (Invitrogen), 2 μl of diluted poly-A RNA controls and nuclease free water (Affymetrix) (volume was determined according to the volume of RNA). The RNA/Primer hybridization mix was incubated at 70 °C for 10 minutes, 25 °C for 10 minutes and then was chilled to 4 °C in a thermal cycler (Applied Biosystems, 96-well GeneAmp® PCR System 9700). While cycling, cDNA synthesis mix was prepared in a PCR tube by adding 7.5 μl 200 U/μl SuperScript II™ Reverse Transcriptase and 12 μl of 5X first strand buffer (Invitrogen), 6 μL 100mM DTT (Affymetrix), 3 μl 10mM dNTP (Invitrogen) and 1.5 μl 20U/μl SUPERase•In™. Then the cDNA synthesis mix (30 μl) from to the RNA/primer hybridization mix reaction mixture (30 μl) was added. The total 60 μl solution was incubated in thermal cycler at 25 °C for 10 minutes, 37 °C for 60 minutes, 42 °C for 60 minutes and 70 °C for 10 minutes, and then was chilled to 4 °C.

2.5.3 Removal of RNA

In order to remove RNA, 20 μl of 1N NaOH (Merck) was added on cDNA/RNA solution and kept at 65 ^{o}C for 30 minutes. After incubation, 20 μl 1N HCl (Merck) was added in order to neutralize NaOH.

2.5.4 Purification and Quantification of cDNA

MinElute PCR Purification Columns (Qiagen) were used to clean up the cDNA synthesis products. The cDNA solution (100 μl) was mixed with 500 μl of Buffer PB, the binding buffer in a microcentrifuge tube. The mixture was vortexed and applied on the MinElute PCR Purification columns (QIAGEN). The column was centrifuged at 17,920g for 1 minute at 20 ^{o}C. The flow-through was discarded and the column was placed back to the same collection tube. 750 μl of washing buffer, Buffer PE, was added on the column and centrifuges at 17,920g for 1 minute at 20 ^{o}C. The flow-through was discarded. The column with the collection tube was centrifuged at 17,920g for additional 1 minute at 20 ^{o}C. The column was placed in a new clean 1.5 ml microcentrifuge tube. 12 μl of the elution buffer was added on the column and incubated at room temperature for 1 minute. The column and the microcentrifuge tube were centrifuged at 17,920g for 1 minute at 20 ^{o}C. The flow-through contained purified single-stranded cDNA in 11 μl elution buffer.

The concentarion of the purified cDNA was determined from the absorbance recorded at at 260nm by micro-volume spectrophotometer (AlphaSpec™). A minimum of 1.5 μg of cDNA was needed for subsequent procedures to obtain sufficient material for hybridization onto the microarray chip.

2.5.5. Fragmentation

Reaction mix was prepared by assembling 10 µl cDNA, 2 µl 10X DNase Buffer (Ambion), DNase I (Ambion, 2U/µl) and nuclease free water (Affymetrix). The amount of DNase I was calculated as 0.6 U DNase I for 1 µg of cDNA. The volume of the nuclease free water was determined according to the volume of DNAse I used. The reaction mix was incubated at 37 ^{o}C for 10 minutes. Then, DNase I was inactivated at 98 ^{o}C for 10 minutes.

2.5.6. Terminal Labeling

Biotin in the GeneChip DNA Labeling Reagent (Affymetrix) was used to label the 3' termini of the fragmentation products. The Terminal Labeling reaction mix was prepared by 20 µl of fragmented cDNA products, 10 µl 5X Reaction Buffer (Promega), 2 µl 7.5mM GeneChip® DNA Labeling Reagent (Affymetrix), 2 µl Terminal Deoxynucleotidy Transferase (Promega, 30 U/µl) and 16 µl nuclease free water (Affymetrix). The reaction mix was incubated in thermal cycler at 37 ^{o}C for 60 minutes and the reaction was stopped by adding 2 µl 0.5M EDTA (Invitrogen, pH 8).

2.5.7. Hybridization

130 µl of hybridization cocktail was prepared for 100 format microarray chips. 1.5 µg of fragmented and labeled cDNA, 2.2 µl 3nM Control Oligo B2, 65 µl 2X hybridization mix, 10.2 µL DMSO, 6.5 µl 20X Hybridization Control and nuclease-free water. The volume of water was determined according to the volume of cDNA) were used for hybridization cocktail.

The GeneChip® Probe Array was completely equilibrated to room temperature. Otherwise rubber septa could crack and lead to leakage of hybridization coctail. A clean pipette tip was inserted into the upper septum to ventilate the array chamber and another pipette tip was placed into the other sepa to load 130 µl hybridization cocktail by using a micropipettor. The GeneChip® Probe Array and the septa are

shown in Figure 2.5. For the hybridization temperature, washing and staining the protocols used for *P. aeruginosa* were selected, since *Rhodobacter capsulatus* have a high GC content (66.6%) like *P. aeruginosa*. The microarray chips were incubated at 50 °C with rotating at 60 rpm at GeneChip® Hybridization Oven 640 for 17 hours.
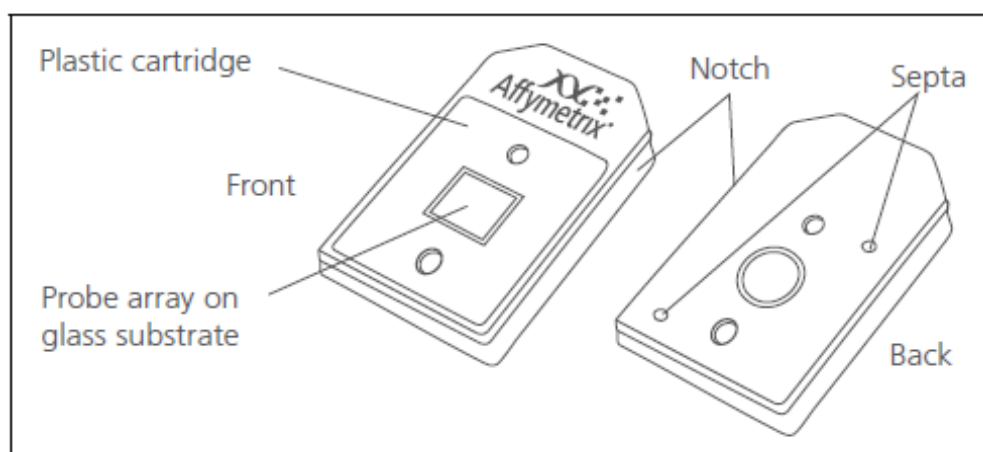
Figure 2. 5 The GeneChip® Probe Array and the septa

2.5.8. Washing and Staining

After the hybridization step, the chips were removed from hybridization oven and a washing and staining protocol was applied at GeneChip® Fluidics Station 450. GeneChip® Operating Software (GCOS) was the program used in the fluidics station. Each experiment was registered in GCOS by filling the Project name, sample name probe array type and experiment name fields. Wash A and Wash B buffers and distilled water were installed in their appropriate locations. Stain Cocktail 1, Stain Cocktail 2 and Array holding buffer were aliquoted into microcentrifuge vials in volumes of 600 µl, 600 µl and 800 µl, respectively, and located into the sample holders 1, 2, and 3 on the fluidics station. Arrays were then placed into the appropriate modules. The fluidics station was then run with the fluidics protocol Flex FS450_0002.

2.5.9. Scanning

GeneChip® Probe Array was removed when fluidics was complete and checked for bubbles. If no bubbles were present, the probe array was scanned by using GeneChip® Scanner 3000, which was operated by GCOS according to instructions of the manufacturer. After scanning of the chips, GCOS generated different files. The .EXP file stores information related with the experimental conditions like the project name, experiment name, sample name, array type. The .DAT file was the image of the scanned array. The .CEL file was derived from .DAT file and it stored the results of the intensity calculations for each probe. The .CHP file was the output file generated from the analysis of a probe array. The .RPT file was generated from .CHP file and it contained information related with the quality criteria (such as average background and noise, percent present and intensity values of controls).

2.5.10. Microarray Data Analysis

CEL files were loaded to GeneSpring GX 11 software (Agilent Technologies, Santa Clara, CA). Raw data from scanned arrays were normalized by Robust Multiarray Analysis (RMA) normalized. After RMA normalization, probe sets were filtered by expression based on the raw intensity values. By this way, probes with very low signal intensity values or with saturated intensity values could be removed. The lower percentile cutoff was set to 20. For, significance analysis p values were calculated by using T-test and p value correction was performed by using Benjamini Hochberg method. The entities which satisfied the significance analysis (corrected P value smaller than 0.1) were further filtered by fold change analysis. Genes with a fold change of at least 1.75 were considered.

2.6 Microarray validation by RT-qPCR

Expression profiles obtained on different nitrogen sources and different acetate concentrations with custom designed *R. capsulatus* GeneChips were validated by RT-qPCR method.

2.6.1 Primer Design

16SrRNA (product: Small Subunit Ribosomal RNA), atpF (product: ATP synthase F0, B subunit), pufM (product: photosynthetic reaction center, M subunit), acnA (product: aconitate hydratase), and oppA (product: oligopeptide ABC transporter, periplasmic oligopeptide-binding protein OppA) genes were selected for validation of microarray data by RT-qPCR. 16SrRNA was selected as the reference gene used to normalize expression values of other genes. Primers were designed by using Primer3 software and PerlPrimer software. NCBI/Primer-BLAST tool was used to check the specifity of the designed primers. Primer syntheses were carried out by Iontek (Istanbul, Turkey). Detailed information related to primers and their products are given in the Table 2.2.

2.6.2. RT-qPCR Protocol

Reverse transcription of RNA to cDNA was performed according to GeneChip Expression Analysis Technical Manual by using SuperScript II (Invitrogen) and random hexamers (Invitrogen). cDNA samples for qPCR were taken as aliquots prior to fragmentation. RT-qPCR experiments were carried out with Roche LightCycler 1.5 which used LightCycler FastStart DNA Master SYBR Green I as reaction mix. Reaction reagents and compositions for qPCR assays are given in Table 2.3.

Table 2. 2 Primer used for validation experiments

Gene (Probe#)	Primer Forward (5'->3')	Primer Reverse (5'->3')
16SrRNA (RCAP_rcr00001)	GCTAGTAATCGCGTAACAGCA	CAGTCACTGAGCCTACCGT
atpF (RCAP_rcc00744)	ACGTTCCTGCTTGTTGCTCT	TCGAGGGAACCTTGAACTTG
pufM (RCAP_rcc00694)	CACCATCGGTGTGTGGTACT	AGACACCACCCTGTTTCAGC
acnA (RCAP_rcc02150)	TCATTCCCTTCGAATTCACC	CCGCCGTTCTTCAGATATTC
oppA (RCAP_rcc02275)	AGGAACTGCTCAAACCGATG	GTCCTTGTAGTCCGCAAACC

Table 2. 3 Reaction reagents and compositions for RT-qPCR assays

Reagent	Volume (µl)	[Final]
dH$_2$O	11.6	
MgCl$_2$ (25mM)	2.4	3mM
DNA Master SYBR Green I	2	
Forward Primer	1	0.5µM for 16SrRNA 0.3µM for pufM,atpF,acnA,oppA
Reverse Primer	1	0.5µM for 16SrRNA 0.3µM for pufM,atpF,acnA,oppA
cDNA Template*	2	
TOTAL VOLUME	20	

*For No Template Control 2µl dH$_2$O is added instead of cDNA template.

RT-qPCR protocol involved 4 programs: pre-Incubation which activated DNA polymerase and denatured DNA; amplification of the target, melting curve for product identification and cooling (Table 2.4).

Table 2. 4 RT-qPCR protocol

Program		Temperature	Time	Cycle
Pre-Incubation		95ºC	10min	1
Amplification	**Denaturation**	95ºC	10s	40
	Annealing	60ºC[1]	5s 2s for pufM	
	Extension	72ºC	Product [bp]/25s*	
Melting Curve		65ºC -95ºC		1
Cooling		40ºC	30s	1

*16srRNA: 146/25=5.84 Extention time: 6
 pufM: 137/25=5.48 Extention time: 5
 afpF: 142/25=5.68 Extention time: 6
 acnA: 211/25= 8.4 Extention time: 8
 oppA :   131/25=5.24 Extention time: 5

Standard curves were constructed for each gene. Serial dilutions of pooled cDNA were prepared to obtain 1000ng, 500ng, 300ng, 100ng, 50ng, 30ng, 10ng standards. Standard curves were obtained by using 5 of these standards as duplicates.

CHAPTER 3

RESULTS AND DISCUSSION

3.1. Physiological Studies with Two *R. capsulatus* Strains SB1003 and DSM1710

The effect of different nitrogen sources on physiology of *Rhodobacter capsulatus* was investigated by using 5mM ammonium chloride and 2mM glutamate. Carbon source was 40mM acetate in both conditions. Effect of different acetate concentrations on physiology of *R. capsulatus* was explored by using 40mM, 60mM and 80mM acetate. Nitrogen source was 2mM glutamate in all conditions. Experiments were carried out 4 times and at least 3 of them were considered.

3.1.1. Physiology of *R. capsulatus* on Different Nitrogen Sources

Glutamate is a good source of nitrogen for hydrogen production purposes via photofermentation. However, it must be noted that ammonium chloride not the glutamate is the nitrogen source used in dark fermentation effluents. For that reason, it is fed to photobioreactors for photofermentation processes (Özgür et al., 2010; Afsar et al., 2010). In this study, effect of 5mM ammonium chloride on growth, hydrogen production and substrate utilization of *Rhodobacter capsulatus* were investigated by comparing the physiology on 2mM glutamate containing medium. Growth profile of *R. capsulatu*s SB1003 is given in Figure 3.1. A

significantly higher (almost twice) biomass accumulation on 5mM ammonium chloride containing medium was observed when compared to that on 2mM glutamate containing medium. The time based hydrogen production profile is shown in Figure 3.2. On 2mM glutamate containing culture, a linear hydrogen production was observed. On the other hand, hydrogen production was completely inhibited on 5mM ammonium chloride containing medium. Similarly, more growth was observed with *R. sphaeroides* on 5mM ammonium chloride containing medium compared to 2mM glutamate containing medium and hydrogen production ceased in photobioreactors containing ammonium chloride concentrations higher than 3mM (Akköse et al., 2009). The increased biomass yield on ammonium chloride in this study might be due to higher concentration of the nitrogen source in the medium and carbon source could be utilized for only growth since hydrogen production was totally inhibited.
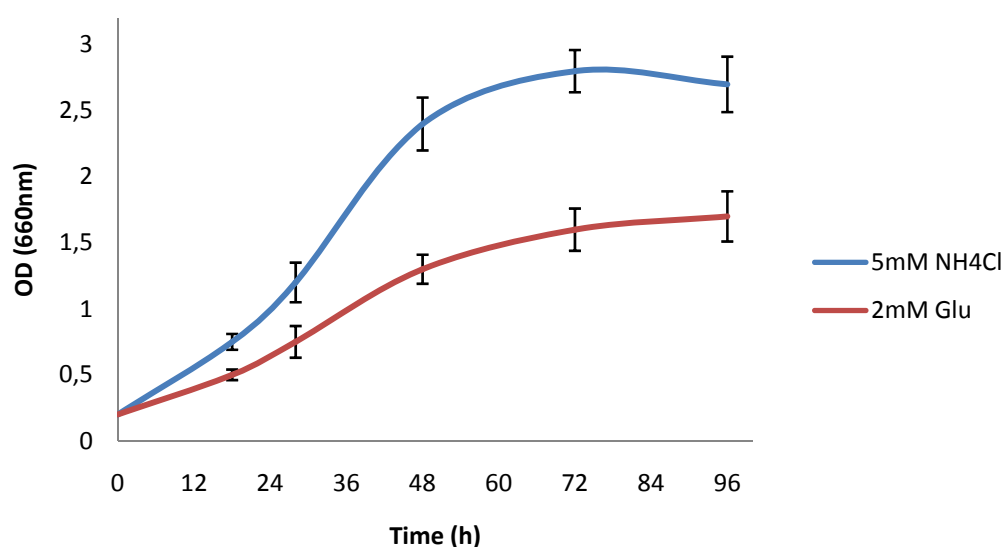
Figure 3. 1 Growth profile of *R. capsulatus* SB1003 on different nitrogen sources. Vertical bars indicate ± SEM values.
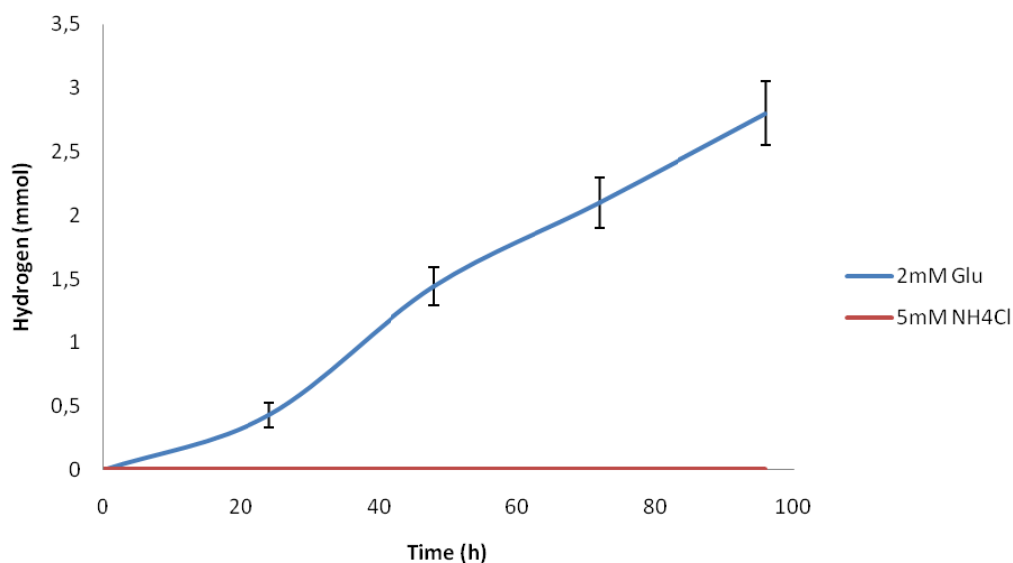
Figure 3. 2 Hydrogen production of *R. capsulatus* SB1003 on different nitrogen sources. Vertical bars indicate ± SEM values.

3.1.2 Physiology of *R. capsulatus* on Different Concentrations of Acetate

Acetate is the main by-product of dark fermentation. For this reason, it has been extensively studied in photofermentation experiments. Previous studies showed that the initial acetate concentration has a significant influence on photofermentation of PNS bacteria (Barbosa 2001; Nath et al.,2005; Özgür 2010; Özsoy 2012). The highest acetate concentration in these studies was in between 50mM and 65mM. However, it is known that acetate concentrations are much higher than these values in dark fermentation effluents (Afsar et al., 2010; Özgür et al, 2010). For this purpose, in addition to 40 and 60mM initial acetate concentration of this study aimed to investigate the effect of a higher acetate concentration 80mM on biomass production, hydrogen production and substrate utilization efficiencies of *R. capsulatus* DSM1710.

3.1.2.1 Growth Profile on Different Initial Acetate Concentrations

Growth of *R. capsulatus* DSM1710 was monitored at different initial acetate concentrations (40-80mM) by measuring optical density at 660nm and growth curve was obtained (Figure 3.3). When the experiment was terminated, bacteria were in death phase at 40mM, in stationary phase at 60mM and in late exponential phase at 80mM acetate containing medium.

The lag phase was missed in all acetate conditions since bacteria were activated in 20mM acetate containing growth media before inoculation. But it could be still understood from the growth curve (Figure 3.3.) that lag phase lasted longer for 80mM compared to 40mM and 60mM acetate conditions. This result might imply that it takes longer for the bacteria to adapt to the 80mM acetate condition. In a recent study which was also performed with acetate adapted *R. capsulatus* DSM1710, lag phase was not observed in cultures grown on acetate concentrations between 10mM and 65mM (Özsoy et al., 2012).

Maximum growth was observed on 80mM and biomass accumulation decreased as concentration decreased. The increase in growth at higher acetate concentrations might be due to higher amount of carbon which is available for growth. A study with *R. capsulatus* showed that max biomass attained increased as acetate concentration in the media increased from 10mM to 65 mM (Özsoy et al., 2012). Another study with *R. capsulatus* reported that 40mM acetate was more beneficial for growth compared to 20mM (Shi and Yu, 2006).
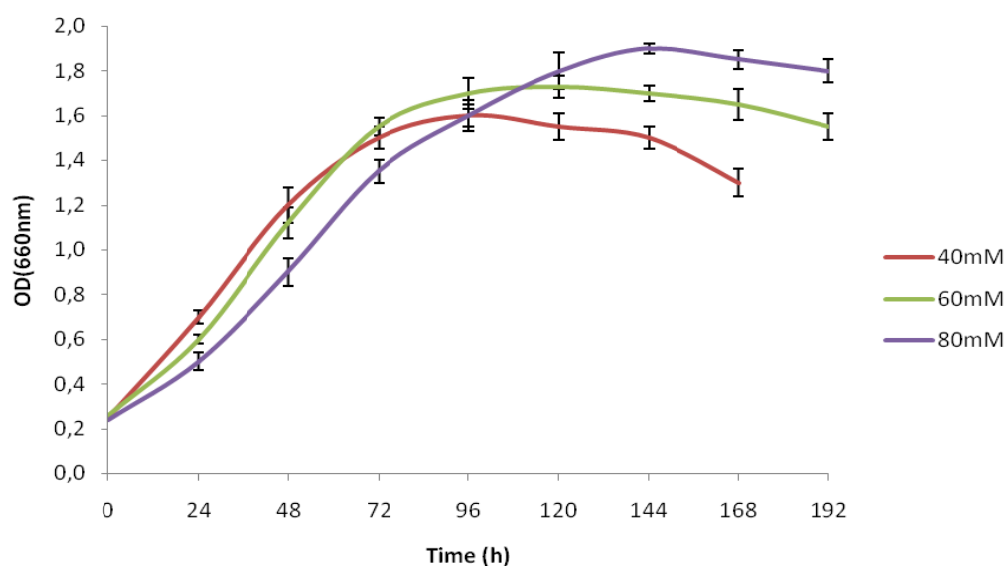
Figure 3. 3 Growth profile of *R. capsulatus* DSM1710 on different acetate concentrations. Vertical bars indicate ± SEM values.

3.1.2.2 Substrate Utilization on Different Initial Acetate Concentrations

Daily acetate utilization character of *R. capsulatus* at different concentration of acetate was followed by HPLC analysis and a time based acetate consumption graph was obtained (Figure 3.4).
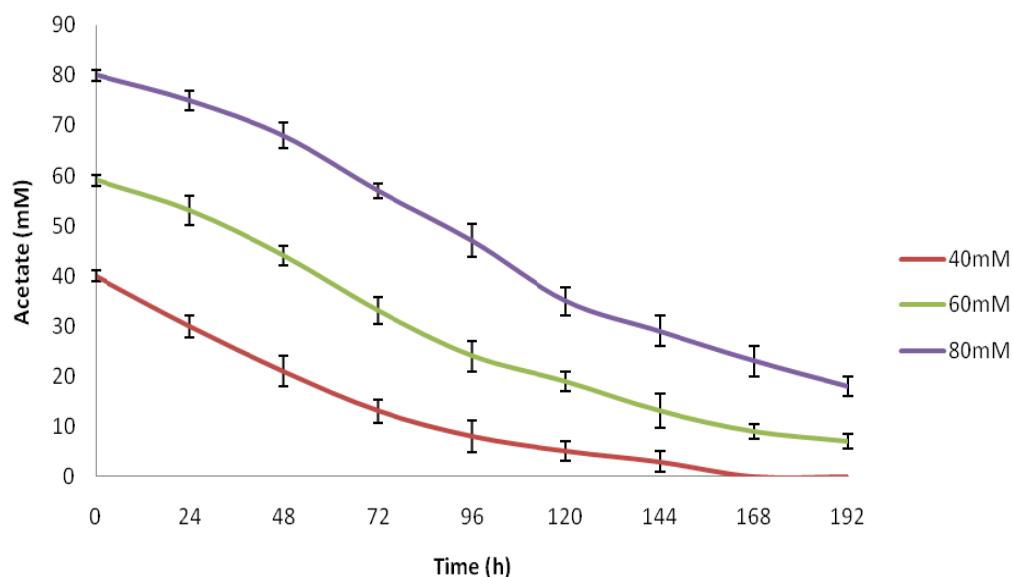
Figure 3. 4 Acetate consumption of *R. capsulatus* DSM1710 on different acetate concentrations. Vertical bars indicate ± SEM values.

It was observed that, 40mM acetate was almost completely utilized (%98) by bacteria after 144 hours. On the other hand, for 60mM acetate and of 80mM acetate containing media consumed amount were %68 and %46 of the initial concentration respectively. It was also noticed that initial substrate consumption rate was slower on 80mM compared to 40 and 60mM conditions which supports a longer lag phase in when grown on 80mM acetate medium. After 24 hours, acetate consumption rate increased as bacteria entered exponential phase. The reason for acetate remaining in the 60mM and 80mM acetate containing media might be due to incomplete metabolism of the substrate when the experiment was terminated.

3.1.2.3. Hydrogen Production on Different Initial Acetate Concentrations

The composition of the collected gas was analyzed by gas chromatography. Evolved hydrogen gas vs time graph is given in Figure 3.5. Cumulative hydrogen gas was higher in 40mM and 60mM than 80mM acetate condition.
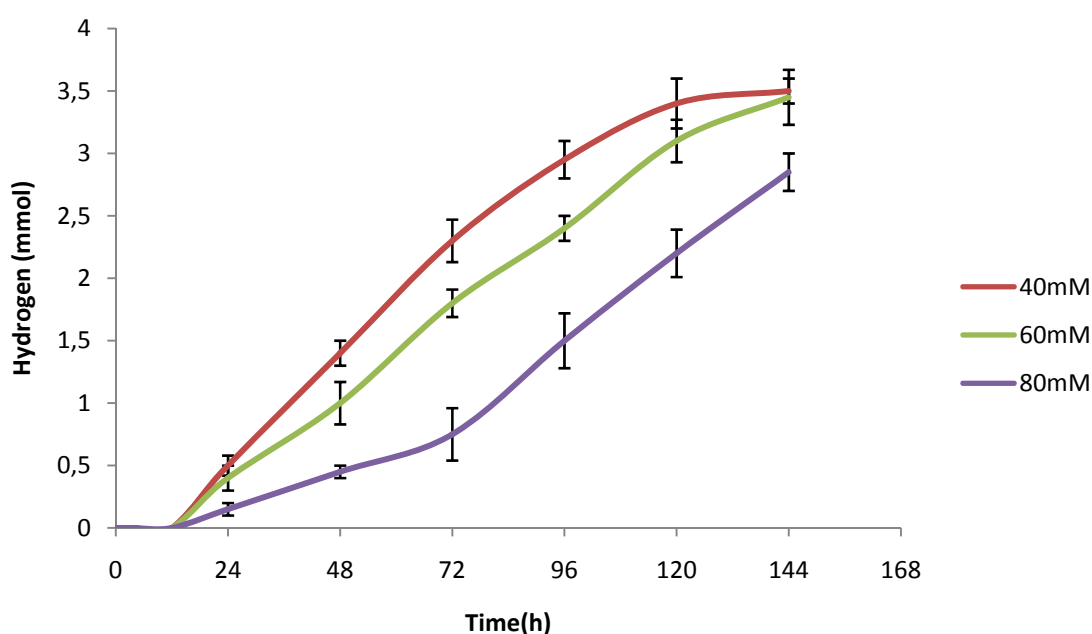
Figure 3. 5 Hydrogen production of *R. capsulatus* DSM1710 on different acetate concentrations. Vertical bars indicate ± SEM values.

Evaluation of hydrogen production performance by just considering total hydrogen produced is not sufficient and there is a need for calculation of some other parameters such as molar productivity, molar yield, product yield factor and light conversion efficiency. Physiological parameters calculated on different acetate concentrations are given in Table 3.1.

Molar Productivity is one of these parameters and can be used to determine the molar hydrogen production rate (amount/time) on the basis of the culture volume. Molar productivity can be calculated from the formula below:

$$\frac{\text{Total } H_2 \text{ (mmol)}}{\text{Volume (L) x time (h)}}$$

The lowest molar productivity was calculated for 80mM acetate medium. Although total hydrogen production for 40mM and 60mM were same, their molar productivity values were significantly different and it was lower on 60mM compared to 40mM acetate condition. The remarkable reduction in molar productivity at higher at 60mM and 80mM indicated that acetate concentrations higher than 40mM results in decrease in hydrogen production rate.

Acetate stands at the intersection point between different metabolic pathways and it can be used for growth, hydrogen production or PHB synthesis. Özgür et al. 2010 suggested that initial acetate concentration has a role on directioning of metabolism. Molar Yield (substrate conversion efficiency) can be defined as the percentage of the ratio of the experimental mmoles of hydrogen produced to the theoretical mmoles of hydrogen that would have been produced if all of the consumed substrate had been utilized for only hydrogen production rather than growth or other by products such as PHB.

$$\frac{\text{Experimental } H_2}{\text{Theoretical } H_2} \times 100$$

In this study, acetate was the sole substrate and theoretical hydrogen production was calculated from the stoichiometric equation. It was assumed that 4 moles of hydrogen was theoretically produced per mole of acetate consumed.

$$CH_3COOH + 2H_2O \rightarrow 4H_2 + 2CO_2$$
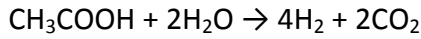
Molar yield decreased as acetate concentration increased from 40mM. Increased biomass accumulation and lower hydrogen production at 60mM and 80mM might indicate that at higher acetate concentrations than 40mM growth might be favored to hydrogen production. This result was also supported by other studies (Özgür et al. 2010; Androga et al., 2011; Özbay et al., 2012).

Light conversion efficiency is calculated from the percentage of the ratio of the total energy amount of the hydrogen to the total energy input to the photobioreactor by light radiation. Light conversion efficiency can be calculated from the formula:

$$\eta\,(\%) = \frac{33.6 \times \rho_{H_2} \times V_{H_2}}{I \times A \times t} \times 100$$

 Where V_{H_2} is the volume (L) of evolved H2, ρH_2 is the density (g/L) of the evolved hydrogen gas, I is the light intensity (W/m^2), A is the irradiated area (m^2) and t is the duration of hydrogen production (h) (Uyar et al., 2007). A decrease in light conversion efficiency was seen with increasing acetate concentrations. Similar results were also observed in different studies with *R. capsulatus* when bacteria were cultivated at higher acetate concentrations. The decrease in light intensity parameter was connected to the increase in biomass which might have created a

shading effect and reduced light penetration into the photobioreactors (Özbay et al. 2012; Barbosa et al., Androga et al., 2011).

Table 3. 1 Physiological parameters on different acetate concentrations

Acetate Concentration (mM)	Molar Productivity (mmol/L_c.h)	Molar Yield (% of theoretical max)	Light Conversion Efficiency (%)
40	0.60	43	0.48
60	0.52	36	0.42
80	0.45	31	0.39

3.1.3. Comparison of Growth and Hydrogen Production Performances of Two Different *R. capsulatus* Strains SB1003 and DSM1710.

R. capsulatus DSM1710 has been the widely used strain in photofermentation studies. On the other hand, SB1003 is the strain whose genome has been sequenced and preferred in molecular studies. In this study, the growth, substrate utilization and hydrogen production capacities of two *R. capsulatus* Strains SB1003 and DSM1710 were compared for the first time on 40mM and 80mM acetate containing media.

When the growth curve of these strains was depicted Figure 3.6), it was seen that growth profile of SB1003 and DSM1710 were very similar and growth was higher at 40mM compared to 80mM acetate. Hydrogen production vs time graph is shown in Figure 3.7. It was seen that there was no significant difference in the real time hydrogen production performances and maximum hydrogen production evolved by these two strains both on 40mM and 80mM acetate. Acetate consumption graph is given in Figure 3.8. Similar to growth and hydrogen production data, acetate utilization trends of SB1003 and DSM1710 were also significantly similar.
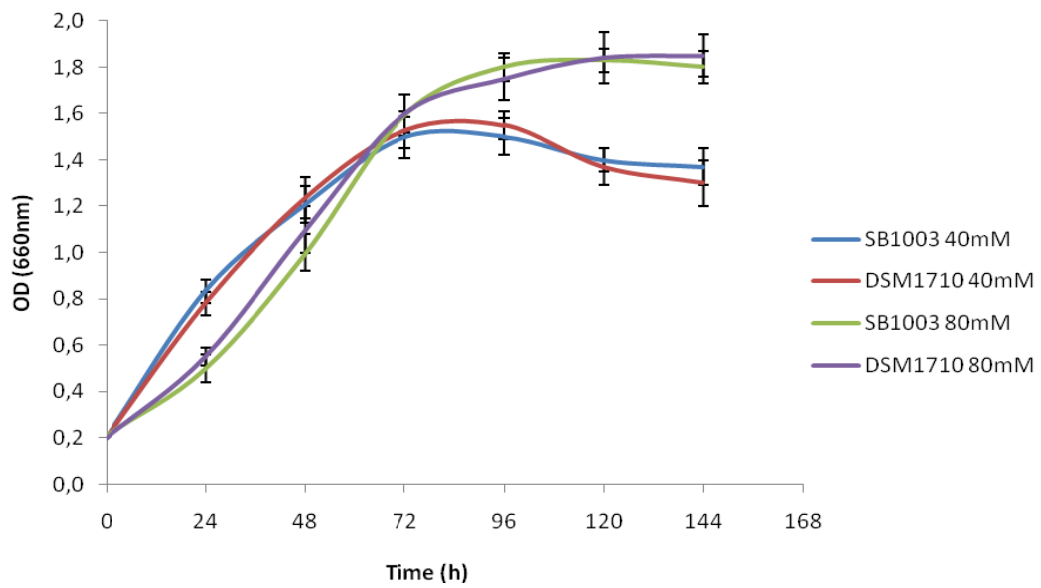
Figure 3. 6 Growth of two different *R. capsulatus* strains SB1003 and DSM1710 on different acetate concentrations. Vertical bars indicate ± SEM values.
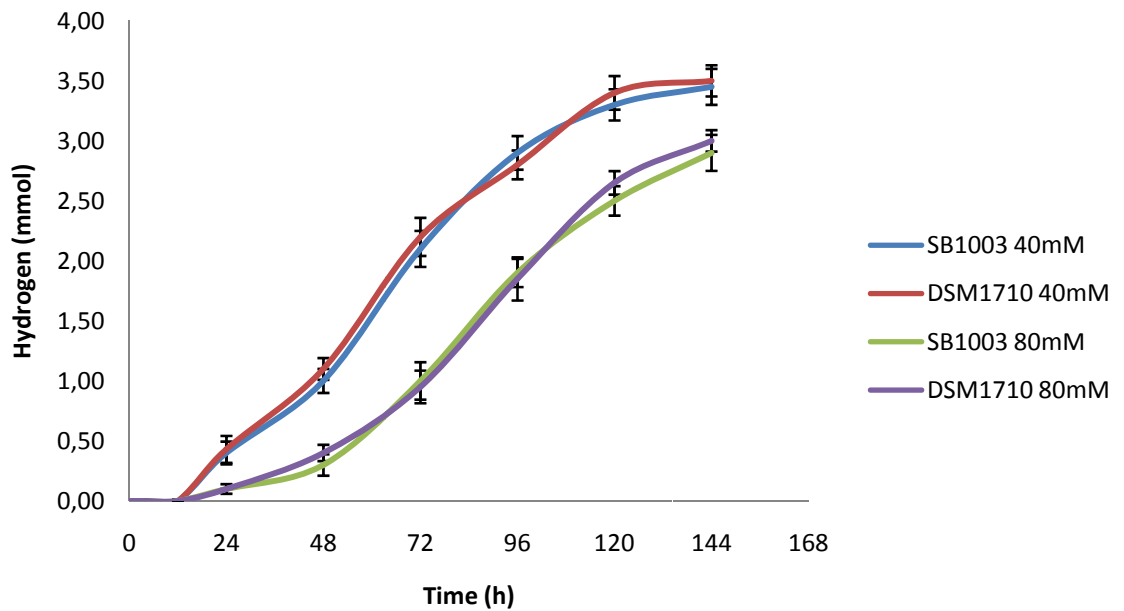
Figure 3. 7 Hydrogen production of two different *R. capsulatus* strains SB1003 and DSM1710 on different acetate concentrations. Vertical bars indicate ± SEM values.

71
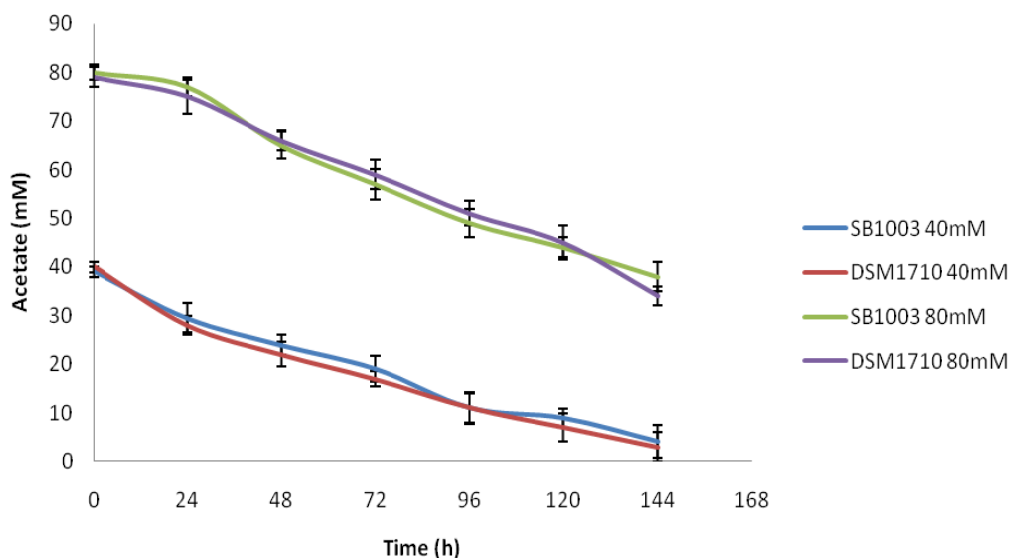
Figure 3. 8 Substrate consumption of two different *R. capsulatus* strains SB1003 and DSM1710 on different acetate concentrations. Vertical bars indicate ± SEM values.

In order to make a more detailed comparison between photofermentation capacities of SB1003 and DSM1710, molar productivity, molar yield, and light conversion efficiency parameters were also calculated on 40mM acetate and 80mM acetate concentrations. Calculations of these physiological parameters were explained previously in section 3.1.2.3. These parameters are summarized in Table 3.2. Although there were slight differences in molar productivity molar yield, product yield factor and light conversion efficiency values of SB1003 and DSM1710, these differences were found to be insignificant and could be due to factors other than strain type such as sampling, inoculation or light intensity differences in the photo bioreactors.

Table 3. 2 Physiological parameters of SB1003 and DSM1710 strains on different acetate concentrations

R.capsulatus Strain	Acetate Concentration (mM)	Molar Productivity (mmol/L$_c$.h)	Molar Yield (% of theoretical max)	Light Conversion Efficiency (%)
SB1003	40	0.69	49	0.40
DSM1710	40	0.66	47	0.40
SB1003	80	0.47	33	0.34
DSM1710	80	0.48	33	0.35

3.2 Microarray Analysis

For an efficient microarray analysis, the quality and the quantity of the RNA and cDNA obtained should be high enough. For this purpose, an RNA isolation protocol was optimized for *R. capsulatus.*

3.2.1 Optimization Studies for RNA Isolation Protocol for *R. capsulatus*

Bacterial cells were immediately centrifuged and frozen in liquid nitrogen in order to stop cellular activity and transcription at the time of sampling. Frozen samples were kept at -80°C until RNA isolation was performed. It is known that there are several parameters which can affect RNA quality and quantity. These parameters include source of sample (such as type of organism), the sampling and RNA isolation protocol used (Jahn et al., 2008). Total RNA extraction can be performed by using commercial kits or manually by using commercial reagents. In this study, a high quantity of RNA (555ng/µl) with a high purity was required (260/280 ratio: 1.8-2.1) since low RNA yield and quality might result in increased noise and signal variability in microarray analysis. For this purpose two different RNA isolation kits RNeasy Mini Kit (QIAGEN), RiboPure–Bacteria Kit (Ambion) and an acid guanidinium thiocyanate–

phenol–chloroform extraction method using a commercial solution TRI REAGENT (Sigma) were compared in terms of the RNA quality and quantity. The purity of the RNA obtained by the kits was high, however the yield was very low (maximum 150ng/μl). Higher concentrations were obtained with TRI reagent (300ng/μl) and it was selected as the RNA isolation protocol. In this procedure, RNA is obtained upon extraction with an acidic solution containing guanidinium thiocyanate, sodium acetate, phenol and chloroform, followed by a centrifugation step. Under acidic conditions, total RNA is located in the upper aqueous phase and precipitated with isopropanol (Chomczynski and Sacchi, 1987). The RNA yield and quality obtained with this protocol were still not enough and some modifications were carried out to increase these parameters to desired values for microarray studies.

Lysozyme treatment: Lysozyme is an enzyme which can be obtained commercially from chicken egg white and it hydrolysis the β-1, 4-glycosidic bond between the N-acetylmuramic acid-N-acetylglucosamine repeating unit of the peptidoglycan layer of the cell walls of bacteria. Its effect is more remarkable when used in combination with EDTA which can chelate metal ions in the outer membrane of gram negative bacteria (Moore et al., 2004). A lysozyme treatment step was added to protocol and it was vigorously vortexed to enhance digestion of *R. capsulatus* cell wall.

Proteinase K treatment: Proteinase K is a serine protease which exhibits endo- and exoproteolytic activity. During RNA isolation, Proteinase K is used to digest proteins in cell lysates. By eliminating protein contamination, it increases purity of the isolated RNA. Morover, it also enhances the total RNA yield since Proteinase K also digests DNase and Rnase enzymes which digests nucleotides. In this study, treatment of cell lysate with proteinase K also increased RNA purity and resulted in an increase in 260/280 ratio.

Change in centrifugation and incubation periods: Incubation time after chloroform addition was extended from 3 min to 6 min. This resulted in a better phase

separation and increased the volume of clear aqueous phase after centrifugation. Extension of centrifugation periods after precipitation and washing steps also increased both purity and yield of isolated RNA.

Determination of initial cell concentration: The manufacturar's manual suggests using an initial bacterial concentration upto $1x10^8$ cells. Effect of different initial cell concentrations on RNA yields was tested. For this purpose, $1x10^8$ cells, $1x10^9$ cells $1.5x10^9$ and $2.0x10^9$ cells were used. It was seen that increasing cell concentration from $1x10^8$ to $1.5x10^9$ resulted in an increase in the quantity of isolated RNA. However, further increase in cell concentration ($2.0x10^9$ cells) did not show a significant effect on yield (Table 3.3).

Table 3. 3 The concentrations and the $OD_{260/280}$ ratios of the RNA obtained with different initial cell concentrations

	RNA Concentration (ng/µl)		
$1x10^8$ Cells	300	409	500
$1x10^9$ Cells	350	450	536
$1.5x10^9$ Cells	800	835	900
$2.0x10^9$ Cells	750	850	890

3.2.2. Characterization of the Isolated RNA

The concentration and $OD_{260/280}$ ratio of total RNA was measured by using a micro-volume spectrophotometer (AlphaSpec™). It is known that for an efficient prokaryotic microarray analysis, isolated RNA should have $OD_{260/280}$ ratio between 1.8 and 2.1 and its concentration should be higher than 555ng/µl. All isolated RNA samples used in this study had $OD_{260/280}$ ratio between 1.8 and 2.1 and their concentration was higher than 555ng/µl (Table 3.4).

Table 3. 4 The concentrations and the $OD_{260/280}$ ratios of the RNA used in the microarray experiments

	RNA	
	$OD_{260/280}$ ratio	Concentration (ng/μL)
40mM Acetate / 2mM Glutamate	1.89	862.2
	1.87	865.6
	1.90	644.6
	1.91	781.8
80mM Acetate / 2mM Glutamate	1.96	594.8
	1.88	598.1
	1.94	649.6
	1,89	634.3
40mM Acetate / 5mM NH₄Cl	1.91	1381.2
	1.92	1419.7
	1.85	1415.1
	1.90	1332.5

The Agilent 2100 Bioanalyzer™ (Agilent Technologies, Santa Clara, CA, USA) is an instrument that allows evaluation of RNA quality in terms of purity and integrity. Its working principle is based on a micro-fluidic capillary electrophoresis in which RNA sample is run with a fluorescent dye and detected with a laser. Its software enables analysis of RNA sample and creates a gel image and an electropherogram. The integrity and purity of isolated RNAs were analysed by Agilent2100 Bioanalyser using Agilent2100 Expert_Prokaryote Total RNA Nano Chip. The gel image of 12 RNA samples is given in Figure 3.9 and a sample RNA electropherograms is given in Figure 3.10. The results showed that RNA samples were in high quality. They were intact and highly pure and could be used for cDNA synthesis.
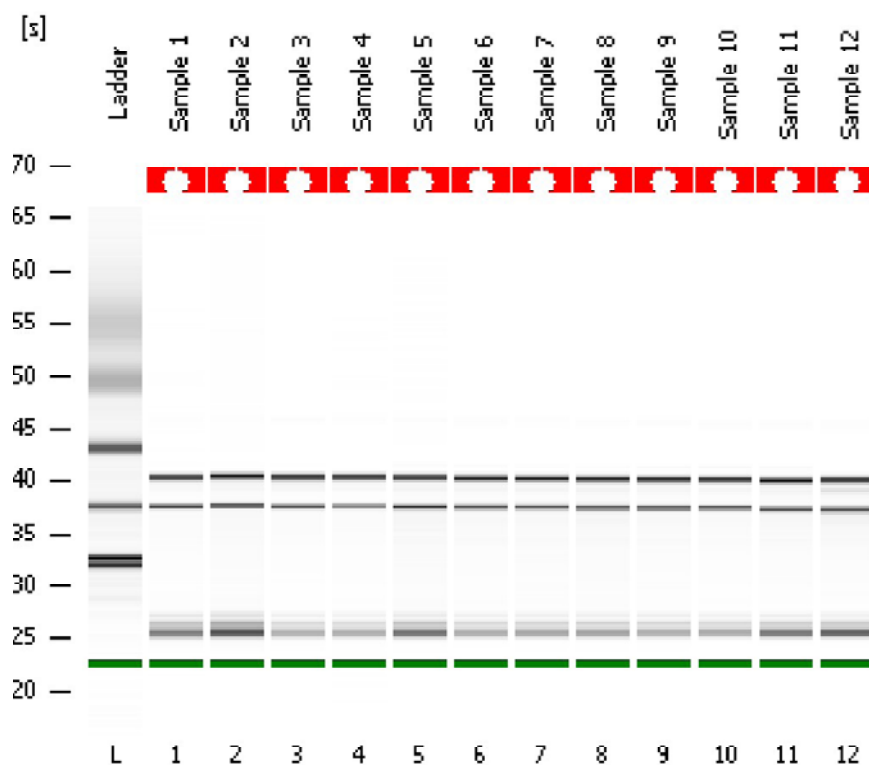
Figure 3. 9 Bioanalyzer gel image for total RNA used in the microarray experiments. Band at 25th s shows 5S rRNA, band at 38th s shows 16S rRNA and band at 40th s indicates 23S rRNA.
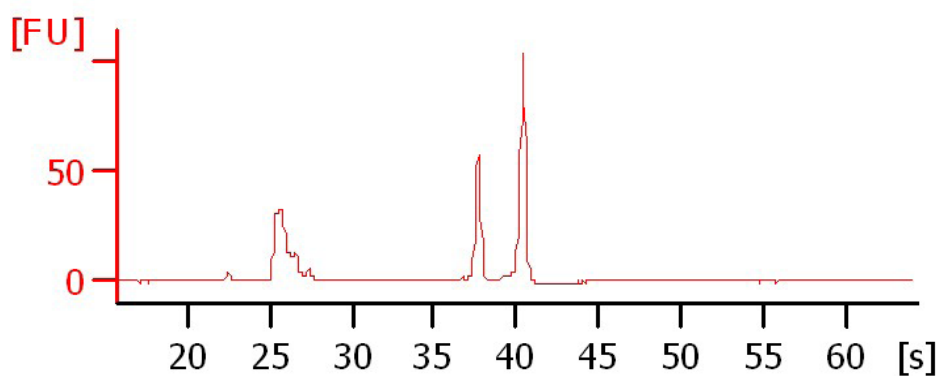
Figure 3. 10 A sample RNA electropherograms

3.2.3. Characterization of the Synthesized cDNA

According to GeneChip®Expression Analysis Technical Manual, a minimum of 1.5 µg of cDNA is needed for subsequent procedures to obtain sufficient material to hybridize onto the array. The concentrations and the $OD_{260/280}$ ratios of the cDNA samples that were used in the microarray experiments are given Table 3.5.

Table 3. 5 The concentrations and the $OD_{260/280}$ ratios of the cDNA

	cDNA	
	260/280 ratio	Concentration (ng/µL)
40mM Acetate / 2mM Glutamate	1.90	458.3
	1.90	443.8
	1.91	493.0
	1.90	501.4
80mM Acetate / 2mM Glutamate	1.92	440.5
	1.92	415.2
	1.91	363.2
	1,89	400.9
40mM Acetate / 5mM NH₄Cl	1.91	399.6
	1.92	419.2
	1.91	418.0
	1.92	365.1

3.2.4. Labeling Efficiency Assessment

It is important to check the efficiency of the labeling procedure in order to prevent hybridizing poorly labeled target onto the probe array. This quality control can be assessed by a bioanalyzer. Unlabelled fragmented cDNA electropherogram and labeled fragmented cDNA electropherogram are given in Figure 3.11 and Figure 3.12 respectively. When these two images are superimposed, the shift due to binding of biotin residues can be seen in Figure 3.13.
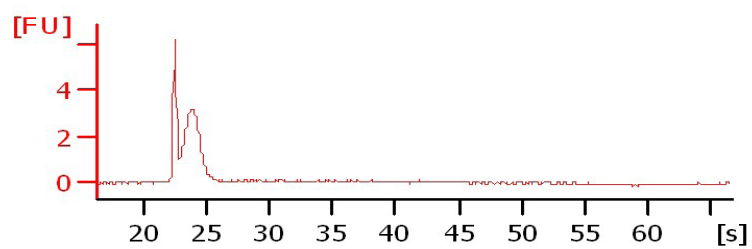
Figure 3. 11 Fragmented cDNA
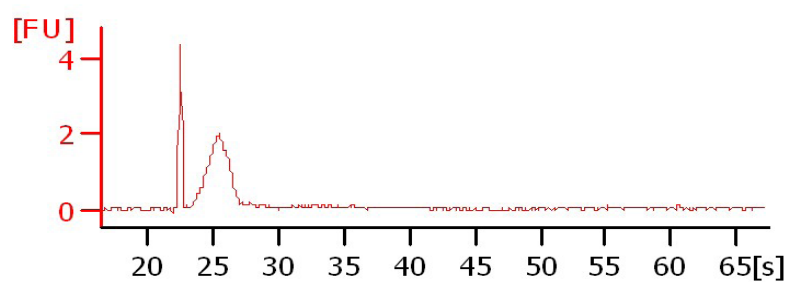
Figure 3. 12 Fragmented and labelled cDNA
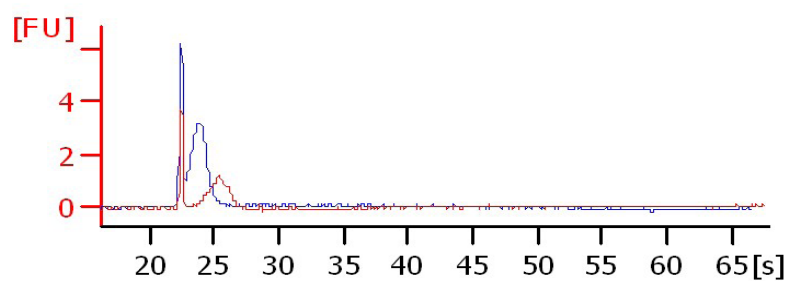
Figure 3. 13 Comparison of labelled and unlabelled cDNA. Blue peak corresponds to cDNA sample before labeling and red peak corresponds to cDNA sample after labeling.

3.2.5. Quality Control for the Microarray Chips

Microarray data were analyzed by using GeneSpring GX (version 11.0.2, Agilent Technologies). Raw data were pre-processed using Robust Multiarray Analysis (RMA) algorithm for background correction, normalization, and log transformation. After pre-processing step, data is analyzed for quality criteria. Quality assessment of samples is important since it ensures that the results obtained at the end of statistical and fold change analysis are meaningful. In order to be able to assess the quality of GeneChip data, a principle component analysis (PCA) was performed. PCA graph is given in Figure 3.14. It was seen that arrays of the same condition were grouped in a similar area and a clear separation was observed for three experimental conditions. This result implied that experiments were carried out in a controlled way and the differences in gene expression values were resulted from the experimental conditions.
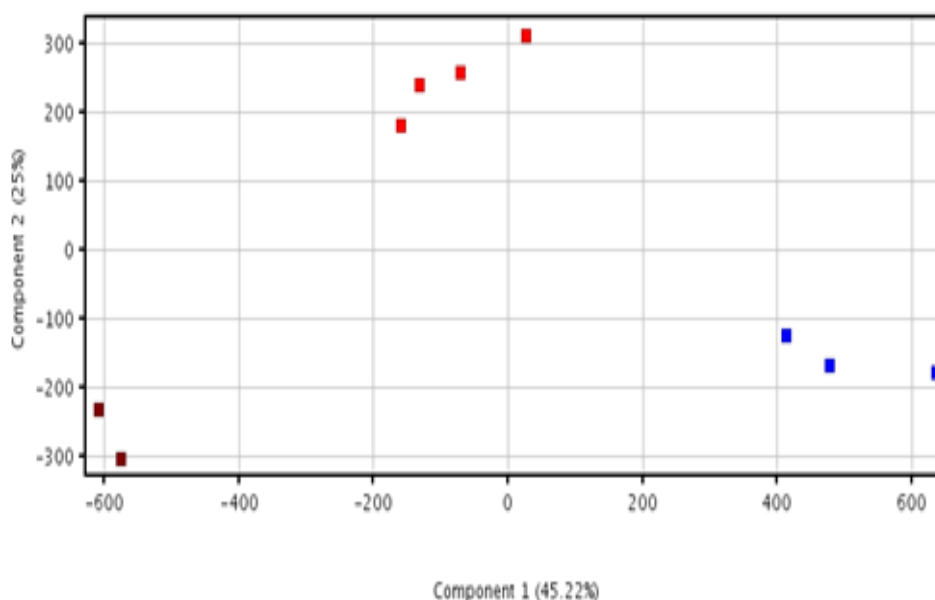
Figure 3. 14 Principle Componant Analysis

3.3. Transcript Profile of *R. capsulatus* on Different Nitrogen Sources

In this study, the effect of different nitrogen sources on *R. capsulatus* metabolism was investigated by comparing transcription profile on 5 mM ammonium chloride and 2 mM glutamate. Concentration of carbon source was 40mM acetate. Probe sets were filtered by expression (lower percentile cut off was set to 20). By this way, probes with very low signal intensity values were eliminated. For the statistical analysis, a one-way ANOVA (p-value <0.05) with a Benjamini-Hochberg p value correction (corrected p-value <0.1) was applied. A fold-change cut-off >1.75 was applied to the significantly changed transcripts. After statistical and fold change analysis, the differentially expressed genes were categorized into groups according to their function.

The profiles plots before and after significance analysis are given in Figure 3.15a and Figure 3.15b respectively. It was observed that 231 transcripts showed a significant difference in expression on ammonium chloride compared to glutamate containing medium. A volcano plot is also given in Figure 3.16. It is a kind of scatter plot that shows changes in expression values of transcripts both according to significance and fold-change. The values that show large magnitude fold changes are located far from the center towards left or right and statistical significance increases from bottom to top.

The functional categories of the significantly changed transcripts on ammonium chloride containing medium compared to glutamate medium is given in pie chart (Figure 3.17).
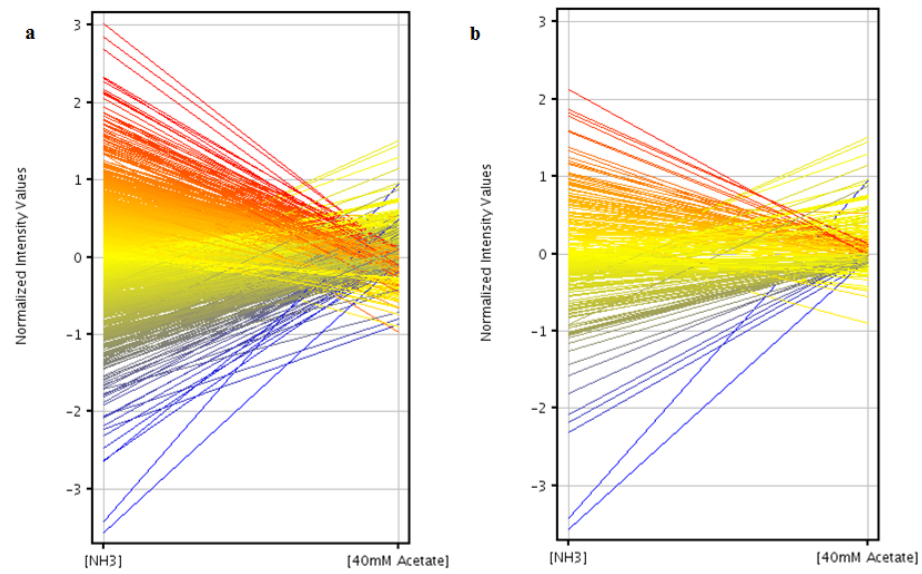
Figure 3. 15 Scatter plot demonstrating the effect of different nitrogen sources a) before significance analysis b) after significance analysis (5mM ammonium chloride vs 2mM glutamate)
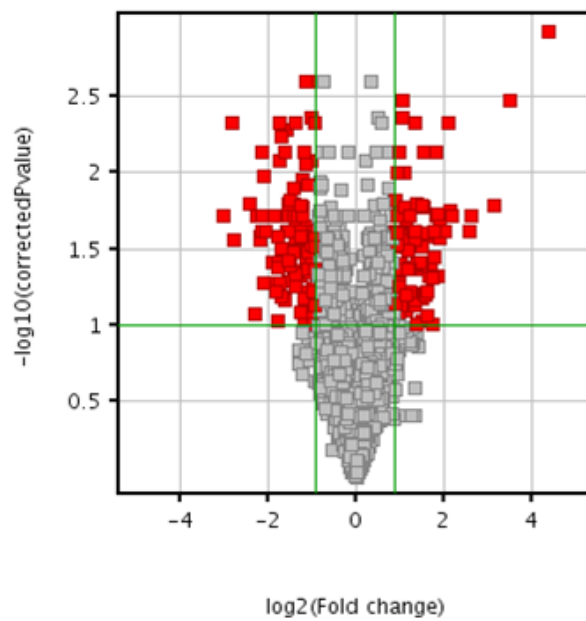
Figure 3. 16 Volcano plot demonstrating the effect of different nitrogen sources (5mM ammonium chloride vs 2mM glutamate)

The most significant changes in expression levels occurred in the energy and central intermediary metabolism (30%) which reflected that the change in nitrogen source shows its primary influence on chemical reactions involved in energy transformations, photosystem, carbon and nitrogen metabolisms. The remarkable changes in expression of genes in the unknown function and hypothetical protein category (28%) might indicate the presence of gaps in the metabolic pathways in this bacterium. A significant difference in the probe sets belonging to 4 intergenic sequences was also observed which showed the possibility of transcribed genes in these regions. The numbers of up and down-regulated transcripts in these functional groups are depicted in the bar graph (Figure 3.18). Total number of up-regulated transcripts was 143 and down-regulated transcripts were 88 on ammonium chloride compared to glutamate medium. The higher number of up-regulated transcripts than that of down-regulated ones on ammonium chloride medium might be due to the higher concentration of nitrogen source in ammonium chloride compared to glutamate medium. Similarly, rich nitrogen source also increased the number of up-regulated proteins in *Rhodospirillum rubrum* when compared to that of nitrogen fixation condition (Selao et al., 2007). The functional categories in which up-regulated transcripts surpassed the down-regulated transcripts are energy and central intermediary metabolism, cellular processes, cell envelope, fatty acid and phospholipid metabolism, signal transduction and regulatory metabolism, transport and binding proteins. On the other hand, the number of down-regulated transcripts was higher in the protein synthesis, protein fate, transcription and unknown and hypothetical protein functional categories on ammonium chloride.
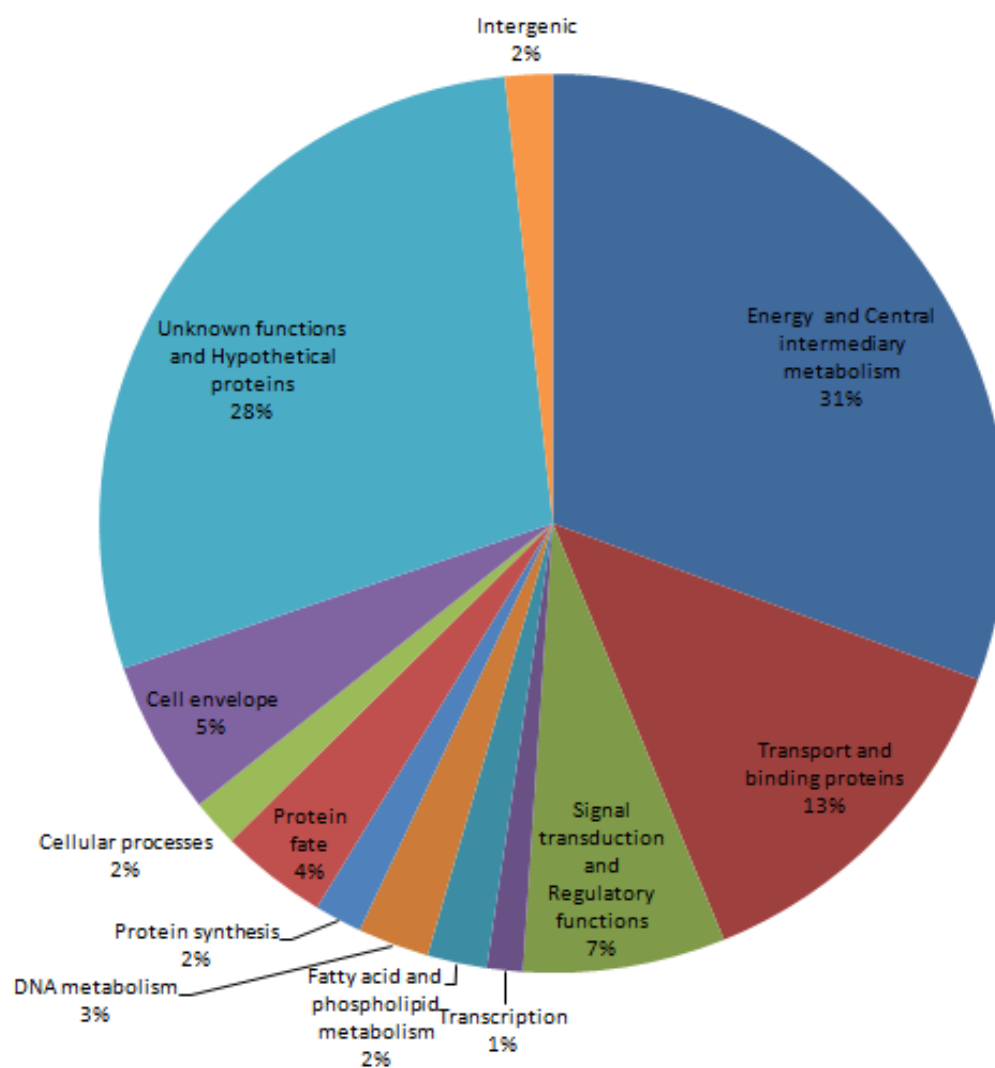
Figure 3. 17 Functional categories of the significantly regulated transcripts on different nitrogen sources (5 mM ammonium chloride vs 2mM glutamate)
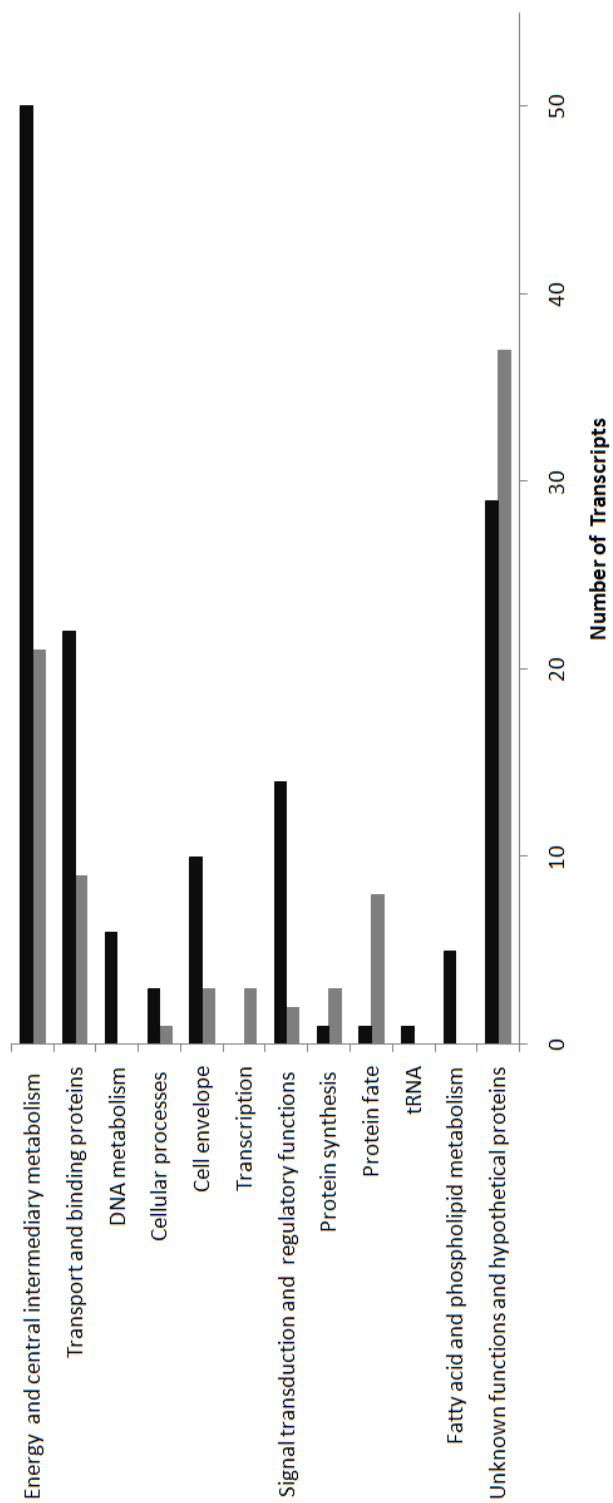
Figure 3. 18 The number of up and down-regulated transcripts in the functrional categories on different nitrogen sources (5mM ammonium chloride vs 2mM glutamate). Black bars indidicate the up-regulated transcripts. Grey bars indicate the down-regulated transcripts.

3.3.1 DNA Metabolism on 5mM Ammonium Chloride vs 2mM Glutamate

Expression of 6 genes related to DNA metabolism functional category showed a significant up-regulation on ammonium chloride medium compared to glutamate medium.

3.3.2. Cellular Processes on 5mM ammonium Chloride vs 2mM Glutamate

In cellular processes functional category, 3 genes exhibited a significant up-regulation, whereas 1 gene showed a down-regulation. Gene expression of FtsA was significantly up-regulated (2.2) on ammonium chloride compared to glutamate containing conditions which indicate the higher rate of cell division. Since it is known that he FtsA protein is involved in bacterial cell division (Goehring and Beckwith, 2005).This result is in accordance with the physiological data since the growth rate of cells in the 5mM ammonium chloride containing medium was lower than the ones in the 2mM glutamate containing medium at the time of cell harvesting. The flaA gene encodes for flagellin protein and involved in flagella synthesis. Its expression was significantly increased (5.34) on ammonium chloride medium compared to glutamate. This result might imply that *R. capsulatus* increases its chemotaxis and mobility abilities towards nutrients in the medium.

3.3.3. Cell Envelope on 5mM Ammonium Chloride vs 2mM Glutamate

Expression of 10 genes in the cell envelope functional category were up-regulated on ammonium chloride. 6 of them are encoding putative cell envelope proteins and their exact function is unknown. On the other hand, expression of 3 genes encoding putative cell envelope proteins significantly down-regulated on ammonium chloride compared to glutamate medium. The fold change difference was around 2 for all differentially expressed genes in this category. However, down-regulation was

remarkable for one gene with probe set ID RCAP_rcc02462_at (11.25). This result might imply that its product might be involved in a function related to glutamate uptake or nitrogen fixation in *R. capsulatus.*

3.3.4. Protein Synthesis on 5mM Ammonium Chloride vs 2mM Glutamate

In protein synthesis functional category, transcription of 4 genes were significantly down-regulated and 1 gene was up-regulated on ammonium chloride compared to glutamate medium. The significantly down-regulated genes (rpsJ, rpmC and rpsQ) were encoding ribosomal protein and given in Table 3.7. Remaining ribosomal proteins which could not pass filtering criteria were also checked for regulation. It was observed that expression of other ribosomal subunit encoding genes were also down-regulated. The genes rpsG and rpsU that showed statistical significant down-regulation with fold changes 1.72 and 1.74 respectively were also included to Table 3.6. The significant down-regulation of ribosomal protein encoding genes on ammonium chloride medium might indicate that cells in the ammonium chloride might have already synthesized majority of the ribosomal proteins. On the other hand, cells were in the early exponential phase in the glutamate medium and were actively synthesizing ribosomal proteins. The translation elongation factor G was significantly up-regulated in ammonium chloride containing medium compared to glutamate medium (Table 3.6). However, the decrease in transcription of fusA gene might not indicate a higher translation alone since other translation initiation and elongation factors did not show a significant change.

87

Table 3. 6 Significantly regulated transcripts in protein synthesis functional category on different nitrogen sources. (FC: Fold Change; NH_4^+ : 5mM Ammonium chloride; Glu: 2mM Glutamate)

Probeset ID	Gene	product	FC and Regulation NH_4^+/Glu*
RCAP_rcc00298_at	rpsJ	30S ribosomal protein S10	1.759↓
RCAP_rcc00308_at	rpmC	50S ribosomal protein L29	2.041↓
RCAP_rcc00309_at	rpsQ	30S ribosomal protein S17	1.778↓
RCAP_rcc00294_at	rpsL	30S ribosomal protein S12	1.96↓
RCAP_rcc00295_at	rpsG	30S ribosomal protein S7	1.72↓
RCAP_rcc00480_at	rpsU	30S ribosomal protein S21	1.74↓
RCAP_rcc01495_at	fusA	translation elongation factor G	2.234↑

*Up-regulation of gene expression is represented with ↑
*Down-regulation of gene expression is represented with ↓

3.3.5. Protein Fate on 5mM Ammonium Chloride vs 2mM Glutamate

When regulation of the genes in the protein fate was investigated, it was observed that 8 genes were significantly down-regulated and only one gene was up-regulated on ammonium chloride medium. In the protein fate functional group, 3 of the down-regulated genes were involved in folding and stabilization; 4 of them were involved in degradation of proteins, peptides, and glycopeptides; 1 of them was involved in protein and peptide secretion; and 1 of them was involved in modification and repair. These results herein might imply that protein metabolism was down-regulated on ammonium chloride containing medium.

3.3.6. Transcription on 5mM Ammonium chloride vs 2mM Glutamate

On ammonium chloride medium, 3 genes were significantly down-regulated in transcription functional category when compared to glutamate medium. The rpoH gene encoding RNA polymerase sigma-32 factor showed a significant down-regulation (2.19) on ammonium chloride medium. Normally, expression of rpoH increases after heat shock and directs expression of heat shock stress proteins such as chaperones and proteases in order to cope with the stress situation at the cellular level. In this study, expression of proteases and chaperons also exhibited a significant down-regulation on ammonium chloride medium which supported the decrease in RNA polymerase sigma-32 factor. Specifically, the clpB gene which encodes the chaperone ClpB was down-regulated (2.25) on ammonium chloride. It is known that clpB promoter is specifically recognized and transcribed by RNA polymerase sigma-32 factor (Kitagawa et al., 1991). In both ammonium chloride and glutamate containing photobioreactors temperature was kept at optimum value which is 30°C for PNS bacteria. For that reason, a shift in the temperature does not seem to be the reason for the higher expression of rpoH gene on glutamate medium. It is known that rpoH expression can also change under several forms of stresses besides heat shock (Ramos et al., 2001). Lower amount of nitrogen source in the glutamate might have created the stress response in *R. capsulatus*.

3.3.7 Signal Transduction and Regulatory Proteins on 5mM Ammonium Chloride vs 2mM Glutamate

In the signal transduction and regulatory proteins functional category, 14 of the significantly changed genes were up-regulated and 2 of them were down-regulated on ammonium chloride medium compared to glutamate medium.

In this study, expression of dksA was significantly up-regulated on ammonium chloride medium compared to glutamate medium. DnaK is a molecular chaperone.

The main role of DnaK is activation of RNA polymerase sigma-32 factor RpoH. The dksA gene encodes a regulatory protein which represses the transcription of DnaK by interacting with DNA. In thisstudy, the increased expression of dksA on ammonium chloride might result in the suppression of DnaK transcription. This result might imply that not only expression of RpoH but also activity could be prevented on ammonium. Expression of 4 genes encoding leucine-responsive regulatory protein family transcriptional regulators significantly increased on ammonium chloride medium. Although they are very widespread in bacteria, their exact function is unknown. However, they are thought to take roles in global and specific regulation of transportation, energy, central metabolism, DNA repair and recombination, bacterial persistence and virulence processes. The remarkable change in these regulators on ammonium chloride compared to glutamate might indicate that they might take part in the regulation of nitrogen metabolism.

RegA is a global regulator which integrates various energy producing and energy utilizing processes in order to be able to regulate redox state of the cell. RegB is the sensor kinase and activates RegA via phosphorylation. In *R. capsulatus*, RegA transcription of genes related to processes that affect reducing equivalents such as photosystem (puf, puc puh operons), components of the respiratory chain (cytochromes, cytochrome bc1 complex), components of the carbon and nitrogen fixation pathways and various dehydrogenases (Elsen et al., 2004; Wu and Bauer, 2008). In this study, expression of RegA significantly increased on ammonium chloride which is in accordance with the increase in pet operon genes encoding cytochrome bc1 complex. The photosynthetic center related genes also showed an up-regulation on ammonium chloride compared to glutamate containing medium. However, the increase was insignificant. For that reason, expression of pufM (FC 1.31 p≥0.2) was examined by qPCR analysis. The RT-qPCR analysis gave a higher fold change difference 1.55. This result might imply the possible role of regA in activation of photosynthesis related gene expression on ammonium containing medium.

The function of up-regulated nitrogen metabolism regulatory protein encoding genes glnB, ntrC genes will be discussed in detail in section 3.10.8.

3.3.8 Fatty acid and phospholipid metabolism on 5mM ammonium chloride vs 2mM glutamate

Significantly regulated genes in fatty acid and phospholipid metabolism functional category on ammonium containing medium is given in table 3.7. In fatty acid and phospholipid metabolism functional category, a significant up-regulation was observed in expression of 5 genes. 4 of them were involved in expression of proteins which take role in the fatty acid and phospholipid degradation (Table 3.7).

Table 3. 7 Significantly regulated genes in fatty acid and phospholipid metabolism functional category on different nitrogen sources. (FC: Fold Change; NH_4^+ : 5mM Ammonium chloride; Glu: 2mM Glutamate)

Probeset ID	Gene	product	FC and Regulation NH_4^+/Glu*
RCAP_rcc00236_at	accD	acetyl-CoA carboxylase, carboxyl transferase, beta subunit	2.38↑
RCAP_rcc01678_at	acpP	acyl carrier protein	2.14↑
RCAP_rcc01884_at		hydrolase, alpha/beta fold family	1.88↑

*Up-regulation of gene expression is represented with↑

3.3.9 Transport and Binding proteins on different nitrogen sources on 5mM ammonium chloride vs 2mM glutamate

31 genes encoding transport and binding proteins showed a significant differential expression on ammonium chloride containing medium compared to glutamate

containing medium. 22 of them showed a significant up-regulation on ammonium chloride compared to glutamate. In these genes 4 of them encode a transporter with an unknown substrate. On the other hand, transcript levels of the 9 transport and binding proteins significantly decreased on ammonium chloride medium compared to glutamate containing medium. Expression of a cation/acetate symporter ActP which is known to be involved in the transport of acetate increased significantly on ammonium chloride medium. The tripartite ATP-independent periplasmic (TRAP) transporters are the most studied family of substrate-binding protein (SBP)-dependent secondary transporters and are present only in prokaryotes (Mulligan et al., 2010). It is encoded by dctPQM genes in *R. capsulatus* (Forward et al., 1997). In this study, expression of dctP, dctM and dctQ genes were significantly up-regulated on ammonium chloride compared to glutamate containing medium and this might imply a higher synthesis of TRAP transporters. It is known that TRAP transporters can bind flexibly to organic acids and have the potential to tranfer organic acids with a variety of different sizes (Fischer et al., 2010). In pseudomonas, a homolog dct TRAP transporter encoded by dctABD genes was found to be involved in transport of several organic acids including acetate (Nam et al., 2003). The significant increase in expression of TRAP transporter on ammonium chloride in this study might imply that it might take role in transport of acetate. The increase in expression of cation/acetate symporter ActP and dct TRAP transporter might indicate that although concentration of acetate was same in both conditions, more acetate was transported, and a higher amount of carbon source was available in the cell.

It is known that the ammonium transporter Amt of *R. capsulatus* takes role in the uptake of ammonium from low-ammonium-concentration solutions where passive diffusion of the ammonia is not sufficient. After binding of NH_4^+ to Amt, it is deprotonated inside the periplasmic interface and is subsequently reprotonated on the cytoplasmic side (Masepohl and Hallenbeck, 2010). *R. capsulatus* possesses two potential amt proteins AmtB and AmtY (Yakunin and Hallenbeck, 2002). Although

the function of the AmtY is still not clear, it was shown that AmtB is involved not only in ammonium transport bu also in sensing of extracellular NH_4^+ concentration and post-translational regulation of nitrogenase (Masepohl and Kranz, 2009; Masepohl and Hallenbeck, 2010). The mechanism for AmtB related regulation of nitrogenase proposed for *R. capsulatus* is discussed in detail in section 3.3.1.11. As expected, in this study expression of amtB gene significantly increased on ammonium chloride containing medium compared to glutamate containing medium and implied the synthesis of ammonium transporter which facilitated the transport of charged ammonium ions.

3.3.10 Energy and Central Intermediary Metabolism on 5mM Ammonium Chloride vs 2mM Glutamate

The number of differentially expressed genes was highest in the energy metabolism and central intermediary metabolism functional group among the other categories. 50 of the genes were significantly up-regulated whereas 21 of them were down-regulated. This result indicated that the major influence of different nitrogen sources was seen on chemical reactions involved in energy transformations, TCA cycle, electron transport, carbon and nitrogen metabolisms. Important processes of energy and central intermediary metabolism and their regulation will be discussed in detail in the following sections.

3.3.10.1 Acetate Assimilation on 5mM Ammonium Chloride vs 2mM Glutamate

Acetate-CoA ligase enzyme is involved regulation of acetate entry to carbon metabolism. A significant up-regulation in expression two genes encoding acetate-CoA ligase (7.349 and 2.006) was noticed on ammonium chloride compared to glutamate containing medium. The obtained result might imply that more carbon source is fed to the TCA cycle for catabolic and anabolic reactions on rich nitrogen

source ammonium chloride. Similarly, expression of acetate-CoA ligase protein increased in *Rhodospirillum rubrum* grown in nitrogen rich medium compared to nitrogen fixing condition (Selao et al., 2007).

Acetate which enters the TCA cycle at the level of acetyl-CoA requires side pathways where C4 acid malate is synthesized. Glyoxylate, citramalate and ethylmalonyl-CoA pathways are the known pathways that take role in different PNS bacteria to utilize acetate (Kars and Gündüz, 2010).

Isocitrate lyase is one of the two main enzymes of the glyoxylate cycle that replenishes TCA cycle intermediates and allows growth on 2 carbon acetate. In this study, expression of isocitrate lyase significantly increased (2.781) on ammonium chloride medium compared to glutamate medium. In literature, isocitrate activity of *R. capsulatus* has been widely studied and conflicting results have been obtained. While several studies reported the complete absence of its activity (Albers and Gottschalk, 1976; Meister et al., 2005), others were able to show its activity on acetate (Kornberg and Lascelles, 1960; Willison, 1988; Petrushkova and Tsygankov, 2011). Petrushkova and Tsygankov (2011) sugested that different isocitrate activities could be obtained even for the same strain of *R. capsulatus* depending on the previous history of the culture and on the growth phase. In this study, the increase in expression value of isocitrate lyase might indicate an active glyoxylate cycle operating in *R. capsulatus*. On contrary to isocitrate lyase, expression of the second main enzyme of glyoxylate pathway which is malate synthase did not exhibit a significant change. This might be due to its constitutive expression under both conditions. Previously, isocitrate lyase activity was detected on acetate grown cells (Willison, 1988) but its expression was found to be constitutive in *R. capsulatus* (Tabita, 1995).

94

KEGG (Kyoto Encyclopedia of Genes and Genomes) PATHWAY database was searched for *R. capsulatus* ethlymalonyl-CoA pathway and it was observed that *R. capsulatus* has the genetic potential for acetate assimilation via ethylmalonyl-coA pathway (Figure 3.19).
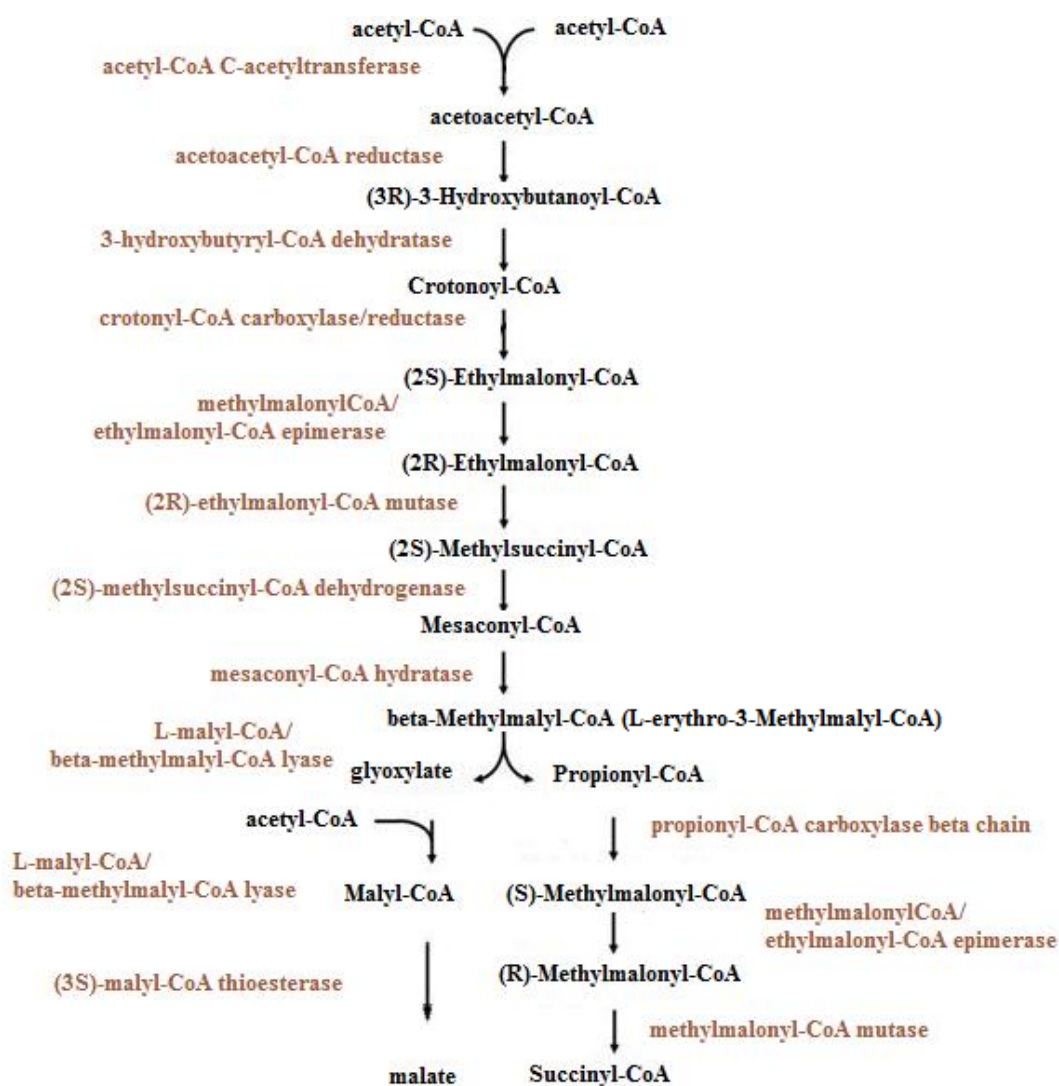
Figure 3. 19 Ethlymalonyl-CoA pathway according to KEGG PATHWAY. Enzyme names are given according to their functional orthologs in the ethlymalonyl-CoA pathway.

However, its presence has not been proven with a molecular study. The screenshot of the KEGG pathway for *R. capsulatus* ethylmalonyl-CoA pathway is given in Appendix C. In this study, 10 enzymes which take role in the ethylmalonyl-CoA pathway showed a statistically significant up-regulation on ammonium containing medium compared to glutamate medium. The fold change values, original annotation and functional orthologs in *R. capsulatus* of the significantly changed transcripts regarding to ethlymalonyl-CoA pathway are given in (Table 3.8). The remaining 3 enzymes of the pathway which are 3-hydroxybutyryl-CoA dehydratase functional ortholog enoyl-CoA hydratase, mesaconyl-CoA hydratase functional ortholog MaoC domain protein and methylmalonyl-CoA mutase also showed a statistical up-regulation but the fold change values were smaller than 1.75 and for that reason they are not included into Table 3.8.

The initial two reactions of the ethylmalonyl-CoA pathway which are catalyzed by acetyl-CoA acetyltransferase and acetoacetyl-CoA reductase overlap with the polyhydroxybutyrate biosynthesis (Figure 3.20). The 3-hydroxybuty-CoA produced can be used for synthetis of polyhydroxybutyrate or assimilated via ethylmalonyl-CoA pathway for malate biosynthesis. Polyhydroxybutyrate synthase is the determinant enzyme for PHB biosynthesis and crotonyl-CoA carboxylase/reductase is seen as the commited step for acetate assimilation in the ethylmalonyl-CoA pathway (Alber, 2011). When the expression values of these two enzymes are compared, although the polyhydroxybutyrate synthase expression did not how a significant change, expression of crotonyl-CoA carboxylase/reductase increased significantly on ammonium chloride compared to glutamate. These results might show that majority of the acetate was utilized for assimilation purposes rather that PHB biosynthesis on ammonium chloride.

Table 3. 8 Genes that are significantly regulated in ethylmalonyl-CoA pathway on different nitrogen sources. (FC: Fold Change; NH_4^+ : 5mM Ammonium chloride; Glu: 2mM Glutamate)

Probe set ID	Gene	Product (original annotation)	Ortholog (KEGG PATHWAY)	FC and Regulation NH_4^+/Glu*
RCAP_rcc03178_at	atoB	acetyl-CoA acetyltransferase	acetyl-CoA acetyltransferase	2.905↑
RCAP_rcc03449_at	atoB	acetyl-CoA acetyltransferase	acetyl-CoA acetyltransferase	3.460↑
RCAP_rcc03179_at	phbB	acetoacetyl-CoA reductase	acetoacetyl-CoA reductase	4.095↑
RCAP_rcc03243_at	ccrA	crotonyl-CoA reductase	crotonyl-CoA carboxylase/ reductase	2.188↑
RCAP_rcc00538_at		methylmalonyl-CoA epimerase	methylmalonyl-CoA/ ethylmalonyl-CoA epimerase	1.917↑
RCAP_rcc03241_at	mutB	methylmalonyl-CoA mutase, large subunit	(2R)-ethylmalonyl-CoA mutase	2.482↑
RCAP_rcc03306_at		acyl-CoA dehydrogenase, medium-chain specific	(2S)-methylsuccinyl-CoA dehydrogenase	1.881↑
RCAP_rcc03164_at	citE	citrate lyase, beta subunit	L-malyl-CoA/beta-methylmalyl-CoA lyase	2.131↑
RCAP_rcc00727_at	citE	citrate lyase, beta subunit	(3S)-malyl-CoA thioesterase	2.003↑
RCAP_rcc00911_at	pccA	propionyl-CoA carboxylase, alpha subunit	propionyl-CoA carboxylase beta chain	1.831↑

*Up-regulation of gene expression is represented with ↑.
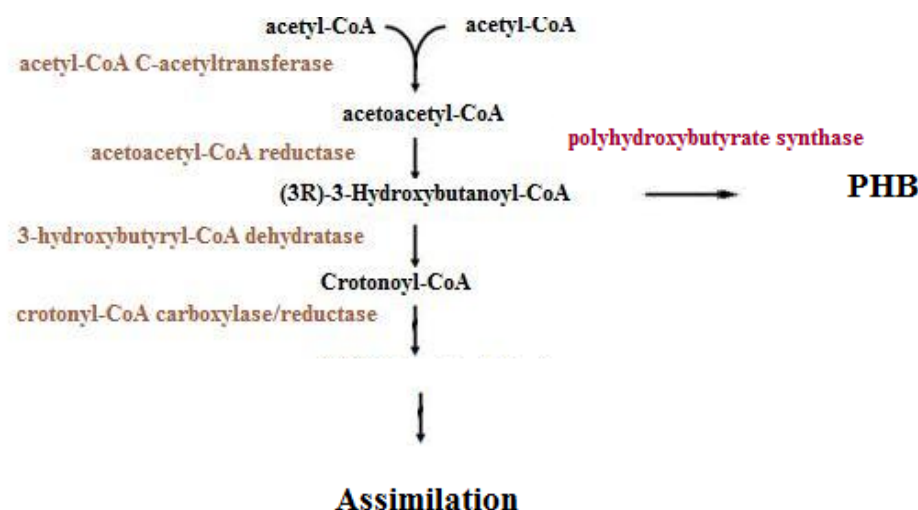
Figure 3. 20 Competing PHB production and ethylmalonyl-CoA pathway in *R. capsulatus*

This study showed for the first time that *R. capsulatus* might assimilate acetate by using both glyoxylate cycle and ethylmalonyl-CoA pathway. Expression of the enzymes of these two routes under the same condition might indicate that, they can be active at the same time or can switch from one route to another. Similarly, it was proposed that another PNS bacteria *R. rubrum* can assimilate acetate by using two different routes, citramalate cycle and/or ethylmalonyl-CoA pathway (Berg and Ivanovsky, 2009).

3.3.10.2 TCA Cycle on 5mM Ammonium Chloride vs 2mM Glutamate

Transcript level of 6 TCA cycle related genes (sucD encoding Succinyl-CoA synthetase (ADP forming), alpha subunit, sucA and sucB for oxoglutarate dehydrogenase, icd for Isocitrate dehydrogenase, acnA for aconitate hydratase and gltA for citrate synthase, maeB for malate dehydrogenase) increased significantly on ammonium containing medium (Table 3.9). The carbon substrate which was acetate in this study is fed into the TCA cycle where it is oxidized to produce CO_2 and electrons for ATP production. In addition to energy production purposes, some of

the TCA cycle genes also take role in acetate assimilation via glyoxylate cycle for biosynthetis of cell components. In addition to the unique gyloxylate cycle enzyme isocitrate lyase, expression of TCA cycle enzymes citrate synthase, aconitate hydratase and malate dehydrogenase which also take role in glyoxylate cycle showed a significant increase. These results suggest that high ammonium concentration stimulates acetate metabolism of *R. capsulatus*.

Table 3. 9 Significantly regulated genes encoding TCA cycle enzymes on different nitrogen sources. (FC: Fold Change; NH_4^+ : 5mM Ammonium chloride; Glu: 2mM Glutamate)

Probeset ID	Gene	Product	FC and Regulation NH_4^+/Glu*
RCAP_rcc00721_at	sucD	Succinyl-CoA synthetase (ADP forming), alpha subunit	2.23↑
RCAP_rcc00724_at	sucA	oxoglutarate dehydrogenase (succinyl-transferring), E1 component	1.91↑
RCAP_rcc00725_at	sucB	dihydrolipoyllysine-residue succinyltransferase (succinyl-transferring), E2 component	2.71↑
RCAP_rcc01887_at	icd	Isocitrate dehydrogenase (NADP(+))	2.85↑
RCAP_rcc02150_at	acnA	aconitate hydratase	3.25↑
RCAP_rcc02364_at	gltA	citrate (Si)-synthase	2.97↑
RCAP_rcc03496_at	maeB	malate dehydrogenase (oxaloacetate-decarboxylating NADP(+))	1.99↑

*Up-regulation of gene expression is represented with ↑.

3.3.10.3. Electron Transport on 5mM Ammonium Chloride vs 2mM Glutamate

NADH-quinone oxidoreductase (complex I) is a multisubunit enzyme catalyzes the oxidation of NADH and pumps protons across the inner membrane of mitochondria or the plasma membrane of many bacteria. It is encoded by the 14 genes of the nuo operon in *Rhodobacter capsulatus* (NuoABCDEFGHIJKLMN) (Brandt, 2006). It is known that NADH-quinone oxidoreductase is involved in photoheterothrophic metabolism of *R. capsulatus* and work in reverse direction to reduce NAD^+ (Herter et al., 1998). The NADH produced is then utilized for biomass synthesis, CO_2 fixation, PHB production and nitrogenase activity via ferredoxin (Golomysova et al., 2010). In this work, expression of 9 nuo genes were significantly up-regulated on ammonium medium which might result in a higher NADH production compared to that on glutamate medium (Table 3.10). In addition to nuo gene cluster, expression of a gene with an orthology to eukaryotic NADH ubiquinone oxidoreductase subunit, NDUFA4, family was also up-regulated. It is thought that this gene encodes an accessory protein that is required for assembly of several accessory eukaryotic NADH-quinone oxidoreductase. The change in this gene might indicate that this gene product might also take role in assembly of prokaryotic NADH-quinone oxidoreductase.

Cytochrome bc1 complex (Complex III) is a multi-subunit membrane bound enzyme that takes role in energy transduction pathways of *R. capsulatus*. It performs the transfer of electrons from the ubiquinol pool to cytochrome c carriers, contribute to the generation of membrane potential by pumping protons from the cytoplasm to the periplasm. The cyt bc1 complex is composed of three subunits (the Fe/S protein, cyt b and cyt c1), which are encoded by three structural genes petA, petB, and petC, respectively (Lanciano et al., 2011). Expression of PetC which encodes cytochrome c1 subunit of Cytochrome bc1 significantly increased 2.298 on ammonium medium which might result in a steeper electrochemical gradient for the ATP synthase compared to that in hydrogen production mediu

Table 3. 10 Significantly regulated genes encoding NADH-quinone oxidoreductase on different nitrogen sources. (FC: Fold Change; NH_4^+ : 5mM Ammonium chloride; Glu: 2mM Glutamate)

Probeset ID	Gene	Product	FC and Regulation NH_4^+/Glu*
RCAP_rcc01521_at	nuoE	NADH-quinone oxidoreductase, E subunit	2.165↑
RCAP_rcc01523_at	nuoF	NADH-quinone oxidoreductase, F subunit	1.957↑
RCAP_rcc01527_at	nuoG	NADH-quinone oxidoreductase, G subunit	2.422↑
RCAP_rcc01529_at	nuoH	NADH-quinone oxidoreductase, H subunit	3.142↑
RCAP_rcc01531_at	nuoI	NADH-quinone oxidoreductase, I subunit	4.475↑
RCAP_rcc01533_at	nuoJ	NADH-quinone oxidoreductase, J subunit	2.476↑
RCAP_rcc01534_at	nuoK	NADH-quinone oxidoreductase, K subunit	3.581↑
RCAP_rcc01535_at	nuoL	NADH-quinone oxidoreductase, L subunit	4.534↑
RCAP_rcc01537_at	nuoN	NADH-quinone oxidoreductase, N subunit	1.790↑
RCAP_rcc01385		NADH ubiquinone oxidoreductase subunit, NDUFA4, family	1.94 ↑

*Up-regulation of gene expression is represented with ↑.

3.3.10.4. ATP Synthases on 5mM Ammonium Chloride vs 2mM Glutamate

The cyclic electron flow through the photosynthetic membrane apparatus results in the generation of a proton motive force and ATP synthase enzyme catalysis ATP production (McKinlay and Harwood, 2010). ATP is then used for for growth, as well as for the hydrogen production activity of nitrogenase.   Ammonium medium resulted in a significant elevation in expression values of ATP synthase F0 and F1 subunit expressions elevated compared to glutamate containing medium which

implied a higher ATP production. Since nitrogen fixation was completely prevented due to high ammonium, produced ATP was most probably utilized for growth and biosynthetic purposes rather than nitrogen fixation.

Table 3. 11 Significantly regulated genes encoding ATP synthase on different nitrogen sources. (FC: Fold Change; NH_4^+ : 5mM Ammonium chloride; Glu: 2mM Glutamate)

Probeset ID	Gene	Product	FC and Regulation NH_4^+/Glu*
RCAP_rcc00744_at	atpF	ATP synthase F0, B subunit	1.968↑
RCAP_rcc02970_at	atpC	ATP synthase F1, epsilon subunit	1.949↑
RCAP_rcc02971_at	atpD	ATP synthase F1, beta subunit	1.769 ↑

*Up-regulation of gene expression is represented with ↑.

3.3.10.5. Calvin Cycle and Redox Balance on 5mM Ammonium Chloride vs 2mM Glutamate

In this study, expression of genes encoding TCA cycle genes and NADH-quinone oxidoreductase subunits significantly increased on ammonium chloride containing medium compared to glutamate containing medium. These results indicated that a higher CO_2 and NADH were generated. Expression and activity of nitrogenase were inhibited by ammonium chloride and for that reason nitrogenase activity could not be used to dissipate excess electrons via NADH oxidation. Other than nitrogenase activity, Calvin cycle is also involved in dissipation of excess electrons in PNS bacteria under photoheterotrophic growth mode. In this study, different nitrogen sources did not result in a significant change in the transcript level of RubisCo and phosphoribulokinase enzymes which catalyzes the two unique reactions of the calvin cycle. These results might imply that higher NADH production on ammonium chloride medium did not cause an increase in Calvin cycle enzyme expression when

compared to glutamate medium and reducing equivalents are dissipated in another way. In addition to acetate assimilation role, the increased expression of ethlymalonyl-CoA pathway enzymes in this study might have a role in redox balance on ammonium chloride containing medium. Since previous studies reported that acetate assimilation via ethylmalonyl-CoA pathway can consume enough reducing equivalents (and CO_2) so that Calvin cycle and hydrogen production are not needed for redox balance (Hadicke et al, 2011; McKinlay and Harwood, 2011) which might be the situation in this study.

3.3.10.6. Nitrogen Fixation on 5mM Ammonium Chloride vs 2mM Glutamate

It is known that ammonium is an inhibitor of nitrogenase transcription and activity. In this study, transcription of Mo-nitrogenase structural genes (*nifHDK),* nitrogenase molybdenum-iron cofactor biosynthesis genes (nifN, nifU and nifX) were significantly down-regulated on ammonium chloride medium compared to glutamate containing medium as expected (Table 3.12). Down-regulation of nitrogenase genes by ammonium has been also reported by other studies (Masepohl and Kranz, 2009, Akköse et al., 2009, Kontur et al., 2011; Pekgöz et al., 2011).

3.3.10.7. Electron Transport to Nitrogenase on 5mM Ammonium chloride vs 2mM Glutamate

The rnfABCDGEH genes of *Rhodobacter capsulatus* encode a membrane protein complex that is essential for nitrogenase enzyme activity. By using the membrane potential, this complex transfers electrons from photosynthetic membrane to ferredoxin which is the ultimate donor for nitrogenase (Jouanneau et al., 1998; Biegel et al., 2011). Similar to nitrogenase genes, Rnf electron transport complex protein structural genes were significantly down-regulated on ammonium chloride

medium compared to glutamate (Table 3.13). Similarly, Kontur et al. (2011) also observed in *R. sphaeroides* that rnf structural genes were down-regulated in ammonium containing medium compared to glutamate containing medium.

Expression of ferredoxin I and ferredoxin V was significantly lower ammonium chloride media compared to glutamate media (Table 3.13). The expression of ferredoxin V was also lower in non-H_2-producing *R. sphaeroides* cells when compared to H_2-producing cells and it was suggested that ferredoxin V may also have a role in electron transport to nitrogenase (Kontur et al., 2011). The lower transcript abundance of ferredoxin V in this study on ammonium rich conditions might indicate that it is only expressed and needed under hydrogen production condition on glutamate for transfer of electrons to nitrogenase.

Table 3. 12 Significantly regulated genes encoding nitrogenase enzyme on different nitrogen sources. (FC: Fold Change; NH_4^+ : 5mM Ammonium chloride; Glu: 2mM Glutamate)

Probeset ID	Gene	Product	FC and Regulation NH_4^+/Glu*
RCAP_rcc00570_at	nifK	nitrogenase molybdenum-iron protein beta chain	3.519 ↓
RCAP_rcc00571_at	nifD	nitrogenase molybdenum-iron protein alpha chain	3.531 ↓
RCAP_rcc00572_at	nifH	nitrogenase iron protein	2.541 ↓
RCAP_rcc03271_at	nifU	nitrogen fixation protein NifU	8.030 ↓
RCAP_rcc03278_at	nifX	nitrogen fixation protein NifX	2.243 ↓
RCAP_rcc03279_at	nifN	nitrogenase molybdenum-iron cofactor biosynthesis protein NifN	1.945 ↓

*Down-regulation of gene expression is represented with ↓.

Table 3. 13 Significantly regulated genes encoding proteins involved in electron transport to nitrogenase on different nitrogen sources. (FC: Fold Change; NH_4^+ : 5mM Ammonium chloride; Glu: 2mM Glutamate)

Probeset ID	Gene	Product	FC and Regulation NH_4^+/Glu*
RCAP_rcc03287_at	rnfA	electron transport complex protein RnfA	3.31↓
RCAP_rcc03288_at	rnfB	electron transport complex protein RnfB	2.27↓
RCAP_rcc03289_at	rnfC	electron transport complex protein RnfC	2.75 ↓
RCAP_rcc03290_at	rnfD	electron transport complex protein RnfD	3.32↓
RCAP_rcc00573_at	fdxD	ferredoxin V	20.6 ↓
RCAP_rcc03284_at	fdxN	ferredoxin I	2.76 ↓

*Down-regulation of gene expression is represented with ↓.

3.3.10.8. Regulation of Nitrogen Fixation on 5mM Ammonium Chloride vs 2mM Glutamate

Nitrogen fixation reaction requires a large input of energy which is 20-30 mol of ATP for reduction of 1 mol N_2. For this reason, this highly energy demanding process is strictly controlled in *R. capsulatus* and in other PNS bacteria. Activation of transcription of the nitrogenase genes in *R. capsulatus* occurs under the control of the NifA protein. At the transcriptional level, the NtrB/NtrC two-component system regulates expression of nifA gene. In turn, NifA protein activates the transcription of the other nif genes, including the structural genes of nitrogenase. At the post translational level, both the NifA and nitrogenase activity can be regulated. (Masepohl and Kranz, 2009; Masepohl and Hallenbeck, 2010).

PII-like signal transduction proteins GlnB and GlnK take role in regulation of nitrogenase activity at the transcriptional and post translational levels. GlnB plays a major role in the transcriptional level control of nifA via NtrBC two-component system. When the cells are under nitrogen limited condition, NtrC is phosphorylated by NtrB and transcription of nifA is activated. On the other hand, when the nitrogen source is in excess GlnB binds to NtrB and prevents phosphorylation of NtrC. NtrC in the dephosphorylated form cannot activate nifA expression (Masepohl and Kranz, 2009; Masepohl and Hallenbeck, 2010). In the present study, there was a significant increase in of glnB (1.82) and NtrC (2.13) expression on ammonium chloride medium, however the decrease in expression of nifA was found to be statistically insignificant. It is known that microarray analysis can underestimate the fold change differences compared to RT-qPCR method and the decrease in nifA expression might be greater in reality. Another possibility is that the small decrease in expression of NifA regulatory protein might have created a greater effect and resulted in significant decrease in nitrogenase related nif genes. In addition to transcriptional control of nifA gene, NifA protein is also regulated at the post translational level. Bacteria were actively producing hydrogen before inoculation to ammonium containing medium so that both NifA protein and nitrogenase might have been present in the cells. It is known that when the nitrogen source is in excess, GlnB and GlnK can bind to NifA and inhibit its activity at the post-translational level. The significant increase in GlnB and GlnK PII-like proteins in this study might be the reason for decrease in NifA activity and nif gene expression. Similarly, either GlnB (1.82) or GlnK (4.29) was enough to prevent NifA activity in *R. capsulatus* after ammonium addition to a nitrogen fixing culture (Drepper et al., 2003).

Nitrogenase activity can be also post-translationally regulated. The ammonium transporter (AmtB) was found to be involved in ammonium sensing and regulation of nitrogen fixation in *R. capsulatus*. PII protein GlnK is most of the time co-transcribed with AmtB and forms a complex with amptB when ammonium is

present in the medium. GlnK-AmptB complex can regulate the activity of nitrogenase at the post translational level. There are two proposed approaches for regulation of nitrogenase GlnK-AmptB complex in R. capsulatus: ADP-ribosylation dependent regulation mediated by DraT (dinitrogenase reductase ADP-ribosyltransferase) and DraG (dinitrogenase-reductase-activating glycohydrolase) or ADP-ribosylation-independent regulation. When nitrogen level in the cell is high, DraT protein modifies dinitrogenase reductase via ADP-ribosylation and swiches off nitrogenase activity. On the other hand, DraG is involved in demodification and reactivation of nitrogenase. Under high ammonium conditions, nitrogenase is in ADP ribosylated form and inactive. The role of GlnK-AmtB complex is thought to sequester DraG and keep it away from its substarate nitrogenase reductase. By this way DraG cannot remove ADP ribosylation and inactive form of nitrogenase accumulates. In the ADP ribosylation independen approach, it is hypothesized that GlnK-AmtB complex could requit one or more components of the Rnf complex and electron supply to nitrogenase is inhibited (Tremblay et al., 2007; Masepohl and Hallenbeck, 2010). In this study both GlnK and AmtB proteins showed a significant increase on ammonium containing medium compared to glutamate containing nitrogen limited medium. These results might indicate that in addition to ammonium transport function of AmtB, it might form a complex with GlnK and regulate nitrogenase activity at the translational level.

3.4 Global Transcription Profile of *R. capsulatus* on Different Acetate Concentrations

The effect of initial acetate concentration on metabolism of *R. capsulatus* was investigated by comparing global transcription profiles on 80mM and 40mM acetate containing media using microarray analysis. Probe sets were filtered by expression (lower percentile cut off was set to 20). One-way ANOVA (p-value <0.05) with a Benjamini-Hochberg p value correction (corrected p-value <0.1) was applied for statistical analysis. A fold-change cut-off >1.75 was applied to the significantly

107

changed transcripts. After statistical and fold change analysis, the differentially expressed genes were categorized into groups according to their function.

The profile plots before and after significance analysis are given in Figure 3.21a and Figure 3.21b respectively. It was observed that 304 transcripts showed a significant change in expression on 80mM acetate containing medium compared to those in 40mM acetate containing medium. The volcano plot was obtained for the significantly changed transcripts and given in Figure 3.22.
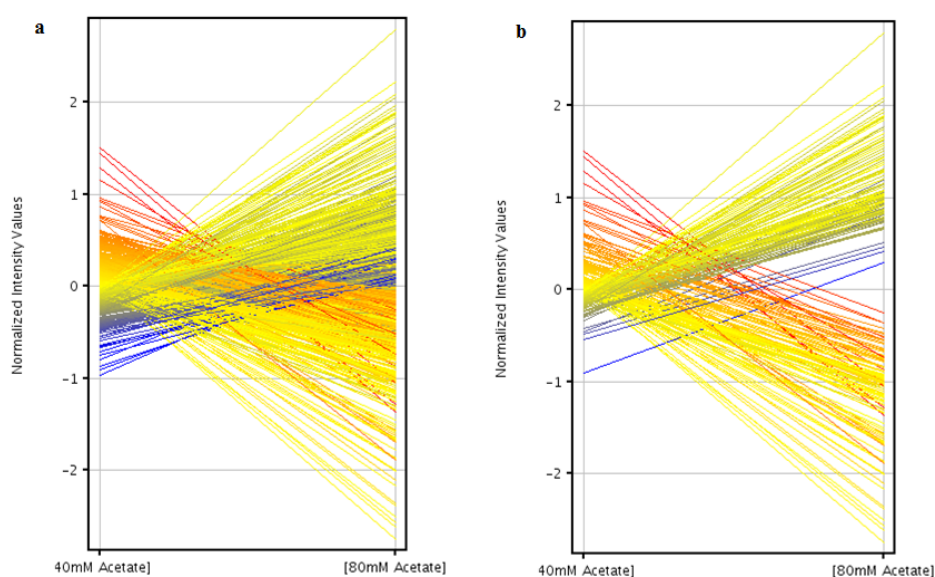
Figure 3. 21 Profile plot demonstrating the effect of different acetate concentrations a) before significance analysis b(after significance analysis (80mM vs 40mM)
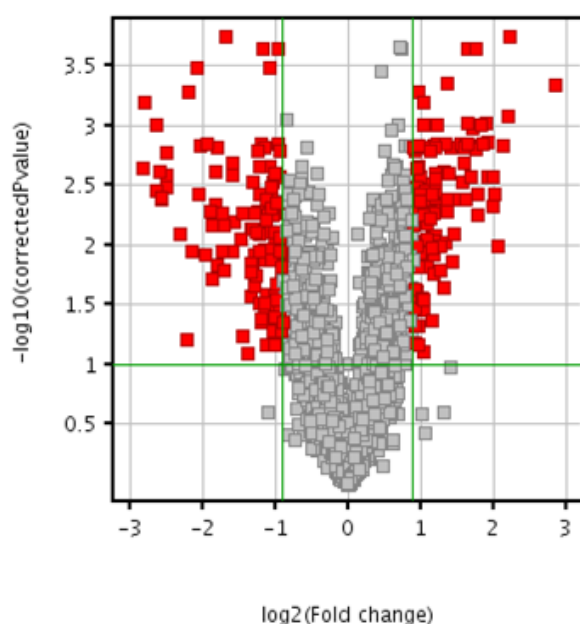
Figure 3. 22 Volcano plot demonstrating the effect of different acetate concentrations

The effect of different acetate concentrations on expression levels of *R. capsulatus* was most remarkable in the energy and central intermediary metabolism (22%) and unknown function and hypothetical protein (28%) functional categories (Figure 3.23). Similar to different nitrogen sources, the primary influence of the change in concentration of acetate was also seen on chemical reactions involved in energy transformations, photosystem, carbon and nitrogen metabolisms. The significant changes in expression levels of genes in the unknown function and hypothetical protein category might indicate the presence of gaps in the metabolic pathways in this bacterium. A significant difference in the probe sets belonging to 7 intergenic sequences was also observed which showed the possibility of transcribed genes in these regions.

The number of up and down-regulated transcripts in these functional groups are depicted in the bar graph (Figure 3.24). The number of up-regulated transcripts was 143 and the number of down-regulated ones are 161.

The functional categories in which up-regulated transcripts surpassed the down-regulated transcripts are purines, pyrimidines, nucleosides and nucleotides; cell envelope; DNA metabolism; transcription; signal transduction and regulatory functions; and unknown and hypothetical proteins. On the other hand, in energy and central intermediary metabolism; amino acid biosynthesis; protein synthesis; fatty acid and phospholipid metabolism; transport and binding proteins.
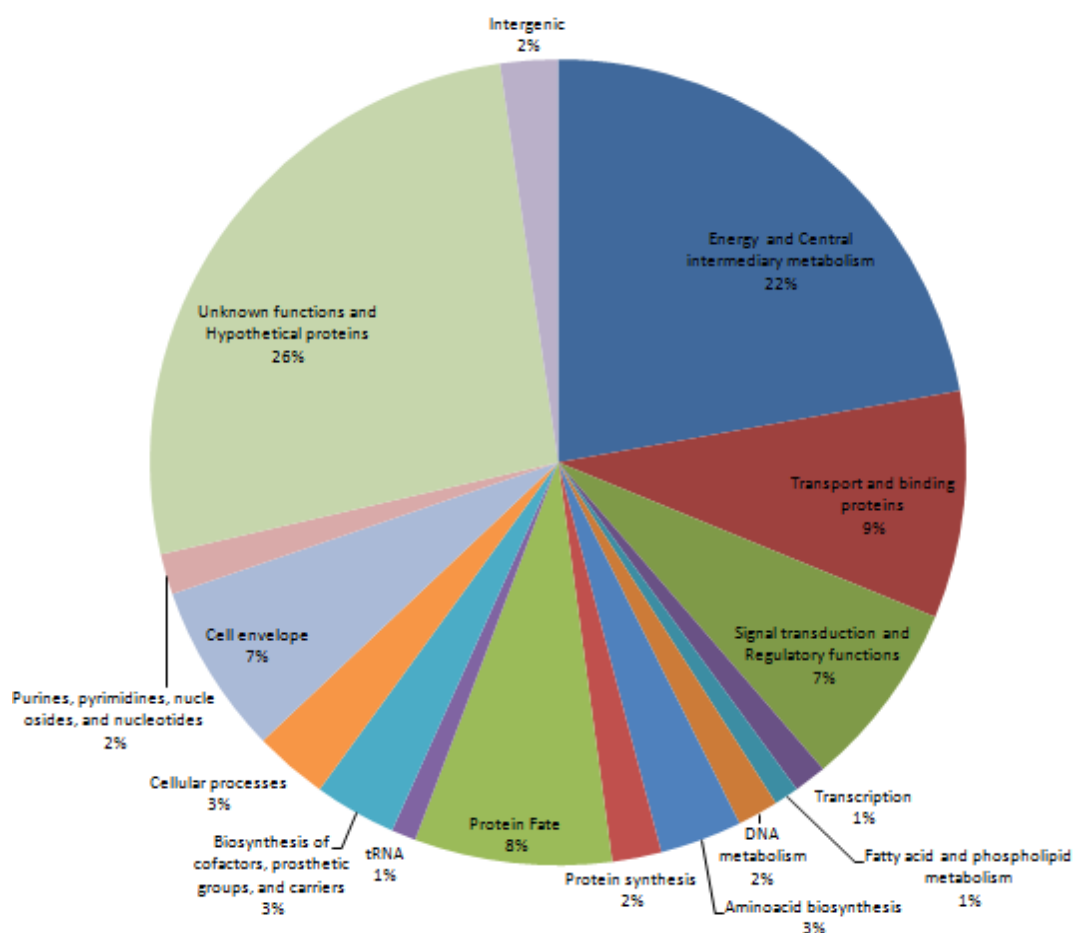
Figure 3. 23 Functional categories of the significantly regulated transcripts on different acetate concentrations (80mM vs 40mM)
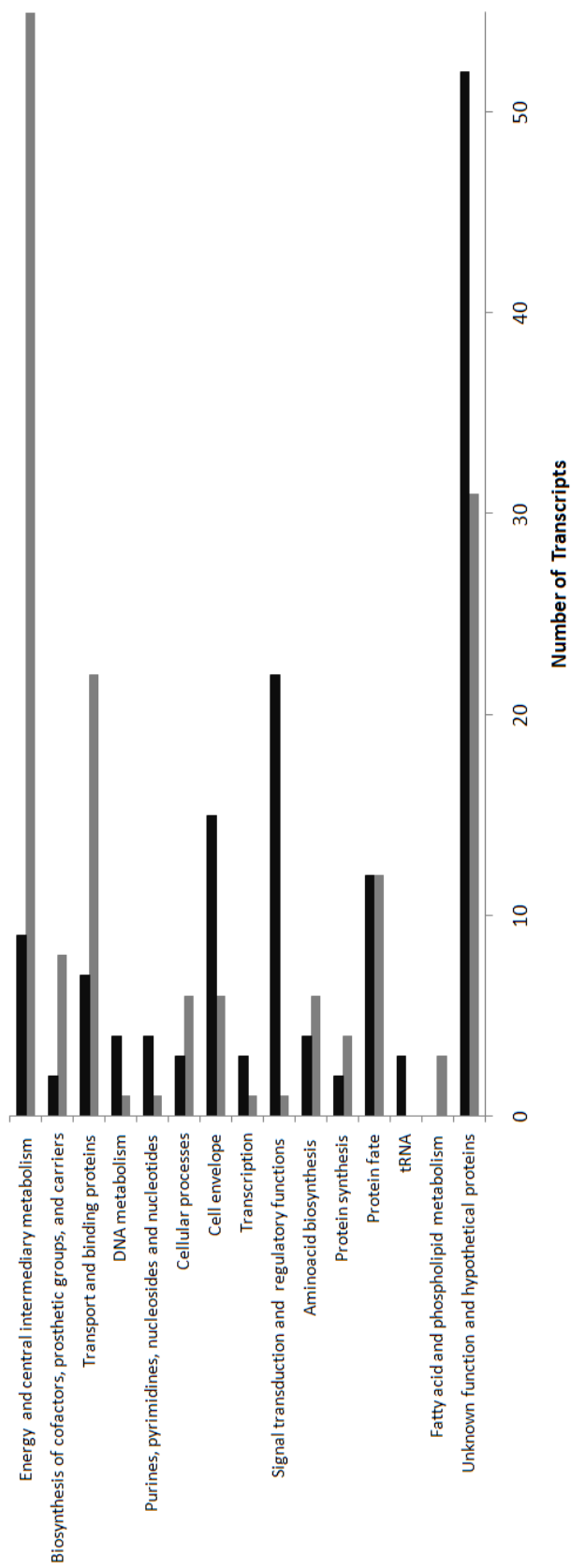
Figure 3. 24 The number of up and down-regulated transcripts in the functional categories on different acetate concentrations (80mM vs 40mM). Black bars indidicate the up-regulated transcripts. Grey bars indicate the down-regulated transcripts.

3.4.1. DNA Metabolism and Purines, Pyrimidines, Nucleosides, and Nucleotides Metabolism on 80mM vs 40mM Acetate

Genes related to metabolism of DNA and purines, pyrimidines, nucleosides, and nucleotides were significantly up-regulated on 80mM compared to 40mM acetate. These results might imply that cell was synthesizing new nucleic acids and increasing DNA replication, in order to be prepared to increase cell number.

3.4.2 Cellular Processes on 80mM vs 40mM Acetate

On 80mM acetate containing medium, 6 genes in the cellular processes functional category showed a significant down-regulation compared to 40mM acetate containing medium. On the other hand, the number of significantly up-regulated genes was 2. The ftsA and ftsK gene products are involved in bacterial cell division Goehring and Beckwith, 2005). In this study, on 80mM acetate cell division proteins ftsA and ftsK were significantly down-regulated 1.98 and 1.89 fold respectively when compared to 40mM acetate containing conditions. These results implied that lower rate of cell division on 80mM acetate. This result is in accordance with the physiological resuts since the growth rate of cells in the 80mM acetate containing medium was lower than the ones in the 40mM acetate containing medium at the time of cell harvesting. Pilus is a surface structure in bacteria and involved in conjugation. It is needed for attachment to recipient cell. In this study, expression of cpaB which encodes a pilus assembly protein showed a down-regulation (1.78) on 80mM acetate which might indicate that a reduced genetic exchange via conjugation compared to 40mM acetate.

3.4.3. Cell Envelope on on 80mM vs 40mM Acetate

In cell envelope funcional category, 10 genes were significantly up-regulated and 2 genes were significantly down-regulated on ammonium chloride containing medium compared to glutamate medium. In the up-regulated transcripts galE (1.81), galU (2.03), lpxC (4.13), wza (2.27) and pncA (1.89) gene products take role in biosynthesis and degradation of surface polysaccharides and lipopolysaccharides. The glmS (1.91) , glmU (1.77) , mepA (3.39) gene products are involved in biosynthesis and degradation of murein sacchulus and peptidoglycan. The two significantly down-regulated genes with probeset numbers RCAP_rcc00435_at and RCAP_rcc00656_at are known to encode putative cell envelope proteins and their function is unknown.

3.4.4. Aminoacid Biosynthesis on 80mM vs 40mM Acetate

In aminoacid biosynthesis functional category, expression of 4 genes significantly up-regulated and expression of the 6 genes significantly down-regulated on ammonium containing medium compared to glutamate. Glutamate synthase enzyme which is composed of two subunits, alpha (gltB) and beta (gltA) is involved in glutamate biosynthesis from 2-oxoglutarate and glutamine by activity according to chemical reaction below.

L-glutamine + 2-oxoglutarate + NADPH + H^+ $\leftrightarrow$ 2 L-glutamate + $NADP^+$ (1.9)
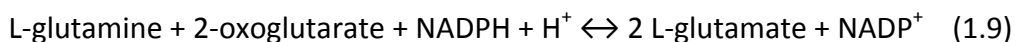
In this study, genes encoding for both subunits were significantly up-regulated (alpha subunit: 2.83; beta subunit; 4.68). These results might indicate that *R. capsulatus* cells are trying to increase glutamate amount on 80mM acetate compared to 40mM acetate.

The glnA gene encodes glutamine synthetase (GS) enzyme which is involved in glutamine production from glutamate and ammonium (Haselkorn et al., 2001). The chemical reaction catalyzed by glutamine synthetase is given below.

Glutamate + ATP + NH_3 → Glutamine + ADP + phosphate   (1.20)
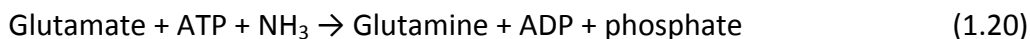
In this study, on 80mM acetate, glnA expression was significantly down-regulated compared to 40mM (1.89) which is expected since glutamate is limiting on 80mM acetate compared to 40mM acetate medium.

3.4.5 Protein Synthesis on 80mM vs 40mM Acetate

In protein synthesis functional category, transcription levels of 4 genes were significantly down-regulated and 2 genes were up-regulated on 80mM acetate compared to 40mM. The significantly down-regulated genes (rpsN, rpsE) were encoding ribosomal protein and shown in Table 3.14. Ribosomal proteins which could not pass filtering criteria were also checked for regulation. It was observed that expression of majority ribosomal subunit encoding genes were also down-regulated. The genes rplE and rplF that showed statistical significant down-regulation with fold changes 1.73 and 1.71 respectively were also included to Table 3.14. Down-regulation of ribosomal protein encoding genes on 80mM acetate might be due to limitation of nitrogen source in the medium. The ribosomal proteins were also significantly down-regulated relative to the proteomes in two different *Prochlorococcus* strains on nitrogen limited condition compared to nitrogen rich condition (Gilbert and Fagan, 2011).

Table 3. 14 Genes that are significantly regulated in protein synthesis functional category on different acetate concentrations. (FC: Fold Change; 80: 80mM acetate; 40: 40mM Acetate)

Probeset ID	Gene	product	FC and Regulation NH_4^+/Glu*
RCAP_rcc00313_at	rpsN	30S ribosomal protein S14	1.86 ↓
RCAP_rcc00317_at	rpsE	30S ribosomal protein S5	1.83↓
RCAP_rcc00312_at	rplE	50S ribosomal protein L5	1.73↓
RCAP_rcc00315_at	rplF	50S ribosomal protein L6	1.71↓

*Down-regulation of gene expression is represented with ↓

3.4.6 Protein Fate on 80mM vs 40mM Acetate

In protein fate functional category, 12 genes were significantly up-regulated and 12 genes were significantly down-regulated on 80mM acetate compared to 40mM acetate containing medium. In 9 of these genes with products involved in protein folding and stabilization, the number of down-regulated genes was 6 and the number of up-regulated genes was 3. Genes with products involved in protein and peptide secretion and trafficking, the number of down-regulated genes was 4 and the number of up-regulated genes was 1. These results might also indicate that protein synthesis was lower on 80mM acetate compared to 40mM acetate.

3.4.7. Transcription on 80mM vs 40mM Acetate

Transcription of RNA polymerase sigma factor sigma-70 family and RNA polymerase omega subunit were significantly up-regulated on 80mM acetate compared to 40mM acetate indicated. These results might imply that there is an overall increase

in transcription regarding to adaptation to high carbon and low nitrogen conditions. Transcription of non ribosomal proteins involved in transcription was slightly higher in nitrogen limited condition compared to nitrogen excess condition in two different *Prochlorococcus* strains (Gilbert and Fagan, 2011).

3.4.8. Signal Transduction and Regulatory Proteins on 80mM vs 40mM Acetate

On 80mM acetate except cspA gene which encodes for a cold shock protein, 22 genes showed a significant up-regulation in the signal transduction and regulatory proteins functional category. These results might indicate that cells are in an adaptation period on 80mM acetate containing medium.

The PpsR protein is a transcriptional regulator for photosynthesic genes and represses of the synthesis of the photosynthetic apparatus under aerobic conditions in *R. capsulatus* and in other PNS bacteria (Kovács et al., 2005). In this study, the ppsR gene expression was significantly up-regulated on 80mM acetate compared to 40mM acetate. This result is in accordance with the down-regulation of genes encoding the photosynthetic apparatus. Increased expression of ppsR gene might indicate that dissolved oxygen could have not been totally utilized on 80mM acetate due to slower growth and metabolism.

Expression of two genes encoding Crp/Fnr family transcriptiol regulator showed a significant increase on 80mM acetate compared to 40mM acetate containing medium. It is known that Crp/Fnr regulators are global transcriptional regulators. They respond to a variety of intracellular or extracellular signals, such as anoxia, carbon monoxide, temperature, nitric oxide, and oxidative and nitrosative stress and regulate metabolic pathways such as photosynthesis, nitrogen fixation, aromatic compound degradation, and respiration. In *E. Coli* it directly interacts with molecular oxygen and controls the metabolic transition between aerobic and anaerobic growth (Zhou et. al, 2012). In this study, up-regulated Crp/Fnr family

transcriptiol regulators might also take role in the regulation of metabolic changes during shift from microaerobic to anaerobic conditions in *R. capsulatus.*

The possible roles of ntrB, ntrC, ntrY, ntrX and nifA gene products on 80mM acetate will be discussed in detail in section 3.3.12.11.

3.4.9 Fatty Acid and Phospholipid Metabolism on 80mM vs 40mM Acetate

3 genes encoding proteins in the fatty acid and phospholipid metabolism functional category showed a significant decrease on 80mM acetate medium compared to 40mM acetate containing medium (Table 3.15). The accD and acpP gene products are involved in biosynthesis of fatty acids and phospholipids. The accD gene encodes the beta subunit of acetyl-CoA carboxylase, carboxyl transferase enzyme and acpP encodes acyl carrier protein. The other down-regulated gene with probeset ID RCAP_rcc01884_at encodes a hydrolase, alpha/beta fold family and is involved in degradation of fatty acids and phospholipids.

Table 3. 15 Genes that are significantly regulated in fatty acid and phospholipid metabolism functional category on different acetate concentrations. (FC: Fold Change; 80: 80mM acetate; 40: 40mM Acetate)

Probeset ID	Gene	product	FC and Regulation 80/40
RCAP_rcc00236_at	accD	acetyl-CoA carboxylase, carboxyl transferase, beta subunit	2.385
RCAP_rcc01678_at	acpP	acyl carrier protein	2.138
RCAP_rcc01884_at		hydrolase, alpha/beta fold family	1.876

*Down-regulation of gene expression is represented with ↓

3.4.10 Transport and Binding Proteins on 80mM vs 40mM Acetate

The transcripts of 7 transport and binding proteins significantly up-regulated on 80mM compared to 40mM acetate. 3 of the up-regulated genes encodes for a transporter with an unknown substrate. The transporters with unknown function might have a role in the adaptation of bacteria to high carbon low nitrogen status on 80mM acetate medium. On the other hand, 21 of the genes encoding transport and binding proteins showed a significant down-regulation on 80mM compared to 40mM. In these genes 4 of them encode a transporter with an unknown substrate. The higher number in down-regulated transcripts than the number of up-regulated transcripts might indicate that less nutrients were tranported into the cell on 80mM acetate compared to 40mM acetate. The lesser amount of nutrient uptake could be the reason for the reduced growth rate on 80mM acetate.

The tripartite ATP-independent periplasmic takes role in transport and utilization of various organic acids (Fischer et al., 2010) including acetate (Nam et al., 2003). The dctPQM genes encode the three subunits of (TRAP) transporter in *R. capsulatus* (Forward et al., 1997). In this research, the transcript levels of dctPQM were significantly up-regulated on 80mM acetate compared to 40mM acetate medium. This result might indicate that TRAP transporter might be involved in transport of acetate into the cell in *R. capsulatus*. Effect of less acetate entering the cell might be one of the reasons for reduced growth on 80mM acetate compared to that on 40mM acetate.

3.4.11 Biosynthesis of Cofactors, Prosthetic Groups, and Carriers on 80mM vs 40mM Acetate

The down regaulated genes in the biosynthesis of cofactrors, prosthetic groups, and carriers were remarkabe (8) compared to up-regulated genes (2). On 80mM acetate, expression of bchM and bchL genes significantly decreased compared to

40mM acetate. It is known that bchM and bchL gene products take role in the biosynthetic pathway for bacteriochlorophyll biosynthesis (Willows and Kriegel, 2009). The significant down-regulation of bchM and bchL might indicate the lower bacteriochlorophyll biosynthesis on 80mM acetate compared to 40mM.

3.4.12. Energy and Cental Intermediary Metabolisn on 80mM vs 40mM Acetate

In energy and central intermediary metabolism functional category, 50 genes were significantly up-regulated and 21 genes were significantly down-regulated on 80mM acetate medium compared to 40mM acetate.

3.4.12.1 Acetate Assimilation on 80mM vs 40mM Acetate

Acetate enters the TCA cycle in the form of acetyl-CoA by the activity of acetate-CoA ligase. The generated acetyl-CoA can enter to the TCA cycle for generation of electrons and for biosynthesis of building blocks. The acsA gene encodes for acetate-CoA ligase. It was observed that different acetate concentrations did not result in a significant change in expression level of acsA.

The three asetate assimilation routes proposed for PNS bacteria are glyoxylate cycle, ethylmalonyl-CoA and citramalate pathways. Similar to acsA, genes of these three pathways did not show a significant change on 80mM acetate compared to 40mM acetate. The two exceptions were two enzymes of the ethylmalonyl-CoA pathway: methylmalonyl-CoA epimerase and propionyl-CoA carboxylase (alpha subunit) which significantly up-regulated and down-regulated, respectively. The two reactions catalyzed by the two enzymes are not the commited steps of ethlymalonyl-CoA pathway. They also take part in other metabolic processes such as amino acid metabolism and propanoate metabolism. The reason for difference in the direction of regulation of these two genes might indicate that their products

take role in different metabolic pathways. These results herein imply that acetate assimilation was not regulated at the transcriptional level on different acetate concentrations.

3.3.12.2. Cytochrome bc1 Complex on 80mM vs 40mM Acetate

Cytochrome bc1 is a multi-subunit membrane bound enzyme that takes role in photosynthetic energy transduction pathways and contribute to the generation of membrane potential by pumping protons from the cytoplasm to the periplasm. The cyt bc1 complex is composed of three subunits (the Fe/S protein, cyt b and cyt c1), which are encoded by three structural genes petA, petB, and petC, respectively (Lanciano et al., 2011). In this study, expression of Pet A and Pet B structural genes encoding Fe/S protein and cyt b were significantly down-regulated under 80mM conditions 3,00 and 3,86 respectively. This might indicate a reduced electron flow to cytochrome c carriers.

3.3.12.3. Cytochromes on 80mM vs 40mM Acetate

Cyt c_y is a membrane bound c-type cytochrome (class I). In *R. capsulatus*, it takes part in cyclic electron transport during photosynthetic growth and transfer electrons from the *bc*1 complex back to the RC (Myllykallio et al., 1997). In *R. capsulatus*, cycY is the structural gene for Cyt c_y and its expression significantly decreased (2.169) under 80mM acetate conditions compared to 40mM.

3.3.12.4. Photosynthetic Membrane Apparatus on 80mM vs 40mM Acetate

Photosynthetic membrane apparatus works in parallel to TCA cycle and converts light energy into ATP. ATP produced is used for biosynthetic pathways and hydrogen production by nitrogenase. The photosynthetic apparatus is composed of

three multimeric transmembrane protein complexes: the antenna or light-harvesting complexes (LHC), the reaction center (RC) and the cytochrome (cyt) $bc1$ complex. In *R. capsulatus*, structural genes that encode components for the photosynthetic apparatus are organized into three operons denoted *puf*, *puc* and *puh.* The *puf* and *puh* operons encode structural proteins of the photosynthetic reaction center and the light harvesting I complex (LHI), while the *puc* operon encodes the structural proteins of light harvesting II complex (LHII) (Dubbs and Tabita, 2004). The bchM, bchL gene products take role in the biosynthetic pathway for bacteriochlorophyll biosynthesis (Willows and Kriegel, 2009). In this study, on 80mM acetate, expression of 10 genes encoding the structural units of photosynthetic reaction center and 2 genes encoding products that take role in bacteriochlorophyll biosynthesis significantly decreased compared to 40mM Acetate (Table 3.16). These results might imply that a significantly reduced photosynthetic activity on 80mM acetate compared to 40mM acetate.

3.3.12.5. TCA Cycle on 80mM vs 40mM Acetate

Acetate is fed into the TCA cycle where it is oxidised to produce CO_2 and electrons. Expression of 4 genes encoding TCA cycle enzymes were significantly down-regulated on 80mM acetate compared to 40mM acetate containing medium (Table 3.17) which indicated a lesser amount of electron generation.

Table 3. 16 Significantly regulated genes encoding photosynthetic membrane apparatus on different acetate concentrations. (FC: Fold Change; 80: 80mM acetate; 40: 40mM Acetate)

Probeset ID	Gene	Product	FC and Regulation 80/40
RCAP_rcc00659_at	puhA	photosynthetic reaction center, H subunit	4.31 ↓
RCAP_rcc00660_at	pucC	PucC protein	2.18 ↓
RCAP_rcc00691_at	pufB	light-harvesting protein B-870, beta subunit	4.00↓
RCAP_rcc00692_at	pufA	light-harvesting protein B-870, alpha subunit	4.21 ↓
RCAP_rcc00693_at	pufL	photosynthetic reaction center, L subunit	4.95 ↓
RCAP_rcc00694_at	pufM	photosynthetic reaction center, M subunit	5.29 ↓
RCAP_rcc00695_at	pufX	intrinsic membrane protein PufX	5.62 ↓
RCAP_rcc02530_at	pucB	light-harvesting protein B-800/850, beta chain	3,36 ↓
RCAP_rcc02531_at	pucA	light-harvesting protein B-800/850, alpha chain	3,51 ↓
RCAP_rcc02533_at	pucDE	light-harvesting protein B-800/850, gamma chain	5.17 ↓
RCAP_rcc00661_at	bchM	magnesium-protoporphyrin O-methyltransferase	1.75 ↓
RCAP_rcc00662_at	bchL	light-independent protochlorophyllide reductase, iron-sulfur ATP-binding protein	1.81 ↓

*Down-regulation of gene expression is represented with ↓.

Table 3. 17 Significantly regulated genes encoding TCA cycle enzymes on different acetate concentrations. (FC: Fold Change; 80: 80mM acetate; 40: 40mM Acetate)

Probeset ID	Gene	Product	FC and Regulation 80/40
RCAP_rcc00718_at	mdh	malate dehydrogenase	1.83 ↓
RCAP_rcc01887_at	icd	Isocitrate dehydrogenase (NADP(+))	2.56 ↓
RCAP_rcc02150_at	acnA	aconitate hydratase	3.16 ↓
RCAP_rcc02364_at	gltA	citrate (Si)-synthase	2.09 ↓

*Down-regulation of gene expression is represented with ↓.

3.3.12.6. NADH-quinone oxidoreductase (complex I) on 80mM vs 40mM Acetate

NADH-quinone oxidoreductase (complex I) catalyzes the oxidation of NADH and pumps protons across the inner membrane of mitochondria or the plasma membrane of many bacteria. It is encoded by the 14 genes of the nuo operon in *Rhodobacter capsulatus* (NuoABCDEFGHIJKLMN) (Brandt, 2006). It is known that NADH-quinone oxidoreductase takes role in photoheterothrophic metabolism of *R. capsulatus* and work in reverse direction to reduce NAD^+ (Herter et al., 1998). The NADH generated is then used for biomass synthesis, CO_2 fixation, PHB production and nitrogenase activity via ferredoxin (Golomysova et al., 2010). In this study, the expression of 3 nuo genes was significantly down-regulated on 80mM acetate compared to 40mM acetate and resulted in a lesser NADH production (Table 3.18).

Table 3. 18 Significantly regulated genes encoding TCA cycle enzymes on different acetate concentrations. (FC: Fold Change; 80: 80mM acetate; 40: 40mM Acetate)

Probeset ID	Gene	Product	FC and Regulation 80/40
RCAP_rcc01518_at	nuoB	NADH-quinone oxidoreductase, B subunit	1.93 ↓
RCAP_rcc01520_at	nuoD	NADH-quinone oxidoreductase, D subunit	2.10 ↓
RCAP_rcc01521_at	nuoE	NADH-quinone oxidoreductase, E subunit	2.03 ↓

*Down-regulation of gene expression is represented with ↓.

3.3.12.7. ATP Synthase on 80mM vs 40mM Acetate

The cyclic electron flow through the photosynthetic membrane apparatus generates a proton motive force and ATP synthase enzyme catalysis ATP production. ATP is required for nitrogenase enzyme to produce hydrogen (McKinlay and Harwood, 2010). On 80mM acetate containing conditions expression level of 10 ATPase structural genes significantly decreased compared to 40mM acetate (Table 3.19).

3.3.12.8 Calvin Cycle and Redox Balance on 80mM vs 40mM Acetate

Expression of type II rubisCo encoding gene cbbm was significantly down-regulated on 80mM acetate containing medium compared to 40mM. In addition to unique calvin cycle enzyme rubisCo expression of other calvin cycle genes such as glyceraldehyde-3-phosphate dehydrogenase, fructose-bisphosphate aldolase, ribulose-phosphate 3-epimerase were also significantly down-regulated on 80mM compared to 40mM acetate. Together these results might imply that Calvin cycle was repressed on 80mM acetate compared to 40mM aceate.

Table 3. 19 Significantly regulated genes encoding TCA cycle enzymes on different acetate concentrations. (FC: Fold Change; 80: 80mM acetate; 40: 40mM Acetate)

Probeset ID	Gene	Product	FC and Regulation 80/40
RCAP_rcc00740_at	atpI	ATP synthase F0, I subunit	2.32 ↓
RCAP_rcc00741_at	atpB	ATP synthase F0, A subunit	3.67 ↓
RCAP_rcc00742_at	atpE	ATP synthase F0, C subunit	6.51 ↓
RCAP_rcc00743_at	atpX	ATP synthase F0, B' subunit	6.67 ↓
RCAP_rcc00744_at	atpF	ATP synthase F0, B subunit	6.12 ↓
RCAP_rcc02971_at	atpD	ATP synthase F1, beta subunit	2.12 ↓
RCAP_rcc02972_at	atpG	ATP synthase F1, gamma subunit	2.32 ↓
RCAP_rcc02973_at	atpA	ATP synthase F1, alpha subunit	2.28 ↓
RCAP_rcc02974_at	atpH	ATP synthase F1, delta subunit	1.80 ↓

*Down-regulation of gene expression is represented with ↓.

3.3.12.9. Nitrogen fixation on 80mM vs 40mM Acetate

Mo-nitrogenase is the major nitrogen fixation (hydrogen producing) enzyme in *R. capsulatus*. In this study, expression of Mo-nitrogenase structural genes (*nifHDK)* on 80mM acetate were not significantly different than that on 40mM acetate containing medium.

3.3.12.10. Electron Transport to Nitrogenase on 80mM vs 40mM Acetate

It is known that both the rnf protein complex and ferredoxin are needed for nitrogenase enzyme activity. By using the membrane potential, rnf complex transfers electrons from photosynthetic membrane to ferredoxin which then donates its electrons to nitrogenase (Biegel et al., 2011). Although expression level of Mo-nitrogenase structural genes were not significantly different on 80mM and 40mM media. A significant down-regulation was observed in transcription of genes encoding rnf system and ferredoxin on 80mM when comapared to their levels on 40mM Acetate (Table 3.20). These results might imply that electron supply to nitrogenase enzyme is lower on 80mM acetate than 40mM acetate.

Table 3. 20 Significantly regulated genes encoding proteins involved in electron transport to nitrogenase on different acetate concentrations. (FC: Fold Change; 80: 80mM acetate; 40: 40mM Acetate)

Probeset ID	Gene	Product	FC and Regulation 80/40
RCAP_rcc03287_at	rnfA	electron transport complex protein RnfA	2.834 ↓
RCAP_rcc03288_at	rnfB	electron transport complex protein RnfB	1.791↓
RCAP_rcc00573_at	fdxD	ferredoxin V	2.701 ↓

*Down-regulation of gene expression is represented with ↓.

3.3.12.11. Regulation of Nitrogen Fixation on 80mM vs 40mM Acetate

The NtrB and NtrC proteins are members of a two-component regulatory system, in which NtrB acts as a sensor kinase and NtrC functions as the response regulator.

Under nitrogen limited conditions, *R. capsulatus* NtrC is phosphorylated by NtrB. Phosphorylated NtrC activates transcription of nifA and ure operon (required for synthesis and activity of urease) (Masepohl et al, 2002) in concert with RNA polymerase containing housekeeping sigma factor, sigma-70. Unlike other bacteria *R. capsulatus* NtrC does not require alternative RNA polymerase sigma factor, sigma-54 but instead uses the house-keeping sigma factor, sigma 70. In *R. capsulatus* similar to ntrB/ntrC, ntrY/ntrX two-component regulatory system is also involved in nitrogen regulation (Masepohl et al., 2004; Gregor et al., 2007). In this study, on 80mM acetate transcript levels of ntrB, ntrC, ntrX and ntrY significantly increased and resulted in an increase in expression of nifA, ureA and ureB (Table 3.21). It is known that nifA activates transcription of nitrogenase structural genes and enhances fixation of nitrogen. The ureA and ureB genes encode gamma and beta subunits of urease enzyme catalyzes the hydrolysis of urea into carbon dioxide and ammonia. These results show that *R. capsulatus* is trying to increase nitrogen content via ntrB/ntrC regulatory system on 80mM acetate where carbon source is in excess and nitrogen source is scarce and limiting for the growth of bacteria compared to 40mM acetate.

3.4 Validation of Microarray by RT-qPCR

Validation of the custom designed *R. capsulatus* GeneChips was carried out by performing RT-qPCR assays. The significance criteria which was 1.75 fold change and corrected p value 0.1 used in the microarray analysis was tested. For this purpose, transcripts with a fold change in the range of 1.3 - 6.12 with a corrected p value in between (0.002 - 0.44) were selected for the RT-qPCR analysis and their expression values were measured under all experimental conditions. Microarray results for the selected genes are given in Table 3.22. The table includes information regarding to statistical analysis, fold change analysis and direction of regulation.

Table 3. 21 Significantly regulated genes encoding proteins involved in regulation of nitrogenase on different acetate concentrations. (FC: Fold Change; 80: 80mM acetate; 40: 40mM Acetate)

Probeset ID	Gene	Product	FC and Regulation 80/40
RCAP_rcc01797_at	ntrB	nitrogen regulation protein NtrB	1.98 ↑
RCAP_rcc01798_at	ntrC	nitrogen assimilation regulatory protein NtrC	2.30 ↑
RCAP_rcc01799_at	ntrY	nitrogen regulation protein NtrB	2.38 ↑
RCAP_rcc01800_at	ntrX	nitrogen assimilation regulatory protein NtrX	1.87 ↑
RCAP_rcc03267_s_at	nifA	Nif-specific regulatory protein	2.10 ↑
RCAP_rcc01218_at	ureA	urease, gamma subunit	2.05 ↑
RCAP_rcc01219_at	ureB	urease, beta subunit	1.93↑

*Up-regulation of gene expression is represented with ↑.

Melt curve analysis gave only one narrow peak which indicated the specificity of primers for the desired gene products. As an example, the melt curve analysis graph of the reference gene 16srRNA in all unknown samples was scanned and given in Figure 3.25.

Slopes of the standard curves were found to be between -3.1 and -3.58 which indicated an acceptable PCR efficiency for each reaction. R^2 values of the standard curves were bigger than 0.985 and acceptable. Equations of the standard curves were used to calculate gene expression levels in unknown samples. Standard curves of the selected genes are given in Appendix F.

Table 3. 22 Comparison of microarray and RT-qPCR results for the selected genes

Gene-Probe ID	NH3 vs Glutamate			80mM vs 40mM		
	corrected p-value	Fold Change	Up/ Down	corrected p-value	Fold Change	Up/ Down
oppA RCAP_rcc2275_at	0.02	4.64	Down	1.48	0.12	Down
acnA RCAP_rcc2150_at	0.08	3.25	Up	3.16	0.02	Down
pufM RCAP_rcc00694_at	0.44	1.31	Up	5.29	0.01	Down
atpF RCAP_rcc00744_at	0.02	1.97	Up	6.12	0.002	Down
16sRNA RCAP_rcc00001_at	0.07	1.01	Down	1.01	0.004	Up
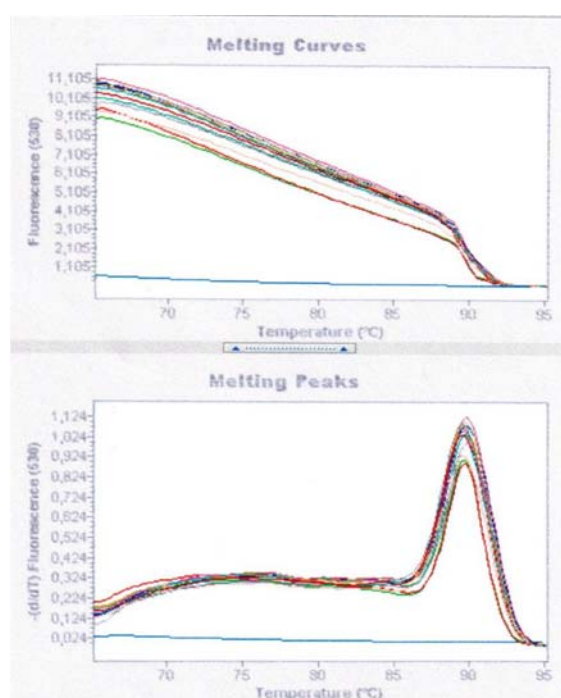
Figure 3. 25 Melt curve analysis graph obtained for 16srRNA

Expression levels of the selected genes measured by RT-qPCR are compared to those from the microarray data in Figure 3.26, Figure 3.27, Figure 3.28 and Figure 3.29. It is seen that the direction of regulation is same in both qPCR and microarray resuts. Fold change values detected by RT-qPCR was higher than that obtained by microarray. This result is consistent with literature since it is known that fold change differences may vary between these two methods and in spite of the fact that microarray can accurately show the direction of regulation, it can underestimate the fold change differences compared to RT-qPCR method (Pappas et. al, 2004; Yuste et al., 2006). For this purpose, the important parameter in validation studies is the concistency in direction of regulation rather than the absolute fold change values and microarray experiments and custom designed *R. capsulatus* GeneChips used in this study were successfully validated by RT-qPCR method.

	Ammonium vs Glutamate	80mM vs 40mM acetate
Microarray	3,25	-3,16
RT-qPCR	5,94	-5,85

■ Microarray ■ RT-qPCR
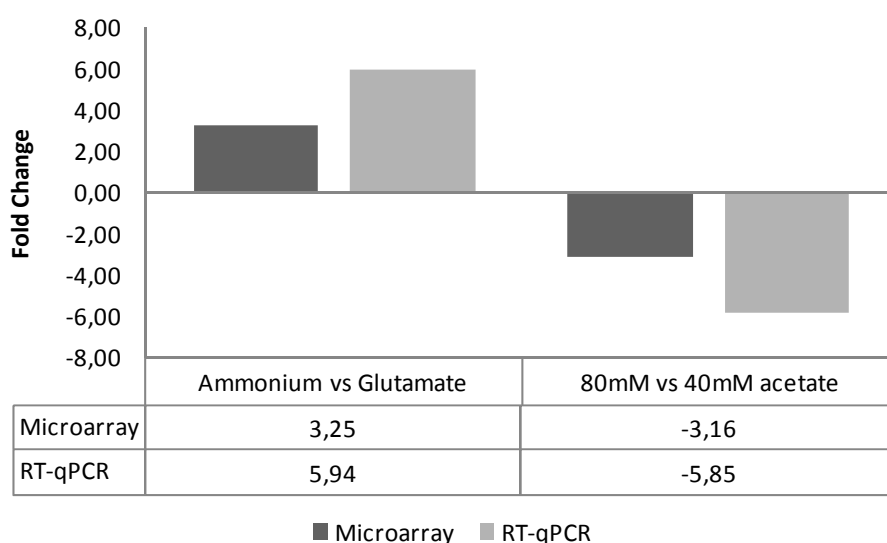
Figure 3. 26 Expression of acnA obtained by RT-qPCR

130

	Ammonium vs Glutamate	80mM vs 40mM acetate
Microarray	1,97	-6,12
RT-qPCR	2,03	-17,00

■ Microarray ■ RT-qPCR
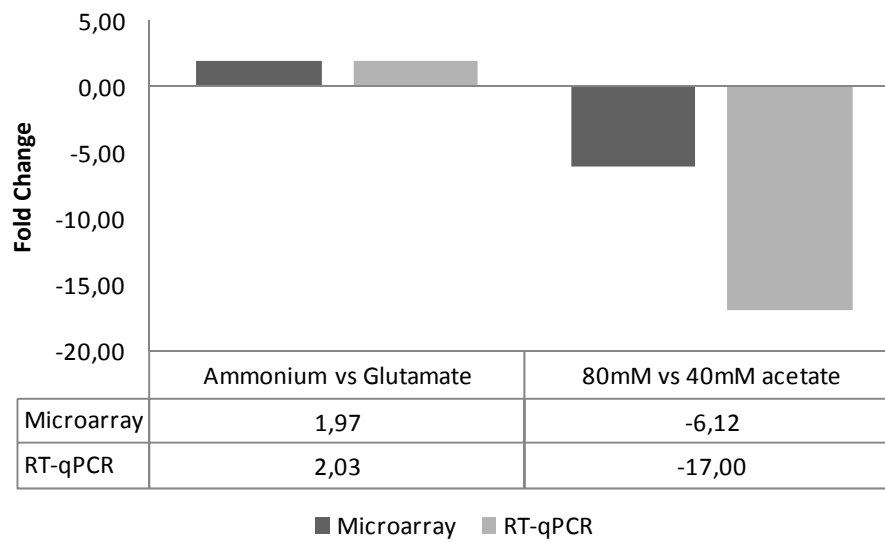
Figure 3. 27 Expression of atpF obtained by RT-qPCR

	Ammonium vs Glutamate	80mM vs 40mM acetate
Microarray	1,31	-5,29
RT-qPCR	1,50	-20,00

■ Microarray ■ RT-qPCR
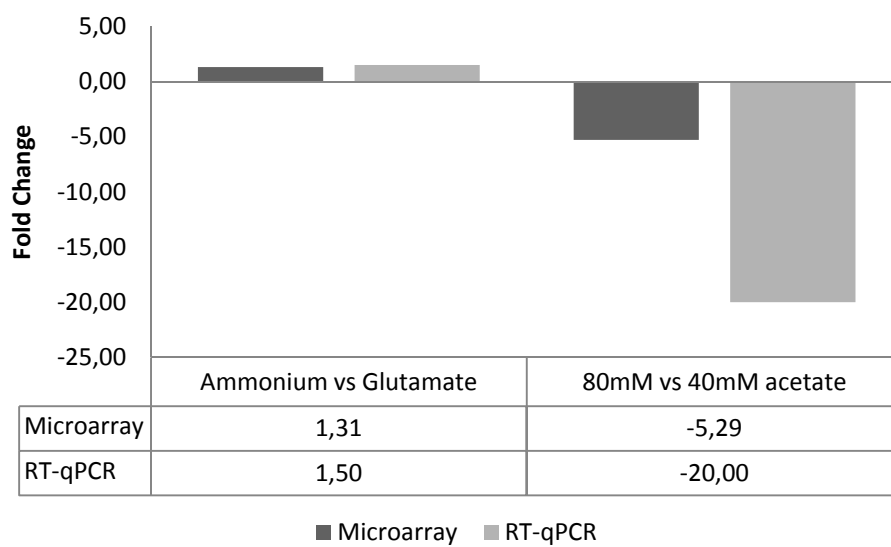
Figure 3. 28 Expression of pufM obtained by RT-qPCR
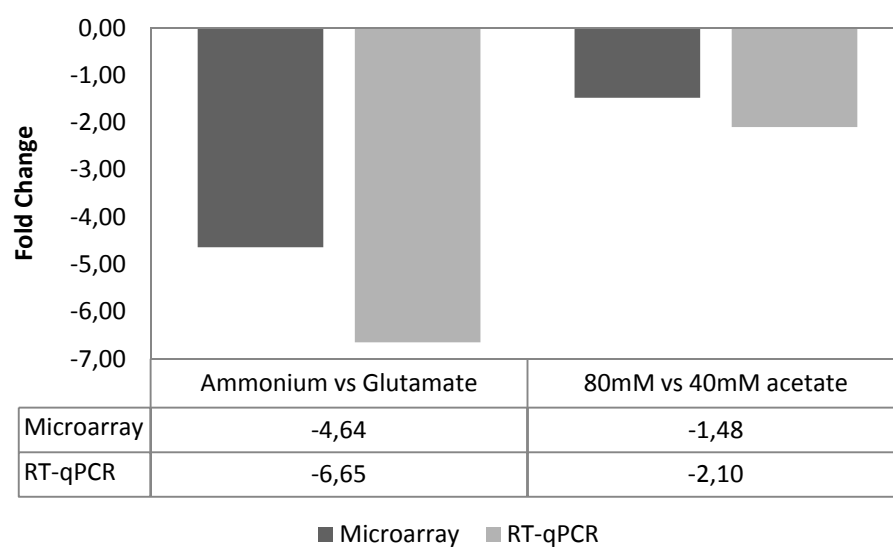
Figure 3. 29 Expression of OppA obtained by RT-qPCR

	Ammonium vs Glutamate	80mM vs 40mM acetate
Microarray	-4,64	-1,48
RT-qPCR	-6,65	-2,10

CHAPTER 4

CONCLUSION

The main goal of this study was to understand the metabolism of *R. capsulatus* on different nitrogen sources which were 5mM ammonium chloride and 2mM glutamate and different acetate concentrations (40mM-80mM) by comprehensive physiological and microarray analyses.

Hydrogen production was totally inhibited and growth was favored on ammonium chloride. When higher acetate concentrations than 40mM was used as carbon source, all physiological parameters regarding the growth, substrate utilization and hydrogen production showed a significant decrease. This effect was remarkable on 80mM acetate. *Rhodobacter capsulatus* strains SB1003 and DSM1710 strains exhibited significantly similar physiological properties on 80mM and 40mM acetate.

A microarray chip for *R. capsulatus* was not commercially available. For that reason, an Affymetrix GeneChip was custom designed in order to be able to study global changes in the transcriptome in response to changing environmental conditions. SB1003 was the strain whose genome has been completely sequenced and used for the chip construction. A high quality and quantity of RNA is required for microarray analysis. For this purpose, an efficient RNA isolation protocol for *R. capsulatus* was optimized in this study by using Trizol reagent. In order to be able to investigate the response and adaptation of *R. capsulatus* cells when transferred to a new medium, RNA samples were collected at 16h when the cells were in the early exponential phase. Microarray experiments and chips used in this study were successfully validated.

In the microarray data analysis, we mainly focused on the differentially regulated transcripts in the energy and central intermediary metabolism; transport and binding proteins; and signal transduction and regulatory proteins functional categories since the main interest of this research was investigation of hydrogen production, carbon assimilation and nitrogen metabolism and their regulations.

Inhibition of hydrogen production was observed on 5mM amonium chloride medium compared to 2mM glutamate medium. This might be due to significant decrease in expression of Mo-nitrogenase structural genes (*nifHDK),* nitrogenase molybdenum-iron cofactor biosynthesis genes (nifN, nifU and nifX) and nitrogenase electron donor rnf complex and ferredoxin encoding genes on ammonium chloride. It is known that NifA protein is the transcriptional regulator of other nif genes. The significant increase in glnB expression might have resulted in decrease in expression of nifA gene or NifA protein activity and consequently inhibition of nitrogenase related genes. Both GlnK and AmtB ammonium transporter proteins exhibited a significant increase on ammonium containing medium compared to glutamate containing medium. This result might imply that in addition to roles in ammonium sensing and transport, AmtB might have an influence on post-translational regulation of nitrogenase enzyme via complex formation with GlnK.

It was speculated that dct TRAP transporters might be involved in transport of acetate. The significant increase in transcript level of cation/acetate symporter ActP and dct TRAP transporter subunits on ammonium chloride might imply that more acetate was transported into the cell as carbon source when compared to glutamate medium.

Significantly increased expression of acetate-CoA ligase, glyoxylate enzyme isocitrate lyase and ethylmalonyl-CoA pathway enzymes on ammonium chloride medium might imply that more acetate was assimilated into the cellular blocks on ammonium chloride medium. These results might be due to higher concentration of nitrogen source in the medium. It was also suggested for the first time that, *R. capsulatus* might assimilate acetate by using both glyoxylate cycle and ethylmalonyl cycle. These two routes might be active at the same time or can switch from one route to another depending on the conditions.

On ammonium chloride medium, the significant increase in expression of genes encoding TCA cycle enzymes, NADH-quinone oxidoreductase subunits, cytochrome bc1 complex subunits and ATP synthase subunits implied that energy metabolism was stimulated compared to glutamate medium.

Increased expression of TCA cycle enzymes and NADH-quinone oxidoreductase might have resulted in increased production of reducing equivalents on ammonium chloride containing medium. In *Rhodobacter capsulatus*, the major routes for excess electron dissipation are Calvin cycle and nitrogenase activity. There was no significant difference in expression of genes encoding Calvin cycle enzymes. Nitrogenase expression and activity were also inhibited on ammonium chloride. According to these results, it was suggested that the excess electrons might be dissipated via ethylmalonyl-CoA pathway during acetate assimilation.

On 80mM acetate containing medium, transcript levels of ntrB, ntrC, ntrX and ntrY regulatory genes significantly increased and might have resulted in an increase in expression of nifA, ureA and ureB. The nifA gene product is involved in activation of transcription of nitrogenase structural genes and the ureA and ureB gene products encode subunits of urease enzyme which is involved in the utilization of urea. Expression levels of genes encoding for alpha (gltB) and beta (gltA) subunits of

glutamate synthase were significantly increased on 80mM acetate might be due to the need of *R. capsulatus* for increasing the primary nitrogen source glutamate., In summary, these results herein might imply that *R. capsulatus* was trying to increase nitrogen content on 80mM acetate where carbon source was in excess and nitrogen source was scarce which might be also the reason for the longer lag phase observed.

In spite of the fact that carbon source was higher in 80mM acetate compared to 40mM acetate containing medium, less acetate might be available for growth due to reduced expression of transporters especially dct TRAP transporters which were suggested to be involved in acetate transport.

Expression of genes related with the acetate assimilation pathways did not show a significant difference on 80mM acetate and 40mM acetate. However, TCA cycle, photosynthetic appararus, electron transport and Calvin cycle genes were significantly decreased on 80mM acetate compared to 40mM acetate which might indicate the repression of energy metabolism on 80mM acetate.

The transcription of signal transduction and regulatory proteins were significantly up-regulated on both conditions. The exact functions of some of the significantly up-regulated transcripts were unknown. These regulatory proteins might have important roles in adaptation to different nitrogen sources and acetate concentrations. For further improvement of hydrogen production capacity and yield of PNS bacteria, functions of these regulatory proteins have to be investigated. The long term aim of this study may be investigation of functions of these regulatory proteins.

REFERENCES

Afsar, N., Özgür, E., Gürgan, M., Akköse, S., Yücel, M., Gündüz, U., Eroğlu, İ., 2011, "Hydrogen productivity of photosynthetic bacteria on dark fermenter effluent of potato steam peels hydrolysate", International Journal of Hydrogen Energy, 36: 432–438.

Afsar, N., Özgür, E., Gürgan, M., Akköse, S., Yücel, M., Gündüz, U., Eroğlu, I., 2011, "Hydrogen productivity of photosynthetic bacteria on dark fermenter effluent of potato steam peels hydrolysate" International Journal of Hydrogen Energy, 36: 432–438.

Akköse, S., Gündüz, U., Yücel, M., Eroğlu, I., 2009, "Effects of ammonium ion, acetate and aerobic conditions on hydrogen production and expression levels of nitrogenase genes in Rhodobacter sphaeroides O.U.001", International Journal of Hydrogen Energy, 24: 8818–8827

Alber, B.E., Spanheimer, R., Ebenau-Jehle C., Fuchs, G., 2006, "Study of an alternate glyoxylate cycle for acetate assimilation by Rhodobacter sphaeroides", Mol Microbiol., 61: 297–309.

Albers, H., Gottschalk, G., 1976, "Acetate metabolism in Rhodopseudomonas gelatinosa and several other Rhodospirillaceae", Arch. Microbiol., 111: 45–49.

Arikawa, E., Sun, Y., Wang, J., Zhou, Q., Ning, B., Dial, S.L., Guo, L., Yang, J., 2008, "Cross-platform comparison of SYBR Green real-time PCR with TaqMan PCR, microarrays and other gene expression measurement technologies evaluated in the MicroArray Quality Control (MAQC) study", BMC Genomics, 9: 328.

Barbosa, M., J., Rocha, J., M., S., Tramper, J., Wijffels, R., H., 2001, "Acetate as a carbon source for hydrogen production by photosynthetic bacteria", Journal of Biotechnology, 85: 25–33.

Basak, N., Das, D., 2007, "The prospect of purple non-sulfur (PNS) photosynthetic bacteria for hydrogen production: the present state of the art", World J. Microbiol. Biotechnol., 23: 31–42

Biebl, H., Pfennig, N., 1981, "Isolation of members of the family Rhodosprillaceae In: The prokaryotes", Editors: Starr, M.P., Stolp, H., Trüper, H.G., Balows, A., Schlegel, H.G., New York: Springer-Verlag, 267–273

Biegel, E., Schmidt, S., González, J.M., Müller, V., 2011, "Biochemistry, evolution and physiological function of the Rnf complex, a novel ion-motive electron transport complex in prokaryotes", Cell Mol Life Sci, 68: 613–634.

Blasco, R., Cardenas, J., Castillo, F., 1991, "Regulation of Isocitrate Lyase in Rhodobacter capsulatus E1F1", Curr. Microbiol., 22: 73–76.

Boehm, D., Herold, S., Kuechler, A., Liehr, T., Laccone, F., 2004, "Rapid detection of subtelomeric deletion/duplication by novel real-time quantitative PCR using SYBR-green dye", Hum. Mutat., 23: 368–378.

Brandt, U., 2006, "Energy converting NADH:quinone oxidoreductase (complex I)" Annu. Rev. Biochem., 75: 69–92.

Claassen, P.A.M., De Vrije, T., 2006, "Non-thermal production of pure hydrogen from biomass: HYVOLUTION", International Journal of Hydrogen Energy, 31: 1416–1423.

Daldal, F., Cheng, S., Applebaum, J., Davidson E., Prince R., 1986, "Cytochrome c2 is not essential for photosynthetic growth of Rhodopseudomonas capsulate", Proc .Natl. Acad. Sci., 83: 2112–2116.

Das, D., Khanna, N., Veziroglu, T.N., 2008, Recent developments in biological hydrogen production processes, Chem Ind Chem Eng Q., 14: 57–67.

Das, D., Veziroğlu, T.N., 2001, "Hydrogen production by biological processes: a survey of literature", International Journal of Hydrogen Energy, 26: 13–28.

Das, D., Veziroğlu, T.N., 2008, "Advances in biological hydrogen production processes" International Journal of Hydrogen Energy, 33: 6046–6057.

D'haene, B., Vandesompele, J., Hellemans, J., 2010, "Accurate and objective copy number profiling using real-time quantitative PCR", Methods, 50: 262–270.

Dixon, R., Kahn, D., 2004, "Genetic regulation of biological nitrogen fixation", Nat. Rev. Microbiol., 2: 621–631.

Drepper, T.,. Groß S., Yakunin A.F., Hallenbeck B.M., Masepohl B., Klipp W., 2003, "Role of GlnB and GlnK in ammonium control of both nitrogenase systems in the phototrophic bacterium Rhodobacter capsulatus", Microbiology, 149: 2203–2212.

Dubbs, J., Tabita, F. R., 2004, "Regulators of nonsulfur purple phototrophic bacteria and the interactive control of CO2 assimilation, nitrogen fixation, hydrogen metabolism and energy generation", FEMs Microbiology Reviews, 28: 353–376

Ediger, V.S, Akar, S., Ugurlu B., 2006, "Forecasting production of fossil fuel sources in Turkey using a comparative regression and ARIMA model", Energy Policy, 34: 3836–3846.

Ehrenreich, A.,2006, "DNA microarray technology for the microbiologist: an overview", Appl Microbiol Biotechnol., 73: 255–273.

Elsen, S., Swem, L.R., Swem, D.L., Bauer, C.E., 2004, "RegB/RegA, a highly conserved redox-responding global two-component regulatory system", Microbiol. Mol. Biol., 68: 263–279.

Erb, T.J., Frerichs-Revermann, L., Fuchs, G., Alber, B.E., 2010, "The apparent malate synthase activity of *Rhodobacter sphaeroides* is due to two paralogous enzymes, (3*S*)-malyl-CoA/β -methylmalyl-CoA lyase and (3*S*)-malyl-CoA thioesterase", J Bacteriol., 192: 1249–1258.

Eroglu E., Melis A., 2011, "Photobiological hydrogen production: Recent advances and state of the art", Bioresource Technology, 102: 8403–8413.

Eurogentec qPCR-guide. Retrieved August 5, 2012 from http://www.eurogentec.com/uploads/qPCR-guide.pdf

Feniouk, B.A., "Biosynthesis of Bacteriochlorophyll in Purple Bacteria", 2009, Editors: Hunter, C.N., Daldal, F., Thurnauer, M.C., Beatty, J.T., The Purple Photosynthetic Bacteria, Dordrecht: Springer Science, 475–493.

Fischer M., Zhang Q.Y., Hubbard R.E., Thomas G.H.,2010, "Caught in a TRAP: substrate-binding proteins in secondary transport", Trends Microbiol, 18: 471–478.

Forward J.A,, Behrendt M.C., Wyborn N.R., Cross R., Kelly D.J., 1997, "TRAP transporters: a new family of periplasmic solute transport systems encoded by the dctPQM genes of Rhodobacter capsulatus and by homologs in diverse gramnegative bacteria" J Bacteriol, 179: 5482–5493.

GeneChip® Expression Analysis Data Analysis Fundamentals. Retrieved July 25, 2012 from
http://media.affymetrix.com/support/downloads/manuals/data_analysis_fundamentals_manual.pdf

GeneChip® customexpress™ array design guide. Retrieved August 1, 2012 from http://media.affymetrix.com/support/technical/other/custom_design_manual.pdf.

GeneChip® expression analysis technical manual. Retrieved Retrieved August 5, 2012 from
http://media.affymetrix.com/support/downloads/manuals/expression_analysis_technical_manual.pdf

Gilbert J.D.J., Fagan W.F., 2010, "Contrasting mechanisms of proteomic nitrogen thrift in *Prochlorococcus*", Mol ecol., 20: 92–104.

Goldberg, I., Nadler, V., Hochman, A., 1987, "Mechanism of nitrogenase switch-off by oxygen", 169: 874–879.

Golomysova, A., Gomelsky, M., Ivanov, P.S., 2010, "Flux balance analysis of photoheterotrophic growth of purple nonsulfur bacteria relevant to biohydrogen production", International Journal of Hydrogen Energy, 35: 12751–12760.

Goehring, N., Beckwith, J., 2005, "Diverse paths to midcell: assembly of the bacterial cell division machinery" *Curr. Biol.* 15: R514–R526.

Gray, K.A., Daldal, F., 1995, "Mutational studies of the cytochrome bc1 complexes", Editors: Blankenship, R.E., Madigan, M.T. And Bauer, C.E., Anoxygenic photosyntetic bacteria , Dordrecht : Kluwer Academic Publishers, 747–774.

Gregor, J., T. Zeller, A. Balzer, K. Haberzettl, Klug G., 2007, "Bacterial regulatory networks include direct contact of response regulator proteins: interaction of RegA and NtrX in*Rhodobacter capsulatus*", J. Mol. Microbiol. Biotechnol, 13: 126–139.

Hadicke, O., Grammel, H., Klamt, S., 2011, "Metabolic network modeling of redox balancing and biohydrogen production in purple nonsulfur bacteria." BMC Systems Biology, 5:150.

Hallenbeck, P. C., Ghosh, D., 2009, "Advances in fermentative biohydrogen production: the way forward", Trends in Biotechnology, 25: 287–297.

Hallenbeck, P., Benemann, J., 2002, "Biological hydrogen production; fundamentals and limiting processes", International Journal of Hydrogen Energy, 27: 1185–1193.

Hallenbeck, P.C., 2009, "Fermentative hydrogen production: Principles, progress, and prognosis", 34: 7379–7389.

Hallenbeck, P.C., Ghosh, D., Skonieczny, M.T., Yargeau, V., 2009, "Microbiological and engineering aspects of biohydrogen production", Indian J Microbiol., 49: 48–59

Hardiman, G., 2004, "Microarray platform comparisons and contrasts", Pharmacogenomics, 5: 487–502.

Haselkorn, R., Lapidus, A., Kogan, Y., Vlcek, C., Paces, J., Paces, V., Ulbrich, P., Pecenkova, T., Rebrekov, D., Milgram, A., 2001, "The *Rhodobacter capsulatus* genome", Proc. Natl. Acad. Sci. USA, 70: 43–52.

Herter, S.M., Kortluke C.M., Drews, G., 1998, "Complex I of Rhodobacter capsulatus and its role in reverted electron transport", Arch. Microbiol., 169: 98-105.

Hobman, J. L., Jones, A., Constantinidou, C., 2007, "Introduction to microarray technology", In: Microarray technology through applications, Editor: Falciani, F., New York :Taylor and Francis Group, 1-52.

Hu, X., Ritz, T., Damjanovic, A., Autenrieth, F., Schulten, K., 2002, "Photosynthetic apparatus of purple bacteria", Q Rev Biophys, 35: 1-62.

Imhoff, J.F., 2006, "The Phototrophic Alpha-Proteobacteria", Prokaryotes, 5: 41-64.

Ivanovsky, R.N., Krasilnikova, E.N., Berg, I.A., 1997, "A proposed citramalate cycle for acetate assimilation in the purple non-sulfur bacterium Rhodospirillum rubrum", FEMS Microbiol. Lett., 153: 399–404.

Jain, I.P., 2009, "Hydrogen the fuel for 21st century", International Journal of Hydrogen Energy, 34: 7368–7378.

Kars, G.; Gündüz, U., 2010, "Towards a super H_2 producer: Improvements in photofermentative biohydrogen production by genetic manipulations", Int J Hydrogen Energy, 35: 6646–6656.

Kitagawa, M,, Wada, C., Yoshioka, S., Yura, T., 1991, "Expression of ClpB, an analog of the ATP-dependent protease regulatory subunit in Escherichia coli, is controlled by a heat shock sigma factor (sigma 32)", J Bacteriol.,173: 4247–4253.

Koku, H., Eroğlu, İ., Gündüz, U., Yücel, M., Türker, M., 2002, "Aspects of the metabolism of hydrogen production by Rhodobacter sphaeroides" International Journal of Hydrogen Energy, 27: 1315–1329.

Kontur, W.S., Ziegelhoffer, E.C., Spero, M.A., Imam, S., Noguera D.R., Donohue, T.J., 2011, "Pathways Involved in Reductant Distribution during Photobiological H2 Production by Rhodobacter sphaeroides", Appl. Environ. Microbiol, 77: 7425-7429.

Kornberg, H.L., Lascelles, J., 1960, "The Formation of Isocitratase by the Athiorhodaceae", J. Gen. Microbiol., 23: 511–517.

Kotay, S.M., Das, D., 2008, "Biohydrogen as a renewable energy resource-Prospects and potentials", International Journal of Hydrogen Energy, 33: 258–263.

Kovacs, A.T., Rakhely, G., Kovacs, K.L., 2005, "The PpsR regulator family", Res Microbiol.,156: 619–625.

Laguna, R., Tabita, F.R., Alber, B.E., 2011, "Acetate-dependent Photoheterotrophic growth and the differential requirement for the Calvin-Benson-Basshamreduc-tivepentosephosphatecycle in Rhodobactersphaeroides and Rhodopseudomonas palustris", Arch. Microbiol., 193: 151–154.

Lanciano, P., Lee, D.W., Yang, H., Darrouzet, E. and Daldal, F., 2011, "Intermonomer electron transfer between the low-potential b hemes of cytochrome bc1", Biochemistry, 50: 1651–1663.

Law, C.J., Roszak, A.W., Southall, J., Gardiner, A.T., Isaacs, N.W., Cogdell, R.J., 2004., "The structure and function of bacterial light-harvesting complexes (review)", Mol. Membr. Biol., 21: 183–191.

Letowski J., Brousseau R., Masson L., 2003, "DNA Microarray Applications in Environmental Microbiology", Analytical Letters, 36: 3165–3184.

Levin, D.B., Pitt, L., Love, M., 2004, "Biohydrogen production: prospects and limitations to practical application", International Journal of Hydrogen Energy, 29: 173–185.

Madigan, M.T. and Jung, D.O., 2009, "An overview of purple bacteria: systematics, physiology, and habitats", Editors: Hunter, C.N., Daldal, F., Thurnauer M.C., Beatty, J.T., The Purple Phototrophic Bacteria. Dordrecht: Springer, 1-15.

Manish, S., Banerjee, R., 2008, " Comparison of biohydrogen production processes." International Journal of Hydrogen Energy, 33: 279–86.

Masepohl, B., Drepper T., Paschen S. G., Pawlowski A., Riedel K., Klipp W., 2002, "Regulation of nitrogen fixation in the phototrophic purple bacterium Rhodobacter capsulatus", J. Mol. Microbiol. Biotechnol., 4: 243–248.

Masepohl, B., Drepper, T. & Klipp, W., 2004, "Nitrogen fixation in the phototrophic purple bacterium Rhodobacter capsulatus In: Genetics and regulation of nitrogen fixation in free-living bacteria" Dordrecht: Kluwer Academic Publischer, 141-173.

Masepohl, B., Drepper, T., Paschen, A., Gross, S., Pawlowski, A., Raabe, K., Riedel, K. U., Klipp, W., 2002. "Regulation of nitrogen fixation in the phototrophic purple bacterium Rhodobacter capsulatus", J Mol Microbiol Biotechnol, 4: 243–248.

Masepohl, B., Hallenbeck, P.C., 2010, "Nitrogen and molybdenum control of nitrogen fixation in the phototrophic bacterium Rhodobacter capsulatus" Editor: Hallenbeck, P.C., Recent Advances in phototrophic prokaryotes, Advances in experimental Medicine and Biology, 675: 49–70.

Masepohl, B., Kranz R.G., 2009, "Regulation of nitrogen fixation", Editors: Hunter, C.N., Daldal, F., Thurnauer, M.C., Beatty, J.T., The purple phototrophic bacteria, Dordrecht: Springer, 759–775.

McKinlay, J.B., Harwood, C.S., 2010, "Photobiological production of hydrogen gas as a biofuel, Current Opinion in Biotechnology", 21: 244–251.

Meister M., Saum, S., Alber B.E., Fuchs, G., 2005, "L-Malyl-coenzyme A/β-methylmalyl-coenzyme A lyase is involved in acetate assimilation of the isocitrate lyase-negative bacterium Rhodobacter capsulatus", J Bacteriol, 187: 1415–1425.

Melis, A., Melnicki, M., 2006, "Integrated biological hydrogen production", Int. J. Hydrogen Energy, 31: 1563–1573.

Miller, M.B., Tang, Y.W., 2009, "Basic concepts of microarrays and potential applications in clinical microbiology", Clin Microbiol Rev., 22: 611–633.

Mulligan, C., Fischer, M., Thomas, G.H., 2010, "Tripartite ATP-independent periplasmic (TRAP) transporters in bacteria and archea", FEMS Microbiol Rev, 35: 68–86.

Myllykallio, H., Jenney, F. E., Moomaw C. R., Slaughter. C., A., Daldal, F., 1997, "Cytochrome cy of Rhodobacter capsulatus is attached to the cytoplasmic membrane by an uncleaved signal sequence-like anchor", J Bacteriol., 179: 2623–2631.

Nam, H.S., Spencer, M., Anderson, A.J., Cho, B.H., Kim, Y.C., 2003, "Transcriptional regulation and mutational analysis of a *dctA* gene encoding an organic acid transporter protein from Pseudomonas chlororaphisO6", Gene, 323: 125–131.

Nath, K., Das, D., 2004, "Improvement of fermentative hydrogen production: various Approaches", Appl. Microbiol. Biotechnol., 65: 520–529.

Özgür, E., Uyar, B., Oztürk, Y., Yücel, M., Gündüz, U., Eroglu, I., 2010,"Biohydrogen Production by R. capsulatus on Acetate at Fluctuating Temperatures", Resources, Conservation and Recycling, 54: 310–314.

Özgür E., Afsar N., de Vrije T., Yücel M., Gündüz U., Claassen P. A. M., 2010. "Potential use of thermophilic dark fermentation effluents in photofermentative hydrogen production by Rhodobacter capsulatus", Journal of Cleaner Production, 18: S23-S28.

Özgür, E., Mars, A.E., Peksel, B., Louwerse, A., Yücel, M., Gündüz, U., Claassen, P.A.M., Eroğlu, İ., 2010, "Biohydrogen production from beet molasses by sequential dark and photofermentation", International Journal of Hydrogen Energy, 35: 511-517.

Özkan, E., Uyar, B., Özgür, E., Yücel, M., Eroglu, I., Gündüz, U., 2012 "Photofermentative hydrogen production using dark fermentation effluent of sugar beet thick juice in outdoor conditions. International Journal of Hydrogen Energy, 37: 2044–2049.

Özsoy B., 2012, Hydrogen and Poly-Beta Hydroxy Butryric Acid Production and Expression Analyses of Related Genes in Rhodobacter Capsulatus at Different Acetate Concentrations. M.Sc. Thesis in Biological Sciences Department, Middle East Technical University, Ankara, Turkey.

Öztürk, Y., Gökçe, A., Peksel, B.,Gürgan, M., Özgür, E., Gündüz, U., Eroğlu, İ.,Yücel, M., 2012, "Hydrogen Production Properties Of Rhodobacter Capsulatus With Genetically Modified Redox Balancing Pathways", International Journal Of Hydrogen Energy, 37: 2014–2020.

Pekgöz G., Gündüz U., Eroğlu I., Yücel M., Kovács K., Rákhely G., 2011, "Effect of inactivation of genes involved in ammonium regulation on the biohydrogen production of *Rhodobacter capsulatus*", International Journal Of Hydrogen Energy, 36 : 13536–13546.

Petrushkova E.P., Tsygankov, A.A, 2011, "Major factors affecting isocitaret lyase activity in Rhodobacter capsulatus B10 under phototrophic conditions", Microbiology, 80: 619-623.

Redwood M.D., Paterson-Beedle M., Macaskie L.E., 2009, "Integrating dark and light bio-hydrogen production strategies: towards the hydrogen economy", Reviews in Environmental Science and Biotechnology, 8: 149–185.

Roche Applied Science Technical Note No. LC 13/2001 Retrieved August 5, 2012 from
http://www.roche-applied-science.com/sis/rtpcr/lightcycler/lightcycler_docs/technical_notes/lc_13.pdf

Roche Applied Science Technical Note No LC 1/99 Retrieved August 5, 2012 from http://www.gene-quantification.de/roche-primer-dimer.pdf

Rubio, L. M., Ludden, P. W, 2008, "Biosynthesis of the iron-molybdenum cofactor of nitrogenase", Annu. Rev. Microbiol., 62: 93–111.

Saei, A.A., Omidi, Y., 2011, "A glance at DNA microarray technology and applications", BioImpacts, 1: 75-86.

Sasikala, K., Ramana, C.V., Raghuveer, R.,P.,, Kovacs, K.,L., 1993, "Anoxygenic phototrophic bacteria: physiology and advances in hydrogen production technology", Adv Appl Microbiol, 38: 211–95.

Schulze, A., Downward, J., 2001, "Navigating gene expression using microarrays – a technology review", Nat. Cell Biol., 3: 190–195.

Selao, T.T., Nordlund, S., Noren, A., 2008, "Comparative proteomic studies in *Rhodospirillum rubrum* grown under Different Nitrogen conditions", J Proteome, 7: 3267-3275.

Sevinç, P., 2010, "Kinetic analyses of the effects of temperature and light intensity on growth, hydrogen production, and organic acid utilization by *Rhodobacter capsulatus.*" M.Sc. Thesis in Biotechnology Engineering Department, Middle East Technical University, Ankara, Turkey.

Sevinç, P., Gündüz, U., Eroglu, I., Yucel, M., 2012, "Kinetic analysis of photosynthetic growth, hydrogen production and dual substrate utilization by *Rhodobacter capsulatus* " doi:10.1016/j.ijhydene.2012.02.176:1-7.

Shin I., Park S., Lee M.R., 2005, "Carbohydrate microarrays: an advanced technology for functional studies of glycans", Chemistry-A European Journal, 11: 2894–2901.

Smith, C.J., Osborn, A.M., 2009, "Advantages and limitations of quantitative PCR(q-PCR)-based approaches in microbial ecology", FEMS Microbiology and Evolution, 67: 6–20.

Strnad, H., Lapidus, A., Paces, J., Ulbrich, P., Vlcek, C., Paces, V., Haselkorn.,R., 2010, "Complete genome sequence of the photosynthetic purple nonsulfur bacterium *Rhodobacter capsulatus* SB 1003. J. Bacteriol. 192: 3545–3546.

Swem, L.R., Elsen, S., Bird, T.H., Swem, D.L., Koch, H.G., Myllykallio, H., Daldal, F. Bauer, C.E., 2001, "The RegB/RegA two-component regulatory system controls synthesis of photosynthesis and respiratory electron transfer components in Rhodobacter capsulatus", J. Mol. Biol., 309: 121–138.

Tabita F.R., 1995, "The biochemistry and metabolic regulation of carbon metabolism and CO2 fixation in purple bacteria. In: Blankenship R E, Madigan M T, Bauer C E, editors. Anoxygenic photosynthetic bacteria", Dordrecht: Kluwer Academic Publishers, 885-914.

Tang, K.H., Tang, Y.J., Blankenship, R.E.,2011, "Carbon metabolic pathways in phototrophic bacteria and their broader evolutionary implications", Front Microbio, 2: 1-23.

Tichi, M.A., Tabita, F.R., 2001, "Interactive control of Rhodobacter capsulatus redox-balancing system during phototrophic metabolism", J Bacteriol, 183: 6344-6354.

Tremblay, P., Drepper, T., Masepohl, B., Hallenbeck, P.C., 2007, "Membrane sequestration of PII proteins and nitrogenase regulation in the photosynthetic bacterium Rhodobacter capsulatus", J Bacteriol, 189: 5850–5859.

Uyar, B., Eroglu, I., Yücel, M., Gündüz, U., Türker, L., 2007, "Effect of light intensity, wavelength and illumination protocol on hydrogen production in photobioreactors", International Journal of Hydrogen Energy, 32: 4670 – 4677.

Uyar, B., 2008, "Hydrogen Production by Microorganisms in Solar Bioreactor", Ph.D. Thesis in Biotechnology Engineering Department, Middle East Technical University, Ankara, Turkey.

Uyar, B., Schumacher, M., Gebicki, J., Modigell, M., 2009, "Photoproduction of hydrogen by Rhodobacter capsulatus from thermophilic fermentation effluent", Bioprocess and Biosystem Engineering, 32: 603–606.

VanGuilder, H.D., Vrana, K.E., Freeman, W.M., 2008, Twenty-five years of quantitative PCR for gene expression analysis", Biotechniques, 44: 619–626.

Vignais, P.M., Magnin, J.P., Willison, J.C., 2006, "Increasing biohydrogen production by metabolic engineering", International Journal of Hydrogen Energy ,31: 1478–1483.

Willison, J.C., 1988, "Pyruvate and Acetate Metabolism in the Photosynthetic Bacterium Rhodobacter capsulatus" J. Gen. Microbiol., 134: 2429–2439.

Willows R. D., Kriegel A. M., "Biosynthesis of Bacteriochlorophyll in Purple Bacteria", Editors: Hunter, C.N., Daldal, F., Thurnauer, M.C., Beatty, J.T., The purple phototrophic bacteria, Dordrecht: Springer: 57–79.

Wong, M.L., Medrano, J.F., 2005, "Real-time PCR for mRNA quantitation", Biotechniques, 39: 75–85 .

World Energy Outlook 2011 Special Report Factsheet, "Are we entering a golden age of gas". Retrieved August 5, 2012 from http://www.worldenergyoutlook.org/media/weowebsite/2011/WEO2011_GAG_FactSheet.pdf

Wu, J., Bauer C.E., 2008, "RegB/RegA, A Global Redox-Responding Two-Component Regulatory System", Advances in Experimental Medicine and Biology, 631: 131-148.

Yuste, L., Hervás, A.B., Canosa, I., Tobes I., Jiménez, J.I., Nogales, J., Pérez-Pérez, M.M., Santero, E., Díaz, E., Ramos, J., Lorenzo, V., Rojo, F., 2006, "Growth-phase dependent expression of the Pseudomonas putida KT2440 transcriptional machinery analyzed with a genome-wide DNA microarray", Environ Microbiol., 8: 165–177.

Zannoni, D., 1995, "Aerobic and anaerobic electron transport chains in anoxygenic phototrophic bacteria", Editors: Blankenship, R.E., Madigan, M.T., Bauer, C.E., Anoxygenic Photosynthetic Bacteria, Advances in Photosynthesis and Respiration, Dordrecht:Springer, 949-971

Zarzycki, J, Schlichting, A., Strychalsky, N., Müller, M., Alber, B.E., Fuchs, G., 2008, "Mesaconyl-coenzyme A hydratase, a new enzyme of two central carbon metabolic pathways in bacteria", J Bacteriol, 190: 1366-1374.

Zhou, A., Chen, Y.I., Zane, G.M., He, Z., Hemme, C.L., Joachimiak, M.P., Baumohl, J.K., He, Q., Fields, M.W., Arkin, A.P., Wall, J.D., Hazen, T.C., Zhou, J., 2012, "Functional characterization of Crp/Fnr-type global transcriptional regulators in Desulfovibrio vulgaris Hildenborough", Appl Environ Microbiol, 78: 1168-77.

Zhou, J., Thompson, D.K., 2004, "DNA microarray technology" Editors: Zhou, J., Thompson, D.K., Xu, Y., Tiedje, J.M, Microbial functional genomics. Hoboken: Wiley, 141–176.

COMPOSITIONS OF MEDIA

Table A. 1 Composition of MPYE medium

Component	Amount
Bactopeptone	3 g
Yeast extract	3 g
MgCl2	1.6 ml from 1M stock
CaCl2	1 ml form 1M stock

The constituents are dissolved in 1000ml of distilled water and sterilized by autoclaving.

Table A. 2 Composition of culture media for 1 L

Composition	Amount
KH2PO4	3 g
MgSO4.7H2O	0.5 g
CaCl2.2H2O	0.05 g
Vitamin Solution (10x) *	0.1 ml
Trace Element Solution *(10x)	0.1 ml
Fe-citrate (50x)*	0.5 ml
Nitrogen source	Varied
Carbon source	Varied

Vitamin, trace element and Fe-citrate solutions are added after dissolving and autoclaving of the other constituents.

Fe-citrate (50x): 5 g ferric citrate is dissolved in 100 ml distilled water and sterilized by autoclaving

Table A. 3 Nitrogen and carbon sources used in culture media

Medium	Nitrogen Source Amount	Carbon Source Amount
20mM Acetate/10mM Glutamate	1.85 g	1.15 ml
40mM Acetate/ 2mM Glutamate	0.36 g	2.30 ml
60mM Acetate/ 2mM Glutamate	0.36 g	3.45 ml
80mM Acetate/ 2mM Glutamate	0.36 g	4.6 ml
40mM Acetate/ 5 mM NH_4Cl	0.27 g	2.30

Table A. 4 The composition of 10x vitamin solution

Composition	Amount
Thiamin Chloride Hydrochloride (B1)	500 mg
Niacin (Nicotinic acid)	500 mg
D + Biotin	15 mg

The constituents are dissolved in 100ml of distilled water and sterilized by filtering .

Table A. 5 The composition of 10x trace element solution

Composition	Amount
ZnCl2	70 mg
MnCl2.4H2O	100 mg
H3BO3	60 mg
CoCl2.6H2O	200 mg
CuCl2.2H2O	20 mg
NiCl2.6H2O	20 mg
NaMoO4.2H2O	40 mg
HCl (25% v/v)	1 ml

The constituents are dissolved in 100ml distilled water and sterilized by autoclaving.

COMPOSITION OF TRIS-EDTA BUFFER

1 M Tris-HCl (pH 7.5) stock solution: Dissolve 157.6 g Tris-HCl in 1 L of distilled water

1 mM EDTA (pH 8) stock solution: Dissolve 186.1 g EDTA dissodium salt in 700 ml distilled water, adjust pH to 8 by 5N NaOH, bring volume to 1 L.

Table B. 1 The composition of TE buffer (10mM Tris, 1mM EDTA)

Composition	Amount
1 M Tris-HCl stock solution	1 ml
0.5 M EDTA stock solution	0.2 ml

The constituents are dissolved in 100 mL of distilled water and autoclaved.

ETHYLMALONYL-COA PATHWAY OF *RHODOBACTER CAPSULATUS*
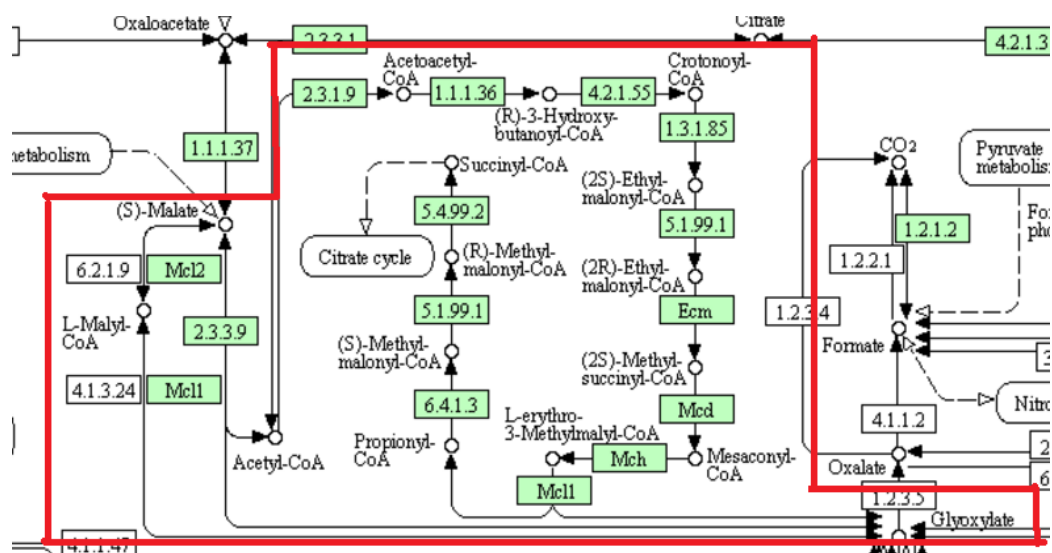
Figure C. 1 Screenshot for ethylmalonyl-CoA pathway of *Rhodobacter capsulatus* from KEGG database

The red line shows the borders for ethylmalonyl-CoA pathway. For the simplecity, the relationship of this pathway with others is not shown. The green boxes indicate the presence of genes in the genome of *R. capsulatus*

.

COMPLETE LIST OF GENES THAT ARE DIFFERENTIALLY REGULATED ON DIFFERENT
NITROGEN SOURCES

Table D. 1 Transcript profile on ammonium chloride vs glutamate

5mM NH3 vs 2mM Glutamate					
Transport and binding proteins					
RCAP_rcc00017_at	xylH	xylose ABC transporter, permease protein XylH	Carbohydrates, organic alcohols, and acids [Transport and binding proteins]	2,025	up
RCAP_rcc00018_at	xylF	xylose ABC transporter, xylose-binding protein XylF	Carbohydrates, organic alcohols, and acids [Transport and binding proteins]	2,987	up
RCAP_rcc00184_at		outer membrane efflux protein	Unknown substrate [Transport and binding proteins]	1,996	up

RCAP_rcc00601_at	mntH	manganese transport protein MntH	Cations and iron carrying compounds [Transport and binding proteins]	1,896	up
RCAP_rcc00704_at	oppC	oligopeptide ABC transporter, permease protein OppC	Amino acids, peptides and amines [Transport and binding proteins]	1,860	up
RCAP_rcc00705_at	oppB	oligopeptide ABC transporter, permease protein OppB	Amino acids, peptides and amines [Transport and binding proteins]	1,904	up
RCAP_rcc01226_at	urtB	urea ABC transporter, urea binding protein UrtB	Amino acids, peptides and amines [Transport and binding proteins]	5,107	up
RCAP_rcc01230_at	urtE	urea ABC transporter, ATP-binding protein UrtE	Amino acids, peptides and amines [Transport and binding proteins]	1,881	up
RCAP_rcc01243_at	potA	polyamine ABC transporter, ATP binding protein PotA	Amino acids, peptides and amines [Transport and binding proteins]	1,762	down
RCAP_rcc01244_at	potD	polyamine ABC transporter, periplasmic polyamine-binding protein PotD	Amino acids, peptides and amines [Transport and binding proteins]	2,534	down
RCAP_rcc01245_at	potB	polyamine ABC transporter, permease protein PotB	Amino acids, peptides and amines [Transport and binding proteins]	3,150	down

Table D.1 (continued)

RCAP_rcc01246_at	potI	polyamine ABC transporter, permease protein PotI	Amino acids, peptides and amines [Transport and binding proteins]	3,256	down
RCAP_rcc01439_at		ABC transporter, ATP-binding/permease protein	Unknown substrate [Transport and binding proteins]	2,303	up
RCAP_rcc01445_at		tonB-dependent receptor	Cations and iron carrying compounds [Transport and binding proteins]	1,990	up
RCAP_rcc02124_2861_at	actP	cation/acetate symporter ActP	Amino acids, peptides and amines [Transport and binding proteins]	3,456	up
RCAP_rcc02183_at	potG	spermidine/putrescine ABC transporter, ATP-binding protein PotG	Amino acids, peptides and amines [Transport and binding proteins]	2,406	up
RCAP_rcc02275_at	oppA	oligopeptide ABC transporter, periplasmic oligopeptide-binding protein OppA	Amino acids, peptides and amines [Transport and binding proteins]	4,642	down
RCAP_rcc02276_at	oppB	oligopeptide ABC transporter, permease protein OppB	Amino acids, peptides and amines [Transport and binding proteins]	3,609	down
RCAP_rcc02277_at	oppC	oligopeptide ABC transporter, permease protein OppC	Amino acids, peptides and amines [Transport and binding proteins]	3,052	down

158

Table D.1 (continued)

RCAP_rcc02278_at	oppD	oligopeptide ABC transporter, ATP-binding protein OppD	Amino acids, peptides and amines [Transport and binding proteins]	2,350	down
RCAP_rcc02373_at		monosacharide ABC transporter, periplasmic monosaccharide-binding protein	Carbohydrates, organic alcohols, and acids [Transport and binding proteins]	3,210	up
RCAP_rcc02417_at	dctP	TRAP dicarboxylate transporter, DctP subunit	Unknown substrate [Transport and binding proteins],Amino acids, peptides and amines [Transport and binding proteins]	2,215	up
RCAP_rcc02534_at	cysA	sulfate ABC transporter, ATP-binding protein CysA	Unknown substrate [Transport and binding proteins]	4,470	up
RCAP_rcc02536_at	cysT	sulfate ABC transporter, permease protein CysT	Anions [Transport and binding proteins]	1,836	up
RCAP_rcc02543_at	fruB	multiphosphoryl transfer protein	Carbohydrates, organic alcohols, and acids [Transport and binding proteins]	1,919	up
RCAP_rcc02621_at	sulP	sulphate transporter	Anions [Transport and binding proteins]	2,160	down
RCAP_rcc02744_at	cysP	sulfate/thiosulfate ABC transporter, periplasmic sulfate/thiosulfate	Anions [Transport and binding proteins]	4,562	up

Table D.1 (continued)

		-binding protein			
RCAP_rcc03022_at	dctM	TRAP C4-dicarboxylate transport system permease, DctM subunit	Carbohydrates, organic alcohols, and acids [Transport and binding proteins]	3,497	up
RCAP_rcc03023_at	dctQ	tripartite ATP-independent periplasmic transporter, DctQ component	Carbohydrates, organic alcohols, and acids [Transport and binding proteins]	4,410	up
RCAP_rcc03024_at	dctP	TRAP dicarboxylate transporter, DctP subunit	Carbohydrates, organic alcohols, and acids [Transport and binding proteins]	3,348	up
RCAP_rcc03386_at	amtB	ammonium transporter	Cations and iron carrying compounds [Transport and binding proteins]	3,560	up
Protein synthesis					
RCAP_rcc00298_at	rpsJ	30S ribosomal protein S10	Ribosomal proteins: synthesis and modification [Protein synthesis]	1,759	down
RCAP_rcc00308_at	rpmC	50S ribosomal protein L29	Ribosomal proteins: synthesis and modification [Protein synthesis]	2,041	down

Table D.1 (continued)

RCAP_rcc00309_at	rpsQ	30S ribosomal protein S17	Ribosomal proteins: synthesis and modification [Protein synthesis]	1,778	down
RCAP_rcc01495_at	fusA	translation elongation factor G	Transcription factors [Transcription],Translation factors [Protein synthesis]	2,234	up
Protein fate					
RCAP_rcc00653_at		ABC-1 domain protein	Protein folding and stabilization [Protein fate]	2,016	down
RCAP_rcc00710_at	hipO	hippurate hydrolase	Degradation of proteins, peptides, and glycopeptides [Protein fate]	2,667	up
RCAP_rcc00762_at	hoxW	hydrogenase maturation factor HowW	Protein modification and repair [Protein fate]	1,942	down
RCAP_rcc02274_at	pip	proline iminopeptidase	Degradation of proteins, peptides, and glycopeptides [Protein fate]	1,888	down
RCAP_rcc02402_at	degP	protease Do	Degradation of proteins, peptides, and glycopeptides [Protein fate]	2,892	down

Table D.1 (continued)

RCAP_rcc02583_at	lon	ATP-dependent protease La	Degradation of proteins, peptides, and glycopeptides [Protein fate]	2,130	down
RCAP_rcc03175_at	ccmG	thiol:disulfide interchange protein DsbE	Protein folding and stabilization [Protein fate]	2,115	down
RCAP_rcc03327_at	lolA	outer membrane lipoprotein carrier protein LolA	Protein and peptide secretion and trafficking [Protein fate]	1,930	down
RCAP_rcc03406_at	clpB	chaperone ClpB	Protein folding and stabilization [Protein fate]	2,253	down
tRNA					
RCAP_rct00032_at	tRNA	tRNA-Ala-GGC	Ala Anticodon-GGC	3,323	up
Energy and Cental Intermediary metabolism					
RCAP_rcc00014_at	xylA	xylose isomerase	Sugars [Energy metabolism]	1,999	up
RCAP_rcc00228_at		oxidoreductase, DSBA family	Aerobic [Energy metabolism]	1,925	down
RCAP_rcc00513_at	etfD	electron transfer flavoprotein-ubiquinone oxidoreductase	Electron transport [Energy metabolism]	2,125	up

Table D.1 (continued)

RCAP_rcc00538_at		methylmalonyl-CoA epimerase	Other [Energy metabolism]	1,917	up
RCAP_rcc00573_at	fdxD	ferredoxin V	Electron transport [Energy metabolism]	18,086	down
RCAP_rcc00721_at	sucD	succinyl-CoA synthetase (ADP-forming), alpha subunit	TCA cycle [Energy metabolism]	2,228	up
RCAP_rcc00724_at	sucA	oxoglutarate dehydrogenase (succinyl-transferring), E1 component	TCA cycle [Energy metabolism]	1,912	up
RCAP_rcc00725_at	sucB	dihydrolipoyllysine-residue succinyltransferase (succinyl-transferring), E2 component	TCA cycle [Energy metabolism]	2,711	up
RCAP_rcc00726_at	lpdA	dihydrolipoyl dehydrogenase	Pyruvate dehydrogenase [Energy metabolism]	2,746	up
RCAP_rcc00727_at	citE	citrate lyase, beta subunit	Fermentation [Energy metabolism]	2,003	up
RCAP_rcc00744_at	atpF	ATP synthase F0, B subunit	ATP-proton motive force interconversion [Energy metabolism]	1,968	up
RCAP_rcc00911_at	pccA	propionyl-CoA carboxylase, alpha subunit	Amino acids and amines [Energy metabolism],Biosynthesis [Fatty acid and phospholipid	1,831	up

			metabolism]		
RCAP_rcc01144_at	gcvP	glycine dehydrogenase (decarboxylating)	Amino acids and amines [Energy metabolism]	2,165	up
RCAP_rcc01385_at		NADH ubiquinone oxidoreductase subunit, NDUFA4 family	Electron transport [Energy metabolism]	1,963	up
RCAP_rcc01521_at	nuoE	NADH-quinone oxidoreductase, E subunit	Electron transport [Energy metabolism]	2,165	up
RCAP_rcc01523_at	nuoF	NADH-quinone oxidoreductase, F subunit	Electron transport [Energy metabolism]	1,957	up
RCAP_rcc01527_at	nuoG	NADH-quinone oxidoreductase, G subunit	Electron transport [Energy metabolism]	2,422	up
RCAP_rcc01529_at	nuoH	NADH-quinone oxidoreductase, H subunit	Electron transport [Energy metabolism]	3,142	up
RCAP_rcc01531_at	nuoI	NADH-quinone oxidoreductase, I subunit	Electron transport [Energy metabolism]	4,475	up
RCAP_rcc01532_at	pcaC	4-carboxymuconolactone decarboxylase	Other [Energy metabolism]	2,867	up
RCAP_rcc01533_at	nuoJ	NADH-quinone oxidoreductase, J subunit	Electron transport [Energy metabolism]	2,476	up
RCAP_rcc01534_at	nuoK	NADH-quinone oxidoreductase, K subunit	Electron transport [Energy metabolism]	3,581	up

Table D.1 (continued)

RCAP_rcc01535_at	nuoL	NADH-quinone oxidoreductase, L subunit	Electron transport [Energy metabolism]	4,534	up
RCAP_rcc01537_at	nuoN	NADH-quinone oxidoreductase, N subunit	Electron transport [Energy metabolism]	1,790	up
RCAP_rcc01620_at	aldB	aldehyde dehydrogenase (NADP(+))	Fermentation [Energy metabolism]	8,622	up
RCAP_rcc01705_at	pdhA	pyruvate dehydrogenase complex, E1 component, pyruvate dehydrogenase (acetyl-transferring), alpha subunit	Pyruvate dehydrogenase [Energy metabolism]	1,911	up
RCAP_rcc01830_at	fba	fructose-bisphosphate aldolase	Glycolysis/gluconeogenesis [Energy metabolism]	2,584	down
RCAP_rcc01887_at	icd	Isocitrate dehydrogenase (NADP(+))	TCA cycle [Energy metabolism]	2,850	up
RCAP_rcc02126_at	acsA	acetate--CoA ligase	Other [Energy metabolism]	7,349	up
RCAP_rcc02150_at	acnA	aconitate hydratase	TCA cycle [Energy metabolism]	3,250	up
RCAP_rcc02163_at	ccdA	cytochrome c-type biogenesis protein CcdA	Electron transport [Energy metabolism]	2,040	down
RCAP_rcc02364_at	gltA	citrate (Si)-synthase	TCA cycle [Energy metabolism]	2,967	up

RCAP_rcc02620_at	acsA	acetate--CoA ligase	Other [Energy metabolism]	2,006	up
RCAP_rcc02679_at		pyridine nucleotide-disulphide oxidoreductase family protein	Electron transport [Energy metabolism]	2,063	down
RCAP_rcc02770_at	petC	ubiquinol--cytochrome-c reductase, cytochrome c1 subunit	Electron transport [Energy metabolism]	2,298	up
RCAP_rcc02845_at	torA	trimethylamine-N-oxide reductase	Anaerobic [Energy metabolism]	2,842	down
RCAP_rcc02859_s_at	acsA	acetate--CoA ligase	Other [Energy metabolism]	2,935	up
RCAP_rcc02970_at	atpC	ATP synthase F1, epsilon subunit	ATP-proton motive force interconversion [Energy metabolism]	1,949	up
RCAP_rcc02971_at	atpD	ATP synthase F1, beta subunit	ATP-proton motive force interconversion [Energy metabolism]	1,769	up
RCAP_rcc03062_at	glpX	fructose-1,6-bisphosphatase	Pentose phosphate pathway [Energy metabolism]	1,763	up
RCAP_rcc03164_at	citE	citrate lyase, beta subunit	Fermentation [Energy metabolism]	2,131	up

RCAP_rcc03243_at	ccrA	crotonyl-CoA reductase	Other [Energy metabolism],Biosynthesis of natural products [Cellular processes]	2,188	up
RCAP_rcc03265_at		LRV FeS4 cluster domain protein	Electron transport [Energy metabolism]	1,836	down
RCAP_rcc03287_at	rnfA	electron transport complex protein RnfA	Electron transport [Energy metabolism],Nitrogen fixation [Central intermediary metabolism]	3,310	down
RCAP_rcc03288_at	rnfB	electron transport complex protein RnfB	Electron transport [Energy metabolism],Nitrogen fixation [Central intermediary metabolism]	2,269	down
RCAP_rcc03289_at	rnfC	electron transport complex protein RnfC	Electron transport [Energy metabolism],Nitrogen fixation [Central intermediary metabolism]	2,754	down
RCAP_rcc03290_at	rnfD	electron transport complex protein RnfD	Electron transport [Energy metabolism],Nitrogen fixation [Central intermediary metabolism]	3,316	down
RCAP_rcc03338_at	aceA	isocitrate lyase	TCA cycle [Energy metabolism]	2,781	up

RCAP_rcc03496_at	maeB	malate dehydrogenase (oxaloacetate-decarboxylating) (NADP(+))	Other [Energy metabolism]	1,989	up
RCAP_rcc00143_at	etfA	electron transfer flavoprotein, alpha subunit	Other [Central intermediary metabolism]	1,999	up
RCAP_rcc00524_at	gyaR	glyoxylate reductase	Other [Central intermediary metabolism]	2,317	up
RCAP_rcc00570_at	nifK	nitrogenase molybdenum-iron protein beta chain	Nitrogen fixation [Central intermediary metabolism]	3,519	down
RCAP_rcc00571_at	nifD	nitrogenase molybdenum-iron protein alpha chain	Nitrogen fixation [Central intermediary metabolism]	3,531	down
RCAP_rcc00572_at	nifH	nitrogenase iron protein	Nitrogen fixation [Central intermediary metabolism]	2,541	down
RCAP_rcc01120_at	metK	methionine adenosyltransferase	Other [Central intermediary metabolism]	2,077	up
RCAP_rcc01593_at	cysH	phosphoadenosine phosphosulfate reductase	Sulfur metabolism [Central intermediary metabolism]	2,399	up
RCAP_rcc01724_at	speB	agmatinase	Polyamine biosynthesis [Central intermediary metabolism]	1,942	up
RCAP_rcc02816_at	sat	binfunctional sulfate adenylyltransferas	Sulfur metabolism [Central intermediary	1,923	up

Table D.1 (continued)

		e/adenylyl-sulfate kinase	metabolism]		
RCAP_rcc03271_at	nifU	nitrogen fixation protein NifU	Nitrogen fixation [Central intermediary metabolism]	8,030	down
RCAP_rcc03278_at	nifX	nitrogen fixation protein NifX	Nitrogen fixation [Central intermediary metabolism]	2,243	down
RCAP_rcc03279_at	nifN	nitrogenase molybdenum-iron cofactor biosynthesis protein NifN	Nitrogen fixation [Central intermediary metabolism]	1,945	down
RCAP_rcc03264_at	nifZ	NifZ family protein	Domain [Hypothetical proteins]	1,968	down
RCAP_rcc03294_at	fccB	FAD-dependent pyridine nucleotide-disulphide oxidoreductase	Other [Central intermediary metabolism]	2,268	down
RCAP_rcc03306_at		acyl-CoA dehydrogenase, medium-chain specific	Other [Central intermediary metabolism],Degradation [Fatty acid and phospholipid metabolism]	1,881	up
RCAP_rcc03284_at	fdxN	ferredoxin I	Domain [Hypothetical proteins]	2,761	down
RCAP_rcc03178_at	atoB	acetyl-CoA acetyltransferase	Toxin production and resistance [Cellular processes]	2,905	up

RCAP_rcc03179_at	phbB	acetoacetyl-CoA reductase	Biosynthesis [Fatty acid and phospholipid metabolism]	4,095	up
RCAP_rcc03449_at	atoB	acetyl-CoA acetyltransferase	Toxin production and resistance [Cellular processes]	3,460	up
RCAP_rcc03306_at		acyl-CoA dehydrogenase, medium-chain specific	Other [Central intermediary metabolism],Degradation [Fatty acid and phospholipid metabolism]	1,881	up
RCAP_rcc03241_at	mutB	methylmalonyl-CoA mutase, large subunit	Transposon functions [Mobile and extrachromosomal element functions]	2,482	up
RCAP_rcc01231_at		ubiquinone biosynthesis hydroxylase, UbiH/UbiF/VisC/COQ6 family	Menaquinone and ubiquinone [Biosynthesis of cofactors, prosthetic groups, and carriers]	1,794	down
Cell Envelope					
RCAP_rcc00167_at		glycosyl transferase, family 2/group 1	Biosynthesis and degradation of surface polysaccharides and lipopolysaccharides [Cell envelope]	1,798	up

RCAP_rcc01114_at		OmpA/MotB domain protein	Other [Cell envelope]	1,903	up
RCAP_rcc01132_at	galM	aldose 1-epimerase	Sugars [Energy metabolism] Cell Envelope	1,806	up
RCAP_rcc01127_at		membrane protein, putative	Other [Cell envelope]	1,864	up
RCAP_rcc01746_at		protein of unknown function DUF485, transmembrane	Other [Cell envelope]	3,539	up
RCAP_rcc03226_at		Polysaccharide biosynthesis/export protein family	Biosynthesis and degradation of surface polysaccharides and lipopolysaccharides [Cell envelope]	1,941	up
RCAP_rcc00734_at		lipoprotein, putative	Other [Cell envelope]	1,941	up
RCAP_rcc02596_at		lipoprotein, putative	Other [Cell envelope]	1,801	up
RCAP_rcc02251_at		membrane protein, putative	Other [Cell envelope]	1,938	down
RCAP_rcc01713_at		lipoprotein, putative	Other [Cell envelope]	2,043	down
RCAP_rcc01484_at		membrane protein, putative	Other [Cell envelope]	1,879	up

Table D.1 (continued)

RCAP_rcc02462_at		membrane protein, putative	Other [Cell envelope]	11,246	down
RCAP_rcc02479_at		lipoprotein, putative	Other [Cell envelope]	2,369	up
Cellular processes					
RCAP_rcc00615_at	acrA	acriflavine resistance protein A	Toxin production and resistance [Cellular processes]	2,595	up
RCAP_rcc00825_at	ftsA	cell division protein FtsA	Cell division [Cellular processes]	2,193	up
RCAP_rcc03281_at		peroxiredoxin	Detoxification [Cellular processes]	2,744	down
RCAP_rcc03525_at	flaA	flagellin protein	Chemotaxis and motility [Cellular processes]	5,336	up
DNA metabolism					
RCAP_rcc00201_at		site-specific DNA-methyltransferase (adenine-specific)	Restriction/modification [DNA metabolism]	2,920	up
RCAP_rcc01126_at	ihfB	integration host factor, beta subunit	DNA replication, recombination, and repair [DNA metabolism]	2,167	up
RCAP_rcc01912_at	ihfA	integration host factor, alpha subunit	DNA replication, recombination, and repair [DNA metabolism]	2,335	up

RCAP_rcc02429_at	xthA	exodeoxyribonuclease III	DNA replication, recombination, and repair [DNA metabolism]	1,753	up
RCAP_rcp00031_at		phage integrase	Prophage functions [Mobile and extrachromosomal element functions]	2,425	up
RCAP_rcp00031_x_at		phage integrase	Prophage functions [Mobile and extrachromosomal element functions]	2,451	up
Fatty acid and phospholipid metabolism					
RCAP_rcc00405_at		acyl-CoA dehydrogenase domain protein	Degradation [Fatty acid and phospholipid metabolism]	2,882	up
RCAP_rcc00442_at	prpE	propionate--CoA ligase	Other [Fatty acid and phospholipid metabolism]	2,425	up
RCAP_rcc00475_at		acyl-CoA dehydrogenase domain protein	Degradation [Fatty acid and phospholipid metabolism]	3,014	up
RCAP_rcc00518_at	fadA	fatty acid oxidation complex, beta subunit	Degradation [Fatty acid and phospholipid metabolism]	3,710	up
RCAP_rcc00520_at	fadB	fatty acid oxidation complex, alpha subunit	Degradation [Fatty acid and phospholipid metabolism]	4,269	up

Table D.1 (continued)

			Transcription		
RCAP_rcc00276_at	rbfA	ribosome-binding factor A	RNA processing [Transcription]	1,923	down
RCAP_rcc01171_at		ATP-dependent RNA helicase DbpA	Other [Transcription]	2,539	down
RCAP_rcc02811_at	rpoH	RNA polymerase sigma-32 factor	Transcription factors [Transcription]	2,187	down
			Regulatory functions		
RCAP_rcc00045_at	regA	photosynthetic apparatus regulatory protein RegA	DNA interactions [Regulatory functions]	1,987	up
RCAP_rcc00263_at		two component transcriptional regulator, winged helix family	DNA interactions [Regulatory functions]	2,232	down
RCAP_rcc00473_at		transcriptional regulator, MerR family	DNA interactions [Regulatory functions]	2,554	up
RCAP_rcc00474_at		transcriptional regulator, MerR family	DNA interactions [Regulatory functions]	2,559	up
RCAP_rcc00494_at		transcriptional regulator, AsnC/Lrp family	DNA interactions [Regulatory functions]	1,840	up
RCAP_rcc01597_at		transcriptional regulator, AsnC/Lrp family	DNA interactions [Regulatory functions]	2,106	up

Table D.1 (continued)

RCAP_rcc01673_at	glnB	nitrogen regulatory protein P-II	Protein interactions [Regulatory functions]	1,827	up
RCAP_rcc01798_at	ntrC	nitrogen assimilation regulatory protein NtrC	Other [Regulatory functions]	2,134	up
RCAP_rcc01896_at		transcriptional regulator, GntR family	DNA interactions [Regulatory functions]	1,892	down
RCAP_rcc02440_at		transcriptional regulator, AsnC/Lrp family	DNA interactions [Regulatory functions]	4,759	up
RCAP_rcc02527_at		transcriptional regulator, XRE family	Other [Regulatory functions]	2,105	up
RCAP_rcc02590_at	dksA	DnaK suppressor protein	DNA interactions [Regulatory functions]	2,322	up
RCAP_rcc02594_at		response regulator receiver protein	Protein interactions [Regulatory functions]	2,143	up
RCAP_rcc02771_at		transcriptional regulator, TetR family	DNA interactions [Regulatory functions]	1,813	up
RCAP_rcc02813_at	lrp	leucine-responsive regulatory protein	DNA interactions [Regulatory functions]	2,115	up
RCAP_rcc03387_at	glnB	nitrogen regulatory protein P-II	Protein interactions [Regulatory functions]	4,374	up
Unknown Function and Hypothetical Proteins					

Table D.1 (continued)

RCAP_rcc00088_at		conserved hypothetical protein	Conserved [Hypothetical proteins]	1,997	up
RCAP_rcc00130_at		radical SAM family protein	Enzymes of unknown specificity [Unknown function]	1,789	down
RCAP_rcc00133_at		conserved hypothetical protein	Conserved [Hypothetical proteins]	3,612	down
RCAP_rcc00194_at		ErfK/YbiS/YcfS/YnhG family protein/Tat domain protein	General [Unknown function]	2,039	down
RCAP_rcc00216_at		conserved hypothetical protein	Conserved [Hypothetical proteins]	4,238	up
RCAP_rcc00227_at		protein of unknown function DUF1159	General [Unknown function]	2,150	down
RCAP_rcc00264_at		conserved hypothetical protein	Conserved [Hypothetical proteins]	1,854	up
RCAP_rcc00274_at		protein of unknown function DUF1674	General [Unknown function]	1,757	down
RCAP_rcc00415_at		oxidoreductase, short-chain dehydrogenase/reductase family	Enzymes of unknown specificity [Unknown function]	2,967	up
RCAP_rcc00543_at		protein of unknown function DUF1523	General [Unknown function]	3,368	down

Table D.1 (continued)

RCAP_rcc00565_at	modD	molybdenum utilization protein ModD	General [Unknown function]	1,783	up
RCAP_rcc00728_at	nurU	NnrU family protein	General [Unknown function]	2,042	up
RCAP_rcc00737_at		hypothetical protein		4,632	down
RCAP_rcc00747_at		conserved hypothetical protein	Conserved [Hypothetical proteins]	3,971	down
RCAP_rcc00880_at		CHAP domain protein	Enzymes of unknown specificity [Unknown function]	2,029	down
RCAP_rcc00901_at		conserved hypothetical protein	Conserved [Hypothetical proteins]	3,143	up
RCAP_rcc01116_at		PhoH family protein	General [Unknown function]	1,809	up
RCAP_rcc01155_at		conserved hypothetical protein	Conserved [Hypothetical proteins]	3,366	up
RCAP_rcc01156_at		UspA domain protein	General [Unknown function]	2,488	up
RCAP_rcc01546_at		AMP-dependent synthetase and ligase family protein	Enzymes of unknown specificity [Unknown function]	6,795	up

Table D.1 (continued)

RCAP_rcc01557_at		rhodanese domain protein	General [Unknown function]	2,041	down
RCAP_rcc01579_at		conserved hypothetical protein	Conserved [Hypothetical proteins]	2,834	down
RCAP_rcc01580_at		conserved hypothetical protein	Conserved [Hypothetical proteins]	1,997	down
RCAP_rcc01589_at		ErfK/YbiS/YcfS/YnhG family protein	Unknown substrate [Transport and binding proteins]	3,976	down
RCAP_rcc01753_at		protein of unknown function DUF1330	General [Unknown function]	1,820	up
RCAP_rcc01814_at		conserved hypothetical protein	Conserved [Hypothetical proteins]	2,485	up
RCAP_rcc01897_at		protein of unknown function DUF1127	General [Unknown function]	2,140	down
RCAP_rcc01900_at		hemolysin-type calcium-binding repeat family protein	Enzymes of unknown specificity [Unknown function]	1,959	up
RCAP_rcc02149_at		protein of unknown function DUF1223	General [Unknown function]	2,530	down
RCAP_rcc02182_at		aminotransferase, class III	Enzymes of unknown specificity [Unknown function]	1,813	up

178

Table D.1 (continued)

RCAP_rcc02273_at		conserved hypothetical protein	Conserved [Hypothetical proteins]	2,297	down
RCAP_rcc02385_at		protein of unknown function DUF1127	General [Unknown function]	5,967	down
RCAP_rcc02515_at	rhlE	ATP-dependent RNA helicase RhlE	Other [Transcription],General [Unknown function]	2,890	down
RCAP_rcc02612_at		transthyretin family protein	General [Unknown function]	1,854	up
RCAP_rcc02614_at		cupin domain protein	General [Unknown function]	1,762	up
RCAP_rcc02665_at		hemolysin-type calcium-binding repeat family protein	General [Unknown function]	2,508	up
RCAP_rcc02795_at		sterol-binding domain protein	General [Unknown function]	2,336	up
RCAP_rcc02798_at		transglutaminase domain protein	General [Unknown function]	2,028	up
RCAP_rcc02799_at		protein of unknown function DUF403	General [Unknown function]	3,347	up
RCAP_rcc02800_at		protein of unknown function DUF404	Conserved [Hypothetical proteins]	2,957	up

Table D.1 (continued)

RCAP_rcc02817_at		protein of unknown function DUF1150	General [Unknown function]	1,939	down
RCAP_rcc03108_at		protein of unknown function DUF305	General [Unknown function]	3,545	down
RCAP_rcc03116_at		conserved hypothetical protein	Conserved [Hypothetical proteins]	1,981	down
RCAP_rcc03181_at		protein of unknown function DUF465	Conserved [Hypothetical proteins]	2,248	up
RCAP_rcc03214_at		protein of unknown function DUF1127	General [Unknown function]	2,558	down
RCAP_rcc03272_at		HesB/YadR/YfhF family protein	General [Unknown function]	1,883	down
RCAP_rcc03276_at		protein of unknown function DUF683	General [Unknown function]	2,237	down
RCAP_rcc03325_at		hemimethylated DNA-binding protein family	General [Unknown function]	1,845	up
RCAP_rcc03448_at		serine/threonine-protein phosphatase	Enzymes of unknown specificity [Unknown function]	2,200	down
RCAP_rcc00283_at		conserved hypothetical protein	Conserved [Hypothetical proteins]	4,518	down

Table D.1 (continued)

RCAP_rcc00307_at		conserved hypothetical protein	Conserved [Hypothetical proteins]	1,968	down
RCAP_rcc00319_at		conserved hypothetical protein	Conserved [Hypothetical proteins]	1,920	down
RCAP_rcc00374_at		hypothetical protein	hypothetical protein	2,169	down
RCAP_rcc00837_at		conserved hypothetical protein	Conserved [Hypothetical proteins]	2,005	down
RCAP_rcc01522_at		conserved hypothetical protein	Conserved [Hypothetical proteins]	2,579	up
RCAP_rcc01528_at		conserved hypothetical protein	Conserved [Hypothetical proteins]	2,564	up
RCAP_rcc01541_at		conserved hypothetical protein	Conserved [Hypothetical proteins]	2,260	down
RCAP_rcc02014_at		conserved hypothetical protein	Conserved [Hypothetical proteins]	2,631	down
RCAP_rcc03008_at		conserved hypothetical protein	Conserved [Hypothetical proteins]	1,830	down
RCAP_rcc03009_at		conserved hypothetical protein	Conserved [Hypothetical proteins]	2,478	down
RCAP_rcc03010_at		conserved hypothetical protein	Conserved [Hypothetical proteins]	3,533	down

Table D.1 (continued)

RCAP_rcc03029_at		conserved hypothetical protein	Conserved [Hypothetical proteins]	1,834	up
RCAP_rcc03261_at		TOBE domain protein	Domain [Hypothetical proteins]	2,547	down
RCAP_rcc03394_at		conserved hypothetical protein	Conserved [Hypothetical proteins]	3,241	up
RCAP_rcc02125_2860_at		protein of unknown function DUF485, transmembrane	Other [Cell envelope]	2,847	up
RCAP_rcc03466_at		rubredoxin domain/protein of unknown function DUF125, transmembrane	NULL	1,884	down

COMPLETE LIST OF GENES THAT ARE DIFFERENTIALLY REGULATED ON DIFFERENT
ACETATE CONCENTRATIONS

Table E. 1 Transcript profile on 80mM acetate compared to 40mM acetate

80mM ACETATE vs 40mM ACETATE					
Transport and binding proteins					
RCAP_rcc00190_at		ABC transporter, ATP-binding/permease protein	Unknown substrate [Transport and binding proteins]	2,168	up
RCAP_rcc00184_at		outer membrane efflux protein	Unknown substrate [Transport and binding proteins]	2,700	down
RCAP_rcc00618_at		ABC transporter, ATP-binding/permease protein	Unknown substrate [Transport and binding proteins]	2,494	up
RCAP_rcc00619_at		ABC transporter, permease protein	Unknown substrate [Transport and binding proteins]	2,242	up

RCAP_rcc00705_at	oppB	oligopeptide ABC transporter, permease protein OppB	Amino acids, peptides and amines [Transport and binding proteins]	1,793	down
RCAP_rcc00706_at	oppA	oligopeptide ABC transporter, periplasmic oligopeptide-binding protein OppA	Amino acids, peptides and amines [Transport and binding proteins]	6,799	down
RCAP_rcc00846_at	dppA	dipeptide ABC transporter, periplasmic dipeptide-binding protein DppA	Amino acids, peptides and amines [Transport and binding proteins]	1,952	down
RCAP_rcc00848_at	dppC	dipeptide ABC transporter, permease protein DppC	Amino acids, peptides and amines [Transport and binding proteins]	1,900	down
RCAP_rcc01243_at	potA	polyamine ABC transporter, ATP binding protein PotA	Amino acids, peptides and amines [Transport and binding proteins]	2,696	down
RCAP_rcc01244_at	potD	polyamine ABC transporter, periplasmic polyamine-binding protein PotD	Amino acids, peptides and amines [Transport and binding proteins]	5,676	down
RCAP_rcc01245_at	potB	polyamine ABC transporter, permease protein PotB	Amino acids, peptides and amines [Transport and binding proteins]	6,301	down

RCAP_rcc01246_at	potI	polyamine ABC transporter, permease protein PotI	Amino acids, peptides and amines [Transport and binding proteins]	5,625	down
RCAP_rcc01369_at		ABC transporter, periplasmic substrate-binding protein	Unknown substrate [Transport and binding proteins]	2,154	down
RCAP_rcc01589_at		ErfK/YbiS/YcfS/YnhG family protein	Unknown substrate [Transport and binding proteins]	2,945	up
RCAP_rcc02127_at	phaG	monovalent cation/proton antiporter, G subunit	Cations and iron carrying compounds [Transport and binding proteins]	1,781	down
RCAP_rcc02521_at		pyrimidine ABC transporter, periplasmic pyrimidine-binding protein	Nucleosides, purines and pyrimidines [Transport and binding proteins]	2,304	down
RCAP_rcc02522_at		pyrimidine ABC transporter, permease protein	Nucleosides, purines and pyrimidines [Transport and binding proteins]	2,277	down
RCAP_rcc02524_at		pyrimidine ABC transporter, ATP-binding protein	Nucleosides, purines and pyrimidines [Transport and binding proteins]	2,277	down
RCAP_rcc02529_at		pyridine nucleotide-disulphide oxidoreductase family protein	Amino acid transport and metabolism [Metabolism]	2,306	down

RCAP_rcc02578_at		iron(III) ABC transporter, periplasmic iron(III)-compound-binding protein	Cations and iron carrying compounds [Transport and binding proteins]	2,404	down
RCAP_rcc02789_at	kefC	glutathione-regulated potassium-efflux system protein KefC	Cations and iron carrying compounds [Transport and binding proteins]	2,286	up
RCAP_rcc02959_at	potD	spermidine/putrescine ABC transporter, periplasmic spermidine/putrescine-binding protein	Amino acids, peptides and amines [Transport and binding proteins]	2,525	down
RCAP_rcc03022_at	dctM	TRAP C4-dicarboxylate transport system permease, DctM subunit	Carbohydrates, organic alcohols, and acids [Transport and binding proteins]	2,221	down
RCAP_rcc03023_at	dctQ	tripartite ATP-independent periplasmic transporter, DctQ component	Carbohydrates, organic alcohols, and acids [Transport and binding proteins]	3,116	down
RCAP_rcc03024_at	dctP	TRAP dicarboxylate transporter, DctP subunit	Carbohydrates, organic alcohols, and acids [Transport and binding proteins]	3,507	down
RCAP_rcc02621_at	sulP	sulphate transporter	Anions [Transport and binding proteins]	3,684	up
RCAP_rcc03430_at	livM	branched-chain amino acid ABC transporter,	Amino acids, peptides and amines	3,019	Up

186

		permease			
RCAP_rcc03120_at		ABC transporter, ATP-binding protein	Unknown substrate [Transport and binding proteins]	2,099	down
RCAP_rcc00184_at		outer membrane efflux protein	Unknown substrate [Transport and binding proteins]	2,700	down
Amino acid biosynthesis					
RCAP_rcc00161_at	gltB	glutamate synthase (NADPH), alpha subunit	Glutamate family [Amino acid biosynthesis]	2,829	up
RCAP_rcc00163_at	gltD	glutamate synthase (NADPH), beta subunit	Glutamate family [Amino acid biosynthesis]	4,677	up
RCAP_rcc00379_at	dapA	dihydrodipicolinate synthase	Aspartate family [Amino acid biosynthesis]	1,960	down
RCAP_rcc00421_at	lysC	aspartate kinase	Aspartate family [Amino acid biosynthesis]	2,258	down
RCAP_rcc00438_at	glyA	serine hydroxymethyltransferase	Serine family [Amino acid biosynthesis]	1,878	down
RCAP_rcc00490_at	metF	5,10-methylenetetrahydrofolate reductase	Aspartate family [Amino acid biosynthesis]	2,695	down

187

RCAP_rcc01214_at	ilvC	ketol-acid reductoisomerase	Pyruvate family [Amino acid biosynthesis]	2,287	up
RCAP_rcc01850_at	aroF	3-deoxy-7-phosphoheptulonate synthase	Aromatic amino acid family [Amino acid biosynthesis]	1,841	down
RCAP_rcc02777_at	glnA	glutamine synthetase	Glutamate family [Amino acid biosynthesis]	1,885	down
RCAP_rcc03109_at		serine--glyoxylate aminotransferase/alanine--glyoxylate aminotransferase/serine--pyruvate aminotransferase	Aspartate family [Amino acid biosynthesis]	1,900	up
Protein synthesis					
RCAP_rcc00313_at	rpsN	30S ribosomal protein S14	Ribosomal proteins: synthesis and modification [Protein synthesis]	1,858	down
RCAP_rcc00317_at	rpsE	30S ribosomal protein S5	Ribosomal proteins: synthesis and modification [Protein synthesis]	1,829	down
RCAP_rcc00532_at	aspS	aspartyl-tRNA synthetase	tRNA aminoacylation [Protein synthesis]	1,872	down
RCAP_rcc02461_at	thrS	threonyl-tRNA synthetase	tRNA aminoacylation [Protein synthesis]	3,252	up

RCAP_rcc02464_at	proS	prolyl-tRNA synthetase	tRNA aminoacylation [Protein synthesis]	1,919	down
RCAP_rcc02506_at	rluB	ribosomal large subunit pseudouridine synthase B	tRNA and rRNA base modification [Protein synthesis]	2,439	up
Protein fate					
RCAP_rcc00034_s_at	hslU	ATP-dependent hsl protease ATP-binding subunit hslU	Protein folding and stabilization [Protein fate]	2,026	down
RCAP_rcc00220_at	secA	preprotein translocase, SecA subunit	Protein and peptide secretion and trafficking [Protein fate]	2,127	down
RCAP_rcc00224_at	dnaK	chaperone DnaK	Protein folding and stabilization [Protein fate]	1,763	down
RCAP_rcc00228_at		oxidoreductase, DSBA family	Protein folding and stabilization [Protein fate]	1,792	up
RCAP_rcc00345_at	oxaA	inner membrane protein OxaA	Protein and peptide secretion and trafficking [Protein fate]	1,936	down
RCAP_rcc00507_at		type II secretion system protein	Protein and peptide secretion and trafficking [Protein fate]	1,797	down
RCAP_rcc00617_at		secretion protein, HlyD family	Protein and peptide secretion and trafficking [Protein fate]	2,325	up

RCAP_rcc00653_at		ABC-1 domain protein	Protein folding and stabilization [Protein fate]	4,674	up
RCAP_rcc00710_at	hipO	hippurate hydrolase	Degradation of proteins, peptides, and glycopeptides [Protein fate]	1,945	down
RCAP_rcc00806_at		heat shock protein DnaJ domain protein	Protein folding and stabilization [Protein fate]	1,903	up
RCAP_rcc01167_at	clpS	ATP-dependent Clp protease adaptor protein ClpS	Degradation of proteins, peptides, and glycopeptides [Protein fate]	2,084	up
RCAP_rcc01709_at	ppiA	peptidyl-prolyl cis-trans isomerase A	Protein folding and stabilization [Protein fate]	2,355	down
RCAP_rcc01710_at	ppiB	peptidyl-prolyl cis-trans isomerase B	Protein folding and stabilization [Protein fate]	2,387	down
RCAP_rcc02162_at	mrcA	penicillin-binding protein 1A	Degradation of proteins, peptides, and glycopeptides [Protein fate]	1,860	up
RCAP_rcc02163_at	ccdA	cytochrome c-type biogenesis protein CcdA	Degradation of proteins, peptides, and glycopeptides [Protein fate]	3,679	up
RCAP_rcc02399_at	hflK	HflK protein	Degradation of proteins, peptides, and glycopeptides [Protein fate]	1,883	down
RCAP_rcc02400_at	hflC	HflC protein	Degradation of proteins, peptides, and glycopeptides [Protein fate]	2,224	down

RCAP_rcc02402_at	degP	protease Do	Degradation of proteins, peptides, and glycopeptides [Protein fate]	2,085	up
RCAP_rcc02477_at	groS	chaperonin GroS	Protein folding and stabilization [Protein fate]	2,253	down
RCAP_rcc02478_at	groL	chaperonin GroL	Protein folding and stabilization [Protein fate]	1,899	down
RCAP_rcc03097_at	tldD	protein TldD	Other [Protein fate]	1,846	up
RCAP_rcc03259_at	msrB	peptide-methionin (R)-S-oxide reductase	Protein modification and repair [Protein fate]	3,207	Up
RCAP_rcc03327_at	lolA	outer membrane lipoprotein carrier protein LolA	Protein and peptide secretion and trafficking [Protein fate]	3,036	Up
RCAP_rcc03333_at		peptidase, S16 family	Degradation of proteins, peptides, and glycopeptides [Protein fate]	1,834	Up
tRNA					
RCAP_rct00001_at	tRNA	tRNA-Pro-CGG	Pro Anticodon-CGG	1,793	Up
RCAP_rct00035_at	tRNA	tRNA-Thr-GGT	Thr Anticodon-GGT	1,966	Up
RCAP_rct00039_at	tRNA	tRNA-Ser-GCT	Ser Anticodon-GCT	1,998	Up

			Energy metabolism		
RCAP_rcc00484_at	ald	alanine dehydrogenase	Amino acids and amines [Energy metabolism]	4,554	down
RCAP_rcc00538_at		methylmalonyl-CoA epimerase	Other [Energy metabolism]	1,905	down
RCAP_rcc00573_at	fdxD	ferredoxin V	Electron transport [Energy metabolism]	2,701	down
RCAP_rcc00659_at	puhA	photosynthetic reaction center, H subunit	Photosynthesis [Energy metabolism]	4,314	down
RCAP_rcc00660_at	pucC	PucC protein	Photosynthesis [Energy metabolism]	2,176	down
RCAP_rcc00691_at	pufB	light-harvesting protein B-870, beta subunit	Photosynthesis [Energy metabolism]	4,001	down
RCAP_rcc00692_at	pufA	light-harvesting protein B-870, alpha subunit	Photosynthesis [Energy metabolism]	4,212	down
RCAP_rcc00693_at	pufL	photosynthetic reaction center, L subunit	Photosynthesis [Energy metabolism]	4,950	down
RCAP_rcc00694_at	pufM	photosynthetic reaction center, M subunit	Photosynthesis [Energy metabolism]	5,288	down
RCAP_rcc00695_at	pufX	intrinsic membrane protein PufX	Photosynthesis [Energy metabolism]	5,619	down

RCAP_rcc00718_at	mdh	malate dehydrogenase	TCA cycle [Energy metabolism]	1,827	down
RCAP_rcc00740_at	atpI	ATP synthase F0, I subunit	ATP-proton motive force interconversion [Energy metabolism]	2,318	down
RCAP_rcc00741_at	atpB	ATP synthase F0, A subunit	ATP-proton motive force interconversion [Energy metabolism]	3,660	down
RCAP_rcc00742_at	atpE	ATP synthase F0, C subunit	ATP-proton motive force interconversion [Energy metabolism]	6,510	down
RCAP_rcc00743_at	atpX	ATP synthase F0, B' subunit	ATP-proton motive force interconversion [Energy metabolism]	6,669	down
RCAP_rcc00744_at	atpF	ATP synthase F0, B subunit	ATP-proton motive force interconversion [Energy metabolism]	6,119	down
RCAP_rcc00761_at	hoxH	NAD-reducing hydrogenase HoxS, beta subunit	Electron transport [Energy metabolism]	1,779	down
RCAP_rcc00762_at	hoxW	hydrogenase maturation factor HowW	[Energy metabolism]	3,335	down
RCAP_rcc00767_at	hupA	hydrogenase, small subunit	Electron transport [Energy metabolism]	2,384	down

193

RCAP_rcc00768_at	hupB	hydrogenase, large subunit	Electron transport [Energy metabolism]	3,130	down
RCAP_rcc00769_at	hupC	hydrogenase, cytochrome b subunit	Electron transport [Energy metabolism]	3,555	down
RCAP_rcc00911_at	pccA	propionyl-CoA carboxylase, alpha subunit	Amino acids and amines [Energy metabolism],Biosynthesis [Fatty acid and phospholipid metabolism]	1,882	up
RCAP_rcc01143_at	gcvH	glycine cleavage system H protein	Amino acids and amines [Energy metabolism]	3,174	down
RCAP_rcc01144_at	gcvP	glycine dehydrogenase (decarboxylating)	Amino acids and amines [Energy metabolism]	1,937	down
RCAP_rcc01518_at	nuoB	NADH-quinone oxidoreductase, B subunit	Electron transport [Energy metabolism]	1,927	down
RCAP_rcc01520_at	nuoD	NADH-quinone oxidoreductase, D subunit	Electron transport [Energy metabolism]	2,101	down
RCAP_rcc01521_at	nuoE	NADH-quinone oxidoreductase, E subunit	Electron transport [Energy metabolism]	2,032	down
RCAP_rcc01565_at	mmsA	methylmalonate-semialdehyde dehydrogenase (acylating)	Amino acids and amines [Energy metabolism]	1,787	up
RCAP_rcc01703_at	pdhC	pyruvate dehydrogenase complex, E2 component, dihydrolipoyllysi	Pyruvate dehydrogenase [Energy metabolism]	1,926	down

		ne-residue acetyltransferas e			
RCAP_rcc01704_at	pdhB	pyruvate dehydrogenase complex, E1 component, pyruvate dehydrogenase (acetyl-transferring), beta subunit	Pyruvate dehydrogenase [Energy metabolism]	1,758	down
RCAP_rcc01705_at	pdhA	pyruvate dehydrogenase complex, E1 component, pyruvate dehydrogenase (acetyl-transferring), alpha subunit	Pyruvate dehydrogenase [Energy metabolism]	1,931	down
RCAP_rcc01708_at	pgk	phosphoglycerat e kinase	Glycolysis/glucone ogenesis [Energy metabolism]	2,161	down
RCAP_rcc01723_at	ccpA	cytochrome-c peroxidase	Electron transport [Energy metabolism]	5,480	down
RCAP_rcc01828_at	rpe	ribulose-phosphate 3-epimerase	Pentose phosphate pathway [Energy metabolism]	1,842	down
RCAP_rcc01829_at	cbbM	ribulose bisphosphate carboxylase, large subunit	Photosynthesis [Energy metabolism]	2,271	down
RCAP_rcc01830_at	fba	fructose-bisphosphate aldolase	Glycolysis/glucone ogenesis [Energy metabolism]	2,210	down

RCAP_rcc01887_at	icd	Isocitrate dehydrogenase (NADP(+))	TCA cycle [Energy metabolism]	2,563	down
RCAP_rcc02150_at	acnA	aconitate hydratase	TCA cycle [Energy metabolism]	3,164	down
RCAP_rcc02160_at	gap	glyceraldehyde-3-phosphate dehydrogenase (phosphorylating)	Glycolysis/gluconeogenesis [Energy metabolism]	2,067	down
RCAP_rcc02364_at	gltA	citrate (Si)-synthase	TCA cycle [Energy metabolism]	2,087	down
RCAP_rcc02501_at	cycY	cytochrome c, class I	Electron transport [Energy metabolism]	2,169	down
RCAP_rcc02530_at	pucB	light-harvesting protein B-800/850, beta chain	Photosynthesis [Energy metabolism]	3,362	down
RCAP_rcc02531_at	pucA	light-harvesting protein B-800/850, alpha chain	Photosynthesis [Energy metabolism]	3,510	down
RCAP_rcc02533_at	pucDE	light-harvesting protein B-800/850, gamma chain	Photosynthesis [Energy metabolism]	5,166	down
RCAP_rcc02598_at	bioA	beta-alanine--pyruvate transaminase	Amino acids and amines [Energy metabolism]	2,035	down
RCAP_rcc02679_at		pyridine nucleotide-disulphide oxidoreductase family protein	Electron transport [Energy metabolism]	3,938	up

RCAP_rcc02681_at		cytochrome b561 family protein	Electron transport [Energy metabolism]	2,819	up
RCAP_rcc02768_at	petA	ubiquinol--cytochrome-c reductase, iron-sulfur subunit	Electron transport [Energy metabolism]	2,998	down
RCAP_rcc02769_at	petB	ubiquinol--cytochrome-c reductase, cytochrome b subunit	Electron transport [Energy metabolism]	3,862	down
RCAP_rcc02814_at	trxB	thioredoxin-disulfide reductase	Electron transport [Energy metabolism]	1,814	down
RCAP_rcc02845_at	torA	trimethylamine-N-oxide reductase	Anaerobic [Energy metabolism]	3,959	down
RCAP_rcc02971_at	atpD	ATP synthase F1, beta subunit	ATP-proton motive force interconversion [Energy metabolism]	2,125	down
RCAP_rcc02972_at	atpG	ATP synthase F1, gamma subunit	ATP-proton motive force interconversion [Energy metabolism]	2,319	down
RCAP_rcc02973_at	atpA	ATP synthase F1, alpha subunit	ATP-proton motive force interconversion [Energy metabolism]	2,281	down
RCAP_rcc02974_at	atpH	ATP synthase F1, delta subunit	ATP-proton motive force interconversion [Energy metabolism]	1,800	down

197

RCAP_rcc03161_at	dat	D-amino-acid transaminase	Amino acids and amines [Energy metabolism]	2,023	down
RCAP_rcc03162_at		mandelate racemase/muconate lactonizing enzyme family protein	Other [Energy metabolism]	2,839	down
RCAP_rcc03287_at	rnfA	electron transport complex protein RnfA	Electron transport [Energy metabolism]	2,834	Down
RCAP_rcc03288_at	rnfB	electron transport complex protein RnfB	Electron transport [Energy metabolism]	1,791	Down
RCAP_rcc03334_at	trxA	thioredoxin	Electron transport [Energy metabolism]	1,781	Down
RCAP_rcc00144_at	etfB	electron transfer flavoprotein, beta subunit	Energy metabolism	2,068	down
RCAP_rcc00228_at		oxidoreductase, DSBA family	Electron transport [Energy metabolism]	1,792	up
RCAP_rcc03258_at		cytoChrome c biogenesis protein, transmembrane region	Energy metabolism	3,787	Up
Central intermediary metabolism					
RCAP_rcc01218_at	ureA	urease, gamma subunit	Nitrogen metabolism [Central intermediary	2,053	up

			metabolism]		
RCAP_rcc01219_at	ureB	urease, beta subunit	Nitrogen metabolism [Central intermediary metabolism]	1,934	up
RCAP_rcc02707_at	cynT	carbonate dehydratase	Other [Central intermediary metabolism]	1,883	down
RCAP_rcc03256_at		cytochrome P450 family protein	Other [Central intermediary metabolism]	2,002	Up
RCAP_rcc03257_at	msrA	peptide-methionine-(S)-S-oxide reductase	Other [Central intermediary metabolism]	2,890	Up
Biosynthesis of cofactors, prosthetic groups, and carriers					
RCAP_rcc00235_at	folC	folylpolyglutamate synthase/dihydrofolate synthase	Folic acid [Biosynthesis of cofactors, prosthetic groups, and carriers]	1,775	down
RCAP_rcc00661_at	bchM	magnesium-protoporphyrin O-methyltransferase	Chlorophyll and bacteriochlorphyll [Biosynthesis of cofactors, prosthetic groups, and carriers]	1,753	down
RCAP_rcc00662_at	bchL	light-independent protochlorophyllide reductase, iron-sulfur ATP-binding protein	Chlorophyll and bacteriochlorphyll [Biosynthesis of cofactors, prosthetic groups, and carriers]	1,807	down

199

RCAP_rcc00696_at	dxS	1-deoxy-D-xylulose-5-phosphate synthase	Other [Biosynthesis of cofactors, prosthetic groups, and carriers]	2,181	down
RCAP_rcc01559_at		methyltransferase, type 11 family	Other [Biosynthesis of cofactors, prosthetic groups, and carriers]	1,916	up
RCAP_rcc01878_at	sufD	FeS assembly protein SufD	Other [Biosynthesis of cofactors, prosthetic groups, and carriers]	2,670	down
RCAP_rcc01879_at	sufC	FeS assembly ATPase SufC	Other [Biosynthesis of cofactors, prosthetic groups, and carriers]	2,535	down
RCAP_rcc02840_at	moaC	molybdenum cofactor biosynthesis protein C	Molybdopterin [Biosynthesis of cofactors, prosthetic groups, and carriers]	1,751	down
RCAP_rcc03423_at	ispH	4-hydroxy-3-methylbut-2-enyl diphosphate reductase	Other [Biosynthesis of cofactors, prosthetic groups, and carriers]	1,797	Down
RCAP_rcc03504_at	cbiX	cobalamin biosynthesis protein CbiX	Heme, porphyrin, and cobalamin [Biosynthesis of cofactors, prosthetic groups, and carriers]	5,201	Up
Cell envelope					

RCAP_rcc00124_at	galE	UDP-glucose 4-epimerase	[Cell envelope]	1,815	up
RCAP_rcc00125_at	galU	UTP--glucose-1-phosphate uridylyltransferase	Biosynthesis and degradation of surface polysaccharides and lipopolysaccharides [Cell envelope]	2,028	up
RCAP_rcc00125_x_at	galU	UTP--glucose-1-phosphate uridylyltransferase	Biosynthesis and degradation of surface polysaccharides and lipopolysaccharides [Cell envelope]	1,847	up
RCAP_rcc00827_at	lpxC	UDP-3-O-[3-hydroxymyristoyl] N-acetylglucosamine deacetylase	Biosynthesis and degradation of surface polysaccharides and lipopolysaccharides [Cell envelope]	4,132	up
RCAP_rcc01500_at	glmS	glutamine--fructose-6-phosphate transaminase (isomerizing)	Biosynthesis and degradation of murein sacculus and peptidoglycan [Cell envelope]	1,906	up
RCAP_rcc01501_at	glmU	bifunctional UDP-N-acetylglucosamine diphosphorylase /glucosamine-1-phosphate N-acetyltransferase	Biosynthesis and degradation of murein sacculus and peptidoglycan [Cell envelope]	1,775	up

RCAP_rcc03420_at		LrgB family protein	Other [Cell envelope]	1,814	Up
RCAP_rcc01960_at	wza	polysaccharide export protein Wza	Biosynthesis and degradation of surface polysaccharides and lipopolysaccharides [Cell envelope]	2,267	up
RCAP_rcc01806_at		transglycosylase, Slt family	Biosynthesis and degradation of murein sacculus and peptidoglycan [Cell envelope]	2,568	up
RCAP_rcc03457_at	mepA	penicillin-insensitive murein endopeptidase MepA	Biosynthesis and degradation of murein sacculus and peptidoglycan [Cell envelope]	3,389	Up
RCAP_rcc03468_at	pncA	pyrazinamidase/ nicotinamidase	Biosynthesis and degradation of surface polysaccharides and lipopolysaccharides [Cell envelope]	1,878	Up
RCAP_rcc00435_at		membrane protein, putative	Hypothethical protein	4,694	down
RCAP_rcc00656_at		membrane protein, putative	[Hypothetical proteins]	1,795	down
RCAP_rcc00821_at		membrane protein, putative	[Hypothetical proteins]	1,834	down

202

RCAP_rcc01234_at		membrane protein, putative	[Hypothetical proteins]	1,787	down
RCAP_rcc01560_at		membrane protein, putative	[Hypothetical proteins]	3,058	up
RCAP_rcc01578_at		lipoprotein, putative	[Hypothetical proteins]	2,118	up
RCAP_rcc01739_at		membrane protein, putative	[Hypothetical proteins]	3,046	down
RCAP_rcc01877_at		membrane protein, putative	[Hypothetical proteins]	1,843	down
RCAP_rcc02462_at		membrane protein, putative	[Hypothetical proteins]	2,311	up
RCAP_rcc03429_at		membrane protein, putative	[Hypothetical proteins]	1,967	up
Cellular processes					
RCAP_rcc00432_at	mdtB	multidrug resistance protein MdtB	Toxin production and resistance [Cellular processes]	2,051	down
RCAP_rcc00501_at	cpaB	Flp pilus assembly protein CpaB	[Cellular processes]	1,780	down
RCAP_rcc00825_at	ftsA	cell division protein FtsA	Cell division [Cellular processes]	1,978	down

RCAP_rcc01118_at	corC	magnesium and cobalt efflux protein CorC	Toxin production and resistance [Cellular processes]	1,972	up
RCAP_rcc01253_at		sporulation domain protein	Sporulation and germination [Cellular processes]	2,411	up
RCAP_rcc01738_at	katG	catalase/peroxidase	Detoxification [Cellular processes]	1,765	down
RCAP_rcc02367_at		calcium-binding protein	Chemotaxis and motility [Cellular processes]	1,787	up
RCAP_rcc03328_at	ftsK	cell division protein FtsK	Cellular processes	1,891	Down
RCAP_rcc02311_at	sodB	superoxide dismutase [Fe]	Detoxification [Cellular processes]	1,846	down
DNA metabolism					
RCAP_rcc00201_at		site-specific DNA-methyltransferase (adenine-specific)	Restriction/modification [DNA metabolism]	1,767	down
RCAP_rcc00829_at	recN	DNA repair protein RecN	DNA replication, recombination, and repair [DNA metabolism]	2,291	up
RCAP_rcc02195_at		HNH endonuclease family protein	Restriction/modification [DNA metabolism]	3,125	up

RCAP_rcc03208_at	xerC	tyrosine recombinase XerC	DNA replication, recombination, and repair [DNA metabolism]	2,029	Up
RCAP_rcc02577_at		phage integrase	Prophage functions [Mobile and extrachromosomal element functions]	2,264	up
Purines, pyrimidines, nucleosides, and nucleotides					
RCAP_rcc02324_at	dgt	deoxyguanosinetriphosphate triphosphohydrolase	Nucleotide and nucleoside interconversions [Purines, pyrimidines, nucleosides, and nucleotides]	1,778	up
RCAP_rcc03469_at	pncB	nicotinate phosphoribosyltransferase	Salvage of nucleosides and nucleotides [Purines, pyrimidines, nucleosides, and nucleotides]	1,847	Up
RCAP_rcc01718_at	rihA	pyrimidine-specific ribonucleoside hydrolase RihA	[Purines, pyrimidines, nucleosides, and nucleotides]	2,042	up
RCAP_rcc01720_at	ndk	nucleoside diphosphate kinase	2'-Deoxyribonucleotide metabolism [Purines, pyrimidines, nucleosides, and nucleotides]	2,093	down

205

RCAP_rcc02505_at	tadA	tRNA-specific adenosine deaminase	[Purines, pyrimidines, nucleosides, and nucleotides]	1,746	up
Fatty acid and phospholipid metabolism					
RCAP_rcc00236_at	accD	acetyl-CoA carboxylase, carboxyl transferase, beta subunit	Biosynthesis [Fatty acid and phospholipid metabolism]	2,385	down
RCAP_rcc01678_at	acpP	acyl carrier protein	Biosynthesis [Fatty acid and phospholipid metabolism]	2,138	down
RCAP_rcc01884_at		hydrolase, alpha/beta fold family	Degradation [Fatty acid and phospholipid metabolism]	1,876	down
Transcription					
RCAP_rcc00118_at		sigma 54 modulation protein/ribosomal protein S30EA	Transcription factors [Transcription]	1,804	down
RCAP_rcc01490_at	rnd	ribonuclease D	RNA processing [Transcription]	1,926	up
RCAP_rcc02637_at		RNA polymerase sigma factor, sigma-70 family, ECF subfamily	Transcription factors [Transcription]	2,373	up
RCAP_rcc03318_at	rpoZ	DNA-directed RNA polymerase, omega subunit	DNA-dependent RNA polymerase [Transcription]	1,965	Up

Regulatory functions					
RCAP_rcc00668_at	ppsR	transcriptional regulator PpsR	[Regulatory functions]	2,214	up
RCAP_rcc00739_at		transcriptional regulator, ArsR family	DNA interactions [Regulatory functions]	1,989	up
RCAP_rcc00748_at	phaR	polyhydroxyalka noate synthesis repressor PhaR	[Regulatory functions]	2,907	up
RCAP_rcc00749_at		transcriptional regulator, LysR family	DNA interactions [Regulatory functions]	2,150	up
RCAP_rcc01658_at		two component transcriptional regulator, LuxR family	DNA interactions [Regulatory functions]	2,047	up
RCAP_rcc01797_at	ntrB	nitrogen regulation protein NtrB	Protein interactions [Regulatory functions]	1,984	up
RCAP_rcc01798_at	ntrC	nitrogen assimilation regulatory protein NtrC	Other [Regulatory functions]	2,302	up
RCAP_rcc01799_at	ntrY	nitrogen regulation protein NtrB	Protein interactions [Regulatory functions]	2,383	up
RCAP_rcc01800_at	ntrX	nitrogen assimilation regulatory protein NtrX	Other [Regulatory functions]	1,872	up

RCAP_rcc01801_at	hfq	RNA chaperone Hfq	Other [Regulatory functions]	1,859	up
RCAP_rcc02289_at		two-component response regulator receiver protein	Other [Regulatory functions]	1,759	up
RCAP_rcc02361_at	lexA	LexA repressor	DNA interactions [Regulatory functions]	2,358	up
RCAP_rcc02374_at		transcriptional regulator, LacI family	DNA interactions [Regulatory functions]	1,863	up
RCAP_rcc02460_at	cspA	cold shock protein CspA	DNA interactions [Regulatory functions]	2,084	down
RCAP_rcc02493_at		transcriptional regulator, Crp/Fnr family	DNA interactions [Regulatory functions]	1,774	up
RCAP_rcc02555_at		transcriptional regulator, HxlR family	DNA interactions [Regulatory functions]	1,998	up
RCAP_rcc02581_at		sensor histidine kinase	Other [Regulatory functions]	2,149	up
RCAP_rcc02766_at	petP	transcriptional regulator PetP	DNA interactions [Regulatory functions]	2,291	up
RCAP_rcc02790_at		transcriptional regulator, CarD family	DNA interactions [Regulatory functions]	2,447	up
RCAP_rcc02813_at	lrp	leucine-responsive regulatory protein	DNA interactions [Regulatory functions]	1,822	up

208

RCAP_rcc02893_at	cspA	cold shock protein CspA	DNA interactions [Regulatory functions]	2,089	up
RCAP_rcc03255_at		transcriptional regulator, Crp/Fnr family	DNA interactions [Regulatory functions]	2,027	Up
RCAP_rcc03267_s _at	nifA	Nif-specific regulatory protein	DNA interactions [Regulatory functions]	2,102	Up
Unknown Function and Hypothetical Proteins					
RCAP_rcc00133_at		conserved hypothetical protein	Conserved [Hypothetical proteins]	1,831	down
RCAP_rcc00162_at		conserved hypothetical protein	Conserved [Hypothetical proteins]	3,160	up
RCAP_rcc00185_at		conserved hypothetical protein	Conserved [Hypothetical proteins]	2,193	down
RCAP_rcc00203_at		conserved domain protein	Domain [Hypothetical proteins]	1,850	down
RCAP_rcc00476_at		protein of unknown function DUF1013	unknown function	2,086	up
RCAP_rcc00499_at		conserved hypothetical protein	Conserved [Hypothetical proteins]	4,046	down
RCAP_rcc00575_at		conserved hypothetical protein	Conserved [Hypothetical proteins]	1,805	down

RCAP_rcc00582_at		conserved hypothetical protein	Conserved [Hypothetical proteins]	1,966	up
RCAP_rcc00656_at		Hypothetical protein	Hypothetical protein	1,795	down
RCAP_rcc00657_at		conserved hypothetical protein	Conserved [Hypothetical proteins]	1,820	down
RCAP_rcc00658_at		conserved hypothetical protein	Conserved [Hypothetical proteins]	2,097	down
RCAP_rcc00738_at		conserved hypothetical protein	Conserved [Hypothetical proteins]	2,109	up
RCAP_rcc00747_at		conserved hypothetical protein	Conserved [Hypothetical proteins]	1,761	up
RCAP_rcc00784_at		conserved domain protein	Domain [Hypothetical proteins]	1,913	up
RCAP_rcc00845_at		hypothetical protein	hypothetical protein	1,905	down
RCAP_rcc00901_at		conserved hypothetical protein	Conserved [Hypothetical proteins]	2,080	down
RCAP_rcc00909_at		conserved hypothetical protein	Conserved [Hypothetical proteins]	2,326	up
RCAP_rcc01038_at		conserved domain protein	Domain [Hypothetical proteins]	2,528	up

RCAP_rcc01234_at		Hypothetical proteins	Hypothetical proteins	1,787	down
RCAP_rcc01448_at		conserved hypothetical protein	Conserved [Hypothetical proteins]	2,170	up
RCAP_rcc01522_at		conserved hypothetical protein	Conserved [Hypothetical proteins]	2,193	down
RCAP_rcc01526_at		conserved hypothetical protein	Conserved [Hypothetical proteins]	1,800	down
RCAP_rcc01580_at		conserved hypothetical protein	Conserved [Hypothetical proteins]	1,797	up
RCAP_rcc01677_at		hypothetical protein	hypothetical protein	2,310	down
RCAP_rcc01682_at		conserved hypothetical protein	Conserved [Hypothetical proteins]	3,239	up
RCAP_rcc01732_at		conserved hypothetical protein	Conserved [Hypothetical proteins]	2,214	down
RCAP_rcc02111_at		conserved hypothetical protein	Conserved [Hypothetical proteins]	1,800	up
RCAP_rcc02177_at		conserved hypothetical protein	Conserved [Hypothetical proteins]	2,365	up
RCAP_rcc02465_at		conserved hypothetical protein	Conserved [Hypothetical proteins]	2,144	down

RCAP_rcc02492_at		conserved hypothetical protein	Conserved [Hypothetical proteins]	1,810	up
RCAP_rcc02688_at		conserved hypothetical protein	Conserved [Hypothetical proteins]	1,957	up
RCAP_rcc02708_at		conserved hypothetical protein	Conserved [Hypothetical proteins]	3,661	down
RCAP_rcc02758_at		protein of unknown function DUF149	Conserved [Hypothetical proteins]	2,119	down
RCAP_rcc02999_at		conserved hypothetical protein	Conserved [Hypothetical proteins]	1,828	up
RCAP_rcc03356_at		conserved hypothetical protein	Conserved [Hypothetical proteins]	1,956	Up
RCAP_rcc03379_at		conserved hypothetical protein	Conserved [Hypothetical proteins]	1,751	Down
RCAP_rcc03429_at		[Hypothetical proteins]	[Hypothetical proteins]	1,967	Up
RCAP_rcc00194_at		ErfK/YbiS/YcfS/YnhG family protein/Tat domain protein	General [Unknown function]	2,006	up
RCAP_rcc00212_at		protein of unknown function DUF150	General [Unknown function]	2,466	up
RCAP_rcc00214_at		protein of unknown function DUF448	[Hypothetical proteins]	1,783	up

RCAP_rcc00227_at		protein of unknown function DUF1159	General [Unknown function]	2,733	up
RCAP_rcc00260_at		alanine racemase domain protein	Enzymes of unknown specificity [Unknown function]	3,143	up
RCAP_rcc00828_at	comL	competence lipoprotein ComL	General [Unknown function]	3,444	up
RCAP_rcc00868_at		protein of unknown function DUF156	General [Unknown function]	2,034	up
RCAP_rcc00899_at		staphylococcal nuclease family protein	General [Unknown function]	1,851	up
RCAP_rcc01117_at		protein of unknown function UPF0054	General [Unknown function]	2,003	up
RCAP_rcc01209_at		cell wall hydrolase, SleB	Enzymes of unknown specificity [Unknown function]	1,984	up
RCAP_rcc01349_at		pirin domain protein	General [Unknown function]	2,249	up
RCAP_rcc01717_at		protein of unknown function UPF0061	unknown function	2,428	up
RCAP_rcc01721_at		TfoX domain protein	General [Unknown function]	3,420	up

RCAP_rcc01725_at		protein of unknown function DUF475, transmembrane	unknown function	2,506	down
RCAP_rcc02149_at		protein of unknown function DUF1223	General [Unknown function]	2,971	up
RCAP_rcc02178_at		protein of unknown function UPF0187	General [Unknown function]	1,966	up
RCAP_rcc02187_at		amidohydrolase family protein	Enzymes of unknown specificity [Unknown function]	2,042	down
RCAP_rcc02319_at		protein of unknown function DUF1289	General [Unknown function]	1,755	up
RCAP_rcc02383_at	mraZ	protein MraZ	General [Unknown function]	2,254	down
RCAP_rcc02638_at		calcium-binding EF-hand domain protein	General [Unknown function]	2,425	up
RCAP_rcc02783_at		CoA-binding domain protein	General [Unknown function]	2,174	up
RCAP_rcc02833_at		ATPase, P-loop family	Enzymes of unknown specificity [Unknown function]	1,867	up

RCAP_rcc03067_at		protein of unknown function DUF451	General [Unknown function]	2,665	down
RCAP_rcc03108_at		protein of unknown function DUF305	General [Unknown function]	6,700	up
RCAP_rcc03163_at		protein of unknown function DUF1611	General [Unknown function]	5,881	Down
RCAP_rcc03220_at		protein of unknown function DUF697, transmembrane	unknown function	1,824	Down
RCAP_rcc03237_at		protein of unknown function DUF81, transmembrane	unknown function	2,083	Up
RCAP_rcc03320_at		protein of unknown function DUF88	General [Unknown function]	1,986	Up
RCAP_rcc03459_at		protein of unknown function DUF165	unknown function	2,052	Down
RCAP_rcc01557_at		rhodanese domain protein	General [Unknown function]	2,152	up
RCAP_rcc01796_at	dusB	tRNA-dihydrouridine synthase B	General [Unknown function]	2,698	up
RCAP_rcc01940_at		hemolysin-type calcium-binding repeat family protein	General [Unknown function]	2,054	down

RCAP_rcc02528_at		dihydropyrimidine dehydrogenase (NADP(+))	Enzymes of unknown specificity [Unknown function]	3,856	down
RCAP_rcc02782_at		aminotransferase, DegT/DnrJ/EryC1/StrS family	Enzymes of unknown specificity [Unknown function]	3,072	up
RCAP_rcc03332_at		protein of unknown function DUF343	General [Unknown function]	2,174	Up
RCAP_rcc00737_at		hypothetical protein	hypothetical protein	1,898	up
RCAP_rcc00821_at		Hypothetical protein	Hypothetical protein	1,834	down
RCAP_rcc03511_at		HemY domain protein	General [Unknown function]	1,747	Down
RCAP_rcc03448_at		serine/threonine-protein phosphatase	Enzymes of unknown specificity [Unknown function]	1,901	Up
RCAP_rcc01551_at	bcp	peroxiredoxin	Other [Cell envelope],General [Unknown function]	3,333	up
RCAP_rcc01754_at		glutamine amidotransferase, class-II	Enzymes of unknown specificity [Unknown function]	1,884	up

RCAP_rcc02778_at		glutamine amidotransferase, class I	Enzymes of unknown specificity [Unknown function]	2,470	up
RCAP_rcc01683_at		terminase-like family protein	Unknown function	2,027	up
RCAP_rcc00283_at		conserved hypothetical protein	Conserved [Hypothetical proteins]	1,949	up
RCAP_rcc00307_at		conserved hypothetical protein	Conserved [Hypothetical proteins]	2,985	up
RCAP_rcc02529_at		pyridine nucleotide-disulphide oxidoreductase family protein	Enzymes of unknown specificity [Unknown function]	2,306	down

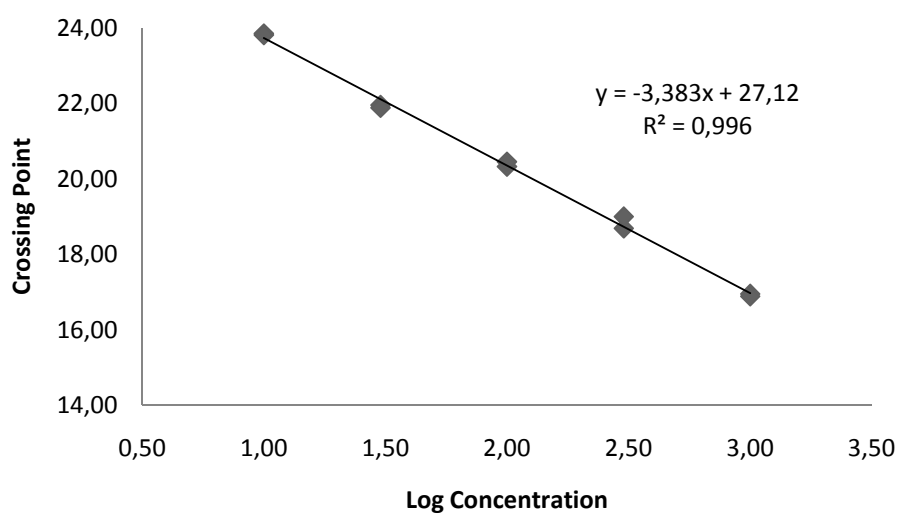## STANDARD CURVES USED FOR RT-QPCR ANALYSIS

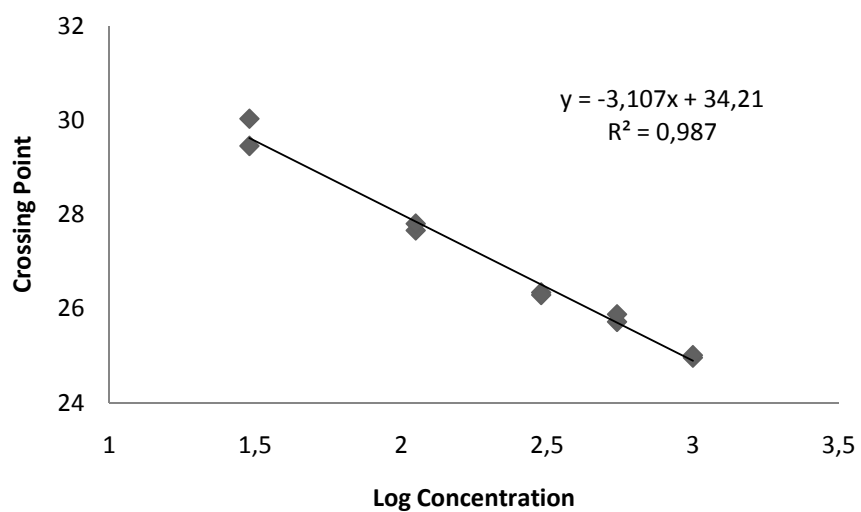**Figure F. 1** Standard curve for 16sRNA gene used for RT-qPCR analysis

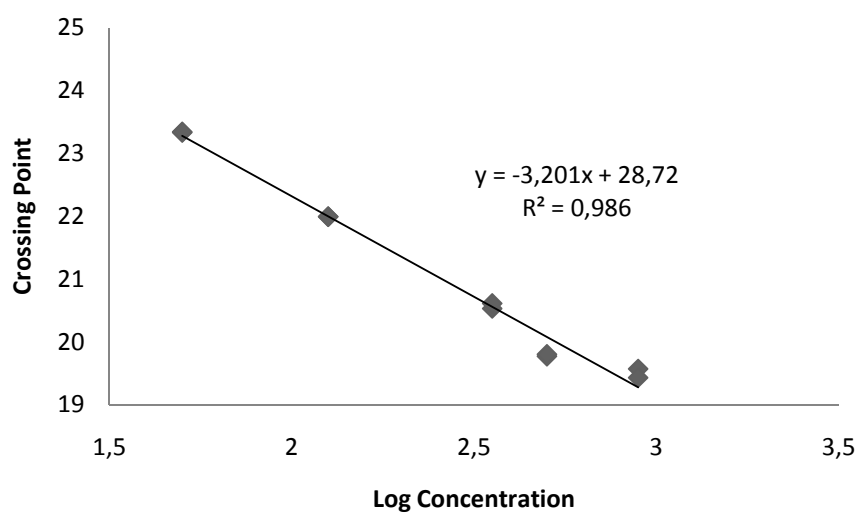**Figure F. 2** Standard Curve for acnA gene for RT-qPCR
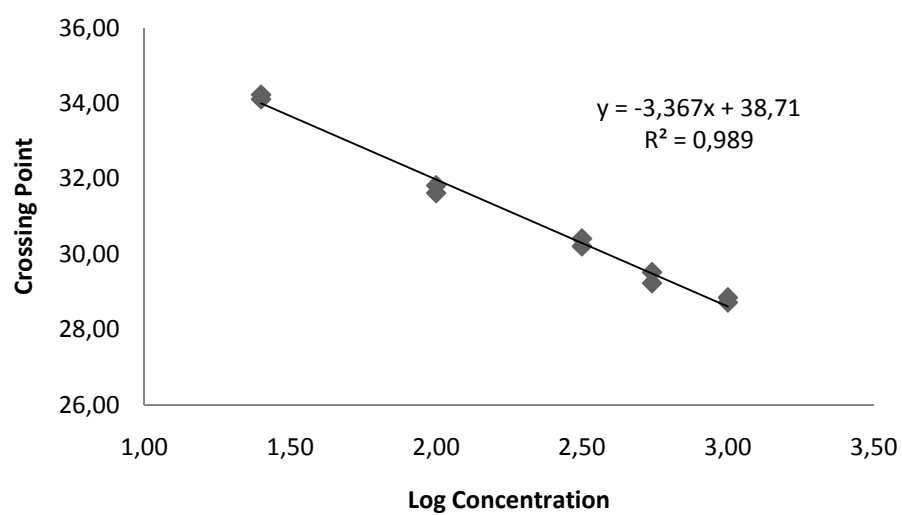
Figure F. 3 Standard Curve for atpF gene for RT-qPCR

$y = -3,367x + 38,71$
$R^2 = 0,989$

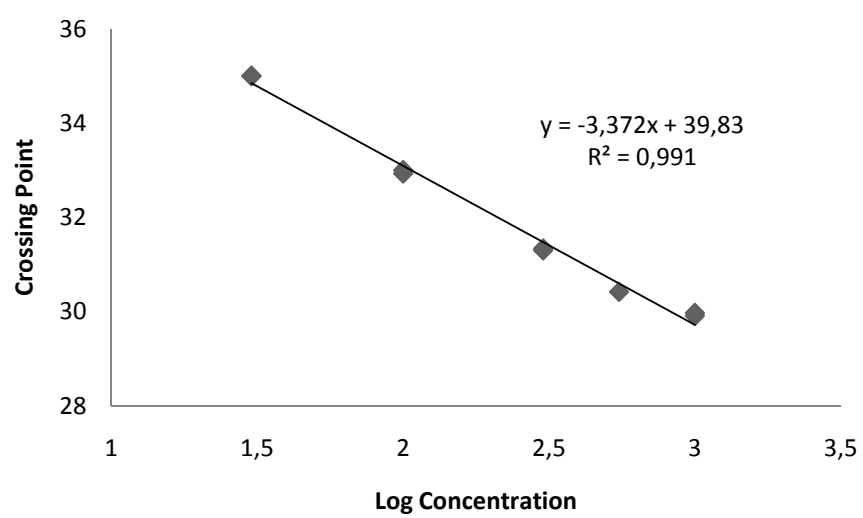**Figure F. 4** Standard curve for pufM for RT-qPCR

Figure F. 5 Standard curve for oppA gene for RT-qPCR

CURRICULUM VITAE

Name, Surname: Afşar Nilüfer

Birth: June 18, 1981, Eskişehir, Turkey

Citizen: Republic of Turkey

Phone: +90 312 287 8122

Mobile: +90 532 4780479

email: niluferafsar@gmail.com

Education:

2012   PhD, METU Department of Biology

2007   MSc, METU Department of Biochemistry

2004   BS, METU Department of Biology

Experiences:

2007-2011 EU project assistant, METU, Hydrogen Research Laboratory

2003   Intern, Abdi Ibrahim Pharmaceuticals, Microbiology Laboratory

Peer-reviewed publications in International Journals

Kayihan, C., Eyidoğan, F., Afsar, N., Oktem H.A., Yucel, M., 2012, "Cu/Zn superoxide dismutase activity and respective gene expression during cold acclimation and freezing stress in barley cultivars", Biologia Plantarum, 56:693-698

Afsar, N., Özgür, E., Gürgan, M., Akköse, S., Yücel, M., Gündüz, U. Eroglu, I., 2011 "Hydrogen productivity of photosynthetic bacteria on dark fermenter effluent of potato steam peels hydrolysate", International Journal of Hydrogen Energy, 36: 432-438

Özgür, E., Afsar, N., de Vrije, T., Yücel, M., Gündüz, U., Claassen, P.A.M., 2010, "Potential use of thermophilic dark fermentation effluents in photofermentative hydrogen production by Rhodobacter capsulatus" Journal of Cleaner Production, 18: S23-S28.

Afsar, N., Özgür, E., Gürgan, M., de Vrije, T., Yücel, M., Gündüz, U., Eroglu, I., 2009, "Hydrogen Production By R. capsulatus on dark fermenter effluent of potato steam peel hydrolysate" Chemical Engineering Transactions, 18: 385-390.

Presentations in International Conferences

Gürgan, M, Afsar, N., Sevinç, P, Özgür, E., Gündüz, U., Eroğlu, İ., Yücel, M. "Effects of Heat and Cold Stress on Biohydrogen Production By Rhodobacter capsulatus" presented at: World Hydrogen Energy Conference 2012 (WHEC2012), Toronto, Canada, 3-7 June, 2012

Afsar, N., Özgür, E., Gürgan, M., Yücel, M., Gündüz, U. Eroglu, I.," Hydrogen Productivity of Different Photosynthetic Bacteria on Dark Fermenter Effluents" presented at: 10th International Conference on Clean Energy, presented at: Famagusta, North Cyprus,15-17 september, 2010

Afsar, N., Özgür, E., Gürgan, M., de Vrije, T., Yücel, M., Gündüz, U., Eroglu, I, "Hydrogen Production By R. capsulatus on dark fermenter effluent of potato steam peel hydrolysate" presented at: 12th International Conference on Process Integration, Modelling and Optimization for Energy saving and Pollution Reduction, Rome, Italy, 10-13 May, 2009.

Afsar, N., Yücel, M., Eyidogan, F.İ. "Effect of Chilling Stress on Antioxidant Response of Winter and Spring Barley (Hordeum vulgare) Cultivars" presented at: International Conference on Responses of Plants to Environmental Stresses, Elena, Bulgaria, 12-18 May, 2008.

Presentations in National Conferences

Afsar, N., Yücel, M., Eyidoğan, F.İ., 'Effect of Cold Stress on Oxidative Stress parameters of Winter and Spring Barley (Hordeum vulgare) Cultivars' presented at 15th National Biotechnology Congress, Antalya, Turkey, 28-31 october, 2007

Memberships   Turkish Biochemical Society

Federation of European Biochemical Societies (FEBS)

Awards

Afsar N., Yücel M.,Eyidogan F. İ. "Effect of Chilling Stress on Antioxidant Response of Winter and Spring Barley (Hordeum vulgare) Cultivars" International Conference on Responses of Plants to Environmental Stresses, Poster presentation: 2nd place, Elena, Bulgaria, 12-18 May, 2008.

Computer Skills

Microsof Office Applications (Word, Excel, Powerpoint, Publisher), Minitab, GCOS, Genespring GX, SPSS, Internet Applications

Languages   Turkish: native language

English: fluent

German: medium